The Development of a Methodology for Analysing a Modular Based Jack-up Concept using Superelements

F. H. van Dongen

Master Thesis

19 April 2017

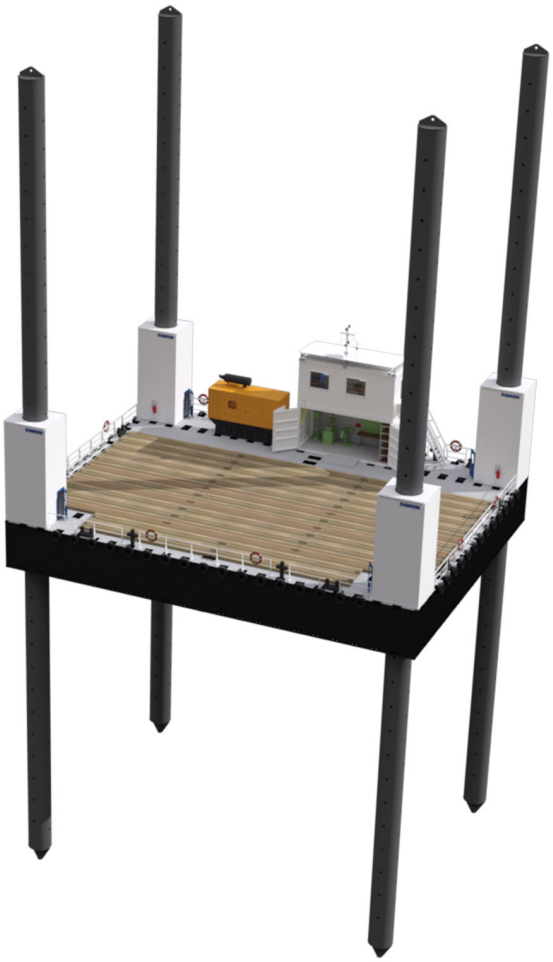

TU Delft Delft University of Technology

DAMEN

The Development of a Methodology for Analysing a Modular Based Jack-up Concept using Superelements

F. H. van Dongen

to obtain the degree of
Master of Science
Offshore & Dredging Engineering
at the Delft University of Technology,
to be defended publicly on Wednesday April 26, 2017

Student number: 4009398
Master program: Offshore & Dredging Engineering

Graduation committee:

Prof. dr. A. Metrikine	TU Delft
Dr. ir. A. Jarquin Laguna	TU Delft
Dr. ir. K.N. van Dalen	TU Delft
Ir. F.A.G. Jacobs	DAMEN
Ir. H.L. Aga	DAMEN

Abstract

A modular jack-up is a platform built from container sized modules which altogether form a deck structure. Benefits of modular building are mobility (e.g. transportable over land) and flexibility in the design. One of the critical aspects of the design are the connections between barges and couplings which can experience significant tensional and shear loading.

The objective of the thesis is to develop a methodology for the analysis of conceptual designs in the early design phase. Following the requirements, the methodology must be capable of analysing the endured loading by couplings. It must be able to consider different configurations and load cases. And lastly, it must provide fast and valid results.

The starting point of the methodology is to create an environment in which configurations and load cases are generated using superelements for the barges and couplings. In Finite Element Analysis a superelement is a grouping of finite elements which, upon assembly, may be regarded as an individual element for computational purposes. From load cases, containing gravitational loading, payload and environmental loading, the displacements in the structure are analysed using the stiffness relations. Using these displacements, the loads between barges and couplings are determined.
The first objective on the development of a methodology is achieved and put in to practice in a model providing valid and accurate results in less than a minute.

The second part of the thesis consists of case studies on a predetermined concept design (see figure). This study investigates the influences of the amount of couplings used, the location of payload on the deck, environmental loading and a punch-through. Also research is performed on the modelling of the leg-hull interaction.

The model performs properly and provides valid results. In load cases considering horizontal loading (e.g. environmental conditions) it must be noted that the P-Δ effect is significant affecting the accuracy of the results. From the findings of the studies, it is concluded that the current connection between barges is insufficient for these jack-up designs even when using the maximum amount of couplings. During the studies it is uncovered that the distribution of loads on the couplings is highly dependent on coupling location. With respect to shear loading, critical locations are found at the couplings close to the legs. For tension these are at the outer edges halfway between the legs.
A punch-through simulation is carried out with the use of this linear model. The soil constraints of the structure are modified replacing simple supports with the use of springs. The results from the simulation are within reasonable boundaries, indicating that this model approximates the results of a punch-through.

Investigations of the overall results show that large loading is introduced into the structure at the leg-hull interfaces influencing the coupling results. From research on the leg-hull interaction it is found that making the connection more flexible in the transverse direction can significantly reduce the maximum shear load in the couplings.

Recommendations are to investigate further on the leg-hull interaction, accounting for the effects on the structure's stiffness considering the gap between leg and guide as well as P-Δ and leg inclination effects. Regarding the simulation of a punch-through, combining the current model with proper modelling of soil characteristics can improve the results.

Acknowledgements

This thesis is written for the completion of my Master's degree in Offshore and Dredging Engineering at the Delft University of Technology. During my internship, I've been in contact with many people who, each in their own way, contributed to this thesis. Here, I would like to express my gratitude.

From the university I want to thank Prof. dr. A. Metrikine for the productive and critical feedback in our progress meetings. Secondly, to Dr. ir. A. Jarquin Laguna for the support and interesting discussions, providing me with new insights on how to go forward. And to Dr. ir. K. N. van Dalen for examining my report for my graduation.

From DAMEN I want to thank Ir. F.A.G. Jacobs, who has continously provided me with the sometimes necessary mental support and much feedback. As well to Ir. H. L. Aga for his guidance throughout this graduation process. The many long Skype calls between Gorinchem and Singapore often resulted in interesting discussions with never a dull moment.

I would like to thank the collegues at DAMEN Singapore and MDEM Ukraine for helping me find my way in NX Nastran. Also a thanks to B. Sekreve for showing me around in the world of modular construction.

To all of the Research & Development department at DAMEN Gorinchem, I want to thank you for letting me be a part of this department for the past year. I've enjoyed my time here as I had the opportunity to meet many people and ask many questions to anyone I could find. This pleasent working environment gave room for lots of laughter and good conversations, which I considered very valuable in this sometimes stressfull period of hard work. This made my experience as a graduate student at DAMEN a truly great one.

Lastly, I would like to give a big word of thanks to my friends and family for the constant support and encouragement along the way.

Contents

List of Figures

List of Tables

Nomenclature

$\bar{u}$	Displacement vector
λ	Wave length [m]
AF	Axial force [N]
BM	Bending moment [Nmm]
COG	Centre of Gravity
DMB	Damen Modular Barge
F	load vector
f_i^e	concentrated element load at node i [N]
f_i	force/moment at node i [N or Nmm]
FEM	Finite Element Method
g	Gravitational acceleration = 9.81 [m/s]
h_{coup}	Coupling height [mm]
K	Stiffness matrix
k_{ij}	Stiffness coefficient of nodes i and j [N/m^2]
L^e	Element length [mm]
q_i	Load per unit length at node i [N/mm]
RBE	Rigid Body Element
SE	Superelement
SF	Shear force [N]
T	Wave period [s]
u_i	displacement of node i [mm or rad]
VBA	Visual Basic for Applications
W	Weight [N]

1 Introduction

1.1. Background

In the offshore industry self-elevating jack-up structures are widely used. This platform is characterized by being a floating as well as a bottom founded structure. A jack-up mainly consists of a buoyant deck with retractable legs. It can be towed (or in some cases self propelled) to a site. It provides a stable work deck for operations by lowering its legs into the seabed and elevate its hull. Additionally, it can be outfitted with equipment like a crane, a helideck or an accommodation facility. These mobile structures are suited for temporary operations like drilling, for maintenance (e.g. windmills, wells), as accommodation or for construction work. These days jack-ups are capable of operation in waters of approximately 120 metres and wave heights of up to 25 metres [8].

1.1.1. Jack-up Operation and Challenges

The main characteristic of a jack-up, being both a floating and a bottom founded structure, directly reveals some challenges [8]. Following the operational phases, the main challenges surrounding a jack-up are described.

At first a jack-up is towed to its working location. During this operation the legs of the structure are pulled up completely. This has influence on the floating stability of the structure as the centre of gravity is higher and the platform is exposed to higher wind loads.

While being towed, the structure moves on the waves experiencing roll and pitch motions. As the legs extend a long way from the deck these can experience large tip movements. This results in moments which have a significant effect on the fatigue life of the structure [30].

Installation begins at arrival on site. The jack-up lowers its legs and makes the transition between being afloat and bottom founded. This is probably the most critical stage of the overall operation. As the jack up moves in an oscillating way in the waves, so do the lowered legs just above the soil. Due to these motions, the feet of these legs can experience large velocities and accelerations. Upon touch down on the soil this may result in large impact loads [13]. Also the shape and layout of the soil is of great importance. Apart from the risk of deploying the legs on pipelines or debris, it is possible that a spud can is set close to an existing footprint made by a jack-up in the past. In this case there is the risk of the spudcan not to penetrate straight downward into the soil, but instead slip into the old hole. This movement can impose a significant bending moment on the leg [22].

The jacking process starts after touchdown. To make sure the structure can withstand all environmental conditions it is expected to encounter, the legs are driven into the soil by preloading.

The weight on the legs is increased using ballast tanks, or by putting all the weight of the structure on two diagonally opposite legs at a time (for jack-ups with more than three legs). The legs will drive deeper into the soil until equilibrium is reached and the structure stands sturdy on the ground.

During the preloading phase a punch-through can occur, which is one of the largest risks for a jack-up[29]. As the legs sink into the soil at different locations, they have different soil beneath them. As one of the legs reaches a softer soil type (e.g. clay), it can break through the hard upper soil and sink several metres. As a result large bending moments will occur in de remaining legs and tipping of the structure is a real threat.

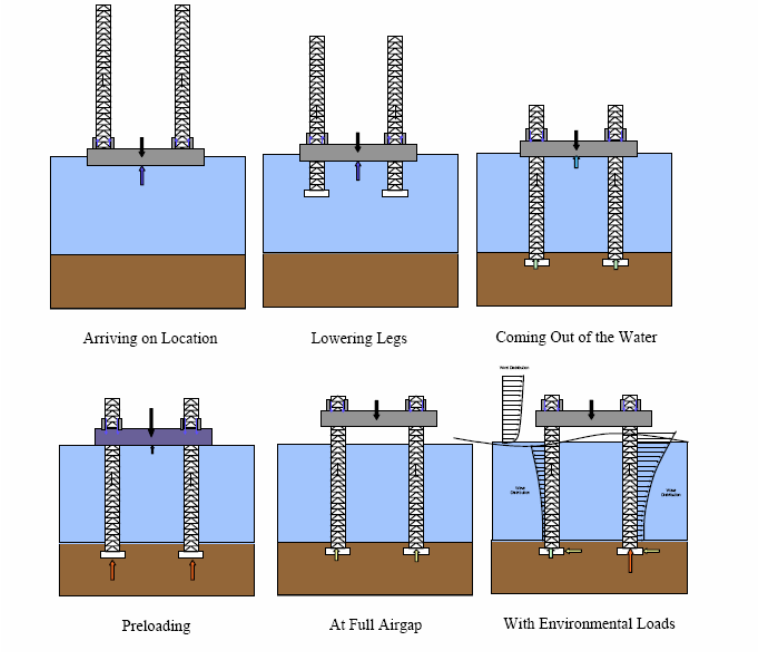

Figure 1.1: Different operational phases of a jack-up structure[26]

It is clear that the interaction between the structure and soil is of great importance. A lot of research is performed in this field to gain insight in the behaviour of a jack-up on different types of soil and in different situations [10] [15] [7].

After preloading and elevation the structure can perform operations. In bottom founded conditions it is exposed to environmental loadings (wind, waves and current). In this field research is performed on the response and behaviour of jack-ups due to external loading [19] [20].

1.1.2. Class Societies

To assure the safety of a jack-up, often its design has to meet criteria defined by class societies. This is done to assure safe operations and required to obtain insurance. There are different class societies[8] with different criteria as jack-ups are produced for different purposes. For example a jack up structure designed for small lifting operations in a lake has different criteria than a large drilling rig towed offshore to ocean waters. The main class societies are : Det Norske Veritas (DNV)[4], Bureau Veritas(BV)[3] and American Bureau of Shipping (ABS)[5]. Many of the criteria in these class societies are based on guidelines of the Society of Naval Architects and Marine Engineers (SNAME)[25].

1.2. Modular Design

Within DAMEN, the department of Civil and Modular Construction (C&MC) designs modular products. The C&MC core component is the DAMEN Modular Barge (DMB). DMBs come in a range of 20 ft. to 40 ft. containers that can be connected. They are easily transported, maintained and operated which makes that they are suitable for a variety of applications. Examples of such applications are: a jetty, a modular ferry and a helideck (Figure 1.2).

(a) Modular jetty (b) Modular ferry (c) Modular Helideck

Figure 1.2: Examples of modular products [1]

1.2.1. Modular Jack-up

Exploring new markets, DAMEN aims to expand their product range by building modular jack-ups which can be used in sheltered, coastal and land locked waters. A large difference with other modular products is that it is not only a floating structure, since it will jack-up. For the connection of these barges, this provides challenges.

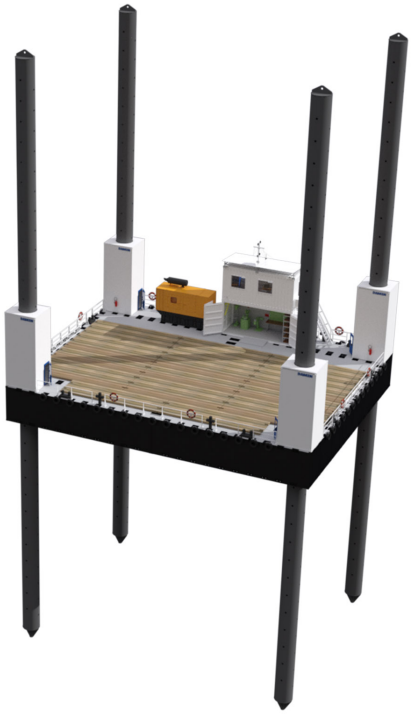

Figure 1.3: Modular jack-up (JUP2420) [1]

Before expanding on these challenges, a DAMEN conceptual design is used for some elaboration on the different main components of the structure.

Figure 1.3 shows a representation of the JUP2420 (appendix B). This four legged jack-up structure is approximately 20 by 24 metres and can operate in waters of a maximum of 25 metres water depth.
It can provide a stable working platform for operations in water. During operation it encounters environmental loading (waves, wind and current) and it has to carry payload installed on the deck. Without a propulsion system, tugs are required to transfer it to its location of operations.
The main components of the JUP2420 are:

- DMBs (figure 1.4)
  These form the deck structure. This design consists of 16 DMBs that are lined up in a two-by-eight manner.

- Couplings (figure 1.4)
  These connect the barges. For the 16 pontoons in this conceptual design 72 couplings are used. 16 in the longitudinal direction and 56 in the transverse direction.

- Jacking mechanism
  This mechanism can lift the structure out of the water.

- Legs
  These carry the weight of the structure, as the deck is lifted. Additionally they experience the majority of the environmental loading from waves and current.

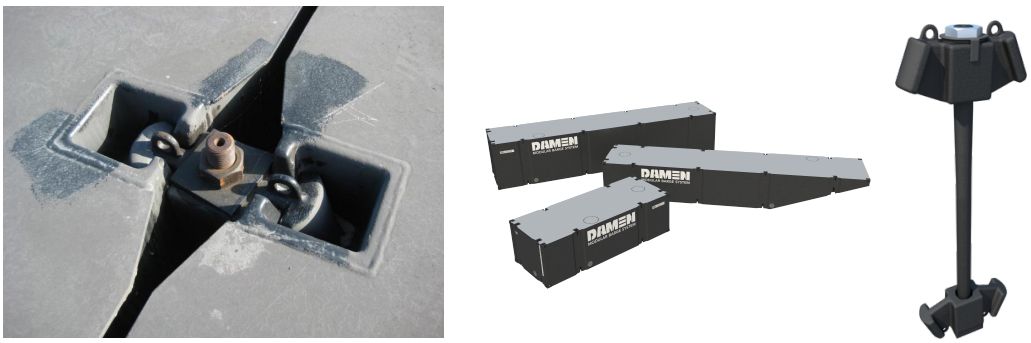

(a) Barges connected by a coupling (b) Damen Modular Barge (DMB) (c) Damen Link

Figure 1.4: The modular components of the deck structure[1]

In the following paragraphs some elaboration is provided on the DMB and coupling forming the deck structure.

DMB
DMBs come in different sizes shown in the table 1.1. These values were attained from the product specifications of DAMEN [12]. In appendix A a more extensive overview of the specifications is shown. These standard barges, originally developed for floating applications, have two and four connection locations on its short and long end respectively. However, for the jack-up more connection locations are considered on the long end. As it is expected that the couplings will endure more loading in comparison to a floating product.

Table 1.1: Standard DMB specifications[12]

DMB dimensions	Minimum:	Maximum:
Length	6.058 m	12.192 m
Width	2.438 m	2.438 m
Height	1.291 m	2.895 m
Deck load	6.8 tons/m^2	

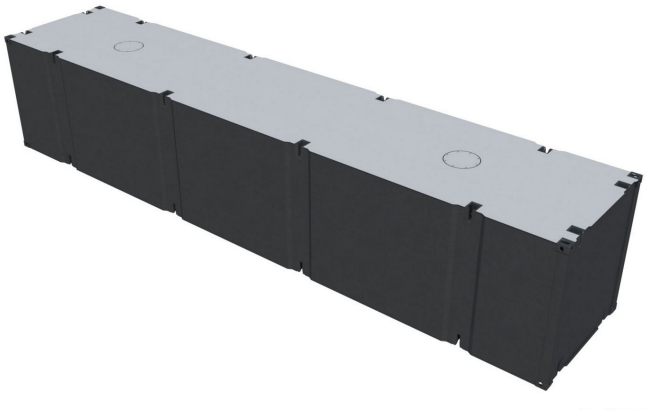

Figure 1.5: A Damen Modular Barge [1]

Coupling and Connection
For the connection the DAMEN Link is used. This is a specifically designed coupling system to join DMBs together. It is a steel construction consisting of three main parts; two hooks at both ends and a main rod connecting them. Furthermore, there is a securing plate at one end of the rod and a washer and nut on the other (figure 1.6).
The connection principle of these couplings is based on the main rod. The hooks slid in the corresponding locks at the top and bottom of the DMBs. The main rod in between the upper and lower hook is pretensioned by fastening the nut. By doing so the hooks are clamped firmly into the locks providing a rigid connection.

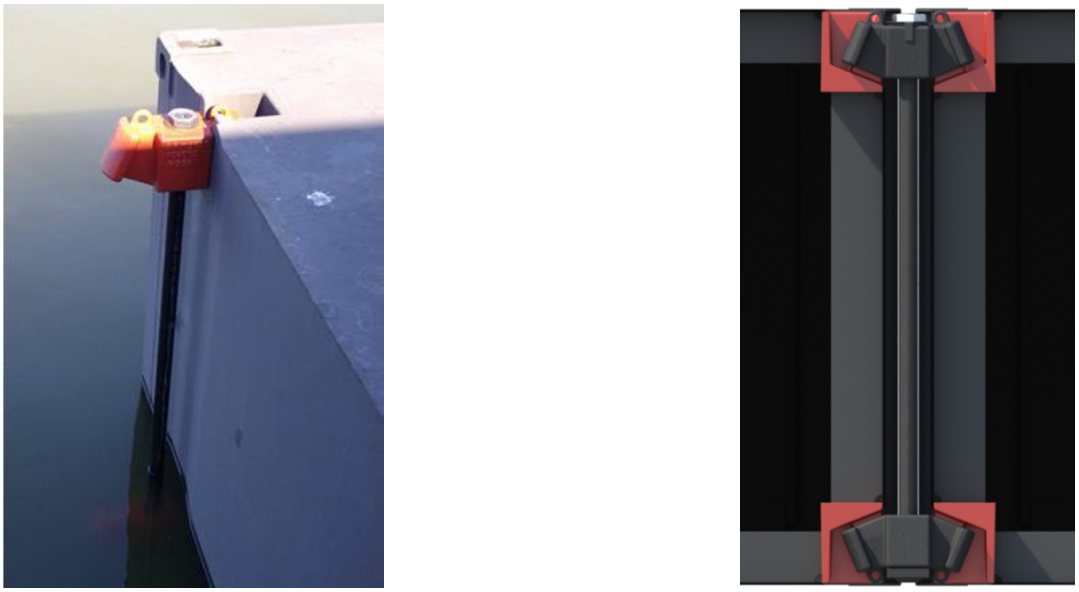

Figure 1.6: A representation and schematic of the connection between a DMB and coupling [1]

The working principle of the coupling is focused on transferring loads from the hooks into the longitudinal direction of the main rod as this is the strongest part of the coupling. Figure 1.7 shows a representation of how loads are transferred due to vertical shearing and bending of two DMBs. This is achieved with the use of the inclined flanges of the hook. Through this inclination the loads are exerted on the coupling by the DMB in a horizontal direction (red arrows in figure 1.7) can be counteracted by vertical forces in the axial direction of the rod (SF and AF)

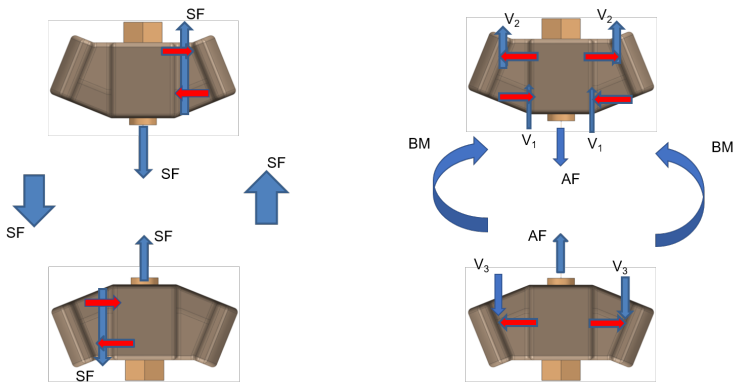

Figure 1.7: Load transfer from DMB movements to the axial direction of coupling rod for loads due to shear force (SF) and bending moment (BM)

These connections between DMBs are the limiting parts of the structure. From an earlier study on the capacity of these couplings different failure modes have been examined based on these shear and bending loads [23]. Different failure modes that can occur are:

- Rod failure
- Loss of pretension (slippage)
- Hook failure
- Lock failure
- Failure of the barge structure around the lock
- Failure of the nut

The failure modes of the coupling system have been examined and the results have been set out in capacity curves. These show at which combination of bending and shear loading a coupling exceeds the limits of a failure mode. These shear and bending loads have been translated to shear and tensional forces at the hooks of a coupling.
The different limits for the different failure modes have been combined into an overall capacity graph shown in figure 1.8.
These results are based on the conventional coupling system that is widely used within DAMEN for floating applications.

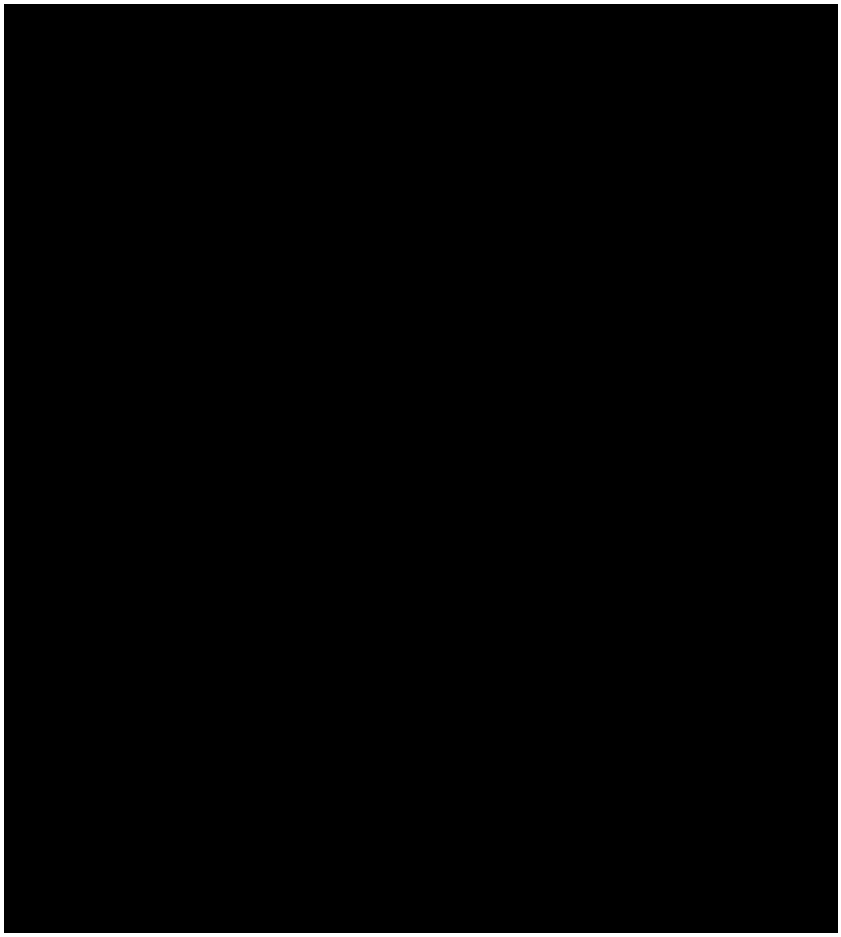

Figure 1.8: Combination of the different capacity curves for a coupling (confidential) [1]

1.3. Design Process

To understand the necessity of this study, it is important to understand the initial process of designing a vessel or structure. The main three phases that can be defined in this process are the sales phase, the engineering phase and the production and delivery phase.

Sales Phase
In DAMEN, generally the stages of design are customer driven. So the process start with a customer providing a request to a sales manager. Often this is done through a tender, where several yards are being approached. The sales manager can involve one or more design and proposal engineers. From the customers request, a set of general requirements is set up to define more specific the clients needs.
With these general requirements an initial concept is created by completing one or more cycles from the project design spiral (figure: 1.9). This cycle is repeated until an initial concept is found that is sufficiently outlined to make a bid for the tender. If the bid is accepted, further iterations are carried out until a sales contract can be set up. This concludes the sales phase.

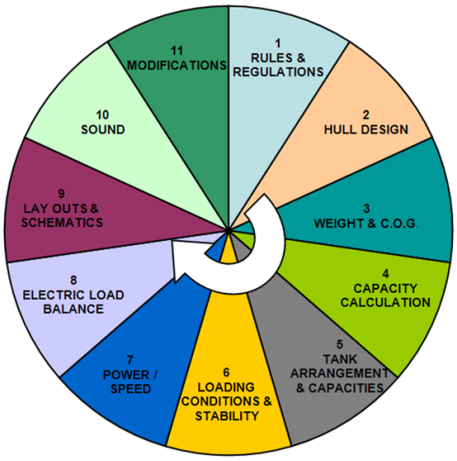

Figure 1.9: The project spiral that is used in DAMEN [6]

Engineering Phase
Once the engineering phase starts, the main constraints are already set for the project. In this phase the engineering department continues to work within the project cycle to improve the product and reduce costs. As the main decisions have already been made, the ability of the engineering department to improve is somewhat limited. The engineering phase is further split in two; the basic engineering and the detailed engineering.
In the basic engineering the overall design is finalized. Choices are made on components to use and the overall structural layout is optimized. On the component level detailed engineering can be necessary to meet specific requirements or for further optimization.
In this phase also an official review is performed on the design to make sure it meets the requirements from class societies involved.

Production and Delivery
In the production phase all the planning and design activities come together and execution of the design starts. During this process, as the product is shaped more and more, it becomes very resistant to changes. In this phase changes to the final design often come at high cost.

1.4. Problem Definition

In developing modular structures design is focused on creating a single standard component that can be combined to form a structure meeting design criteria. Furthermore, ideally the design of these components allows them to be used in different (types and sizes of) structures with various purposes and design criteria.

The main components of a modular jack-up are (besides the legs) the DMBs and the couplings. For proper design of these components insight is needed in the loads they will endure in these different possible configurations. Earlier studies on these structures show that this connection between DMB and coupling is a critical part of the design[24].

This research falls within the early part of the development process. When a tender is put out, an analysis is needed on what it is that the customer requires and what this means for the loading on an initial concept.

Currently this is done using Finite Element Method analysis. This method can provide analysis on highly detailed structures. However, using FEM results in a time consuming process that in the end only provides answers to a single configuration. When more general insight is required in different configurations and load cases a more flexible method is needed.

Focusing on a more flexible method, the objective is to gain knowledge on:

- The degree in which a coupling is loaded in different configurations and loading scenarios.

- How (external) loading is handled by the set of couplings in different configurations all together.
  The transfer of load through a structure gives insight in the increase or decrease of internal loadings due to different external loadings. E.g. it is valuable to know how external load of a crane on the side of a jack-up, is taken on by the total number of couplings. Whether there will be a large increase in loading on a small amount of couplings or a small increase in load on a large amount of couplings.
  When load is equally distributed through a structure, the general design strength of the coupling can be less compared to non-equally distributed load. The described distribution is also valuable considering the redundancy of the structure. In case of failure of one or more couplings, the additional load has to be taken by the others.

Currently there is no method available to can provide a fast analysis on different load cases and configurations in the early design phase.

1.5. Research Objective

The problem definition requires the development of a methodology capable of analysing couplings within a modular deck structure in different structures and load scenarios in the early design phase. The methodology is put into practice in a model that may be used for the design of modular jack-ups.

DAMEN has attempted such a study before using beam theory to simulate the structure. However, this was discontinued. From the knowledge gained from this study the idea was proposed to investigate using superelements.

This model is part of an overall analysing model for jack-up designs. Consequently, the developed model must be compatible with this overall model. Summarizing, the requirements for this methodology are:

- To be capable of analysing the endured loading by couplings
- Provide fast analysis
- Consider different configurations
- Consider different load scenarios
- Be compatible with existing software/tools
- Provide valid results

From this point the overall thesis is divided into two parts:
Part one, consisting of the development of the methodology and investigating the possible use of superelements.
And part two, a case study on a conceptual jack up design. In this study the influences of different external loading will be investigated.

1.6. Scope

The thesis is aimed on structural analysis of (conceptual) jack-up designs. Considering the scope of this thesis the following can be stated:

- The analysis is performed on jack-up designs in standing conditions. Jack-up operational phases regarding transit and preloading are not part of this study.
- The conceptual designs are built up from modular barges. This results in the designs being rectangular and carried by four legs.
- The analyses are based on linear (quasi-) static relations.
- The loads taken into account are gravity, payload and environmental loading due to waves, wind and current.

The following objects are considered out of scope:

- The environmental loading on the structure is attained from external software. The calculation of these loads therefore does not fall under the scope of this thesis.
- The modelling of soil beneath the jack-up does not fall under the scope of this project. The leg soil interaction is considered as a mechanical support, such as a clamped or pinned connection.
- The focus of the methodology lies on forces and moments, stresses are not in the scope of this thesis.

1.7. Research Questions

For the different parts of the thesis the following research questions are formulated:

Part 1:
The first part consists of the development of a methodology and investigates the possible use of superelements. Within this part of the thesis the following research question is examined:
How can superelements be used in the development of a methodology to analyse couplings in a modular deck structure in the early design phase?

To help answer the research question of the first part, the following sub-questions have been defined.

- *What is a superelement?*
- *How can the methodology be put into practice in a model?*
- *How can such a model be validated?*

Part 2:
The second part consists of a case study on a predetermined modular jack-up design. In this study the influences of different forms of external loading will be examined.
This part is split up into different sections considering specific topics on gravitational loading, payload, environmental conditions, punch-through and an overall assessment of the predetermined design. For each section research questions have been formulated:

Gravity
- *What is the influence of the number of couplings on the loading of the structure?*
- *How is the load distributed over the set of couplings in the configuration?*

Focusing on the simplest case in which the structure is only loaded under its self-weight, insight can be attained in the general load distribution in the structure. From here the effect of using different amounts of couplings can be examined.

Payload
- *What is the influence of the location of payload on the loading of the structure?*
- *How is the load distributed over the set of couplings in the configuration?*

The designed jack-ups are often equipped with a mobile crane for lifting operations. The location of this payload may differ for operations which raises the question about the effects of these changes on the couplings.

Environmental conditions

- *What is the influence of the angle of attack of environmental conditions on the loading of the structure?*
- *How is the load distributed over the set of couplings in the configuration?*
- *What is the optimal environmental angle of attack for a JUP2420?*
- *How does the wavelength influence the loading of the structure?*

The presence of environmental conditions introduces horizontal external loading into the structure. These loadings occur in different magnitudes and can come in at different angles. For design purposes it is of interest to know how horizontal loading on the structure (and mainly the legs) may influence the loading of the couplings within the structure. The focus is set to the angle of attack of environmental loading. In addition different wavelengths and periods are examined.

Punch-through

- *How can the developed model be used in the simulation of a punch-through?*
- *How does a punch-through influence the loading of the structure?*
- *To what extent is the current model valid for analysing a punch-through?*

After development of the model and methodology it is investigated whether the specified model is useful for the simulation of a punch-through. This can provide knowledge on the effects such event on the internal forces in the structure.

Overall assessment

- *Is the conceptual design of the JUP2420 sufficient for operation considering the design wave and use of a mobile crane?*

As the case study is performed on a predetermined conceptual design, the last study is focused on determining whether the JUP2420 design is sufficient to withstand the operational loadings examined in the cases above.

Leg implementation

- *What is the influence of the stiffness of the connection between leg and hull on the loadings endured by the couplings?*

Considering that the leg-hull connection has a significant influence on the outcome of the load cases, in this case it is examined how reducing the stiffness of the connection between leg and hull can influence the maximum loading endured by the couplings.

By answering these questions, insight can be obtained on the loading endured by couplings within a standing modular jack-up structure.

1.8. Approach & Thesis Outline

To answer the research questions, research has been performed consisting of a few different stages. These stages are divided in the following chapters:

- *Chapter 1: Introduction*
  The introduction gives background information on the subject. Afterwards, the problem description, research objective and approach is discussed.

- *Chapter 2: Methodology*
  This chapter describes the requirements set up for the methodology. Afterwards, the working principle and scope of the methodology are discussed.

- *Chapter 3: The Model*
  The making of a model makes it possible to simulate physical aspects of a jack up structure.
  In this chapter elaboration is given on a model developed to describe the structural aspects of a deck structure.

- *Chapter 4: Validation of the Model*
  The model can only be of use when it can be validated. Therefore the model should be validated using proven results. This chapter discusses the validation study performed on the model.

- *Chapter 5: Case Study*
  To provide answers to the second part of the research question, a case study is performed on a deck structure. This case study is based on a design developed by DAMEN.

- *Chapter 6: Conclusions and Recommendations*
  A conclusion is written for the entire research and recommendations are provided for further research and for DAMEN.

By doing the research in this manner, structure and validity is attained within this thesis. As a result it will be possible to provide a robust methodology which is of use to the company as well as provide scientific insight in the loading of modular structures.

2

Methodology

2.1. Introduction

In this chapter the methodology is discussed. First the current situation is described after which elaboration is given on the requirements of the methodology. Next the set up of the developed methodology is given, showing the working principle and the cornerstones it is built on. Further details of the methodology are found in chapter 3 where it is put into practice in a model.

2.2. Current Situation

As mentioned in chapter 1 the methodology is for the early design phase, where often different configurations are considered to reach a final concept design.
These concepts are analysed using software based on the Finite Element Method. More elaboration on this method follows in the following sections, but in essence this requires the manual modelling of each different configuration. This process can be costly and time consuming. Analysis of a single load case on a jack-up design using conventional FEM takes days or weeks.

2.3. Requirements for the Methodology

Before starting on a methodology, the requirements listed in section 1.5 are elaborated on separately.

Analysis of Couplings
The main product of the analysis must be the loads endured by the couplings connecting the DMBs.
When in operation, the deck of DMBs will be hanging in the air supported by four legs at the corners. Under its own weight, possible payload and environmental loading these DMBs have the tendency to move with respect to one another (figure 2.1a). These movements are counteracted by the couplings.
This results in corresponding shear and tensional loads in the couplings (figure 2.1b). From former studies on these modular configurations it was found that the connection points where the couplings and DMBs come together are the limiting parts of the design [23].

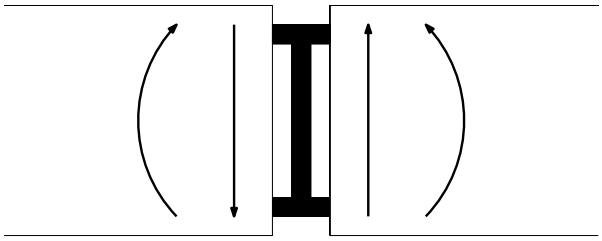

(a) Movements of the DMBs

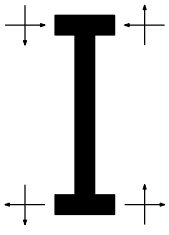

(b) Loads endured by the coupling

Figure 2.1: The main movements and loads focused on within the jack-up

Speed
Comparing to the analysis of a single load case in an hour, the aim is to decrease this time to only minutes for several load cases on different structures.
As mentioned in chapter 1, the methodology will mainly be used in the early design phase, where often a tender has to be won. Therefore, it must be able to do fast analysis on one or more conceptual designs.

Consider Different Configurations
The methodology must be easily applicable on different configurations.
When considering the options for a tender, often more than one concept is created. By analysing and comparing the different initial configurations, an optimal final concept can be attained. Generally different configurations, means different combinations of the standard modules. In addition the methodology must also (if necessary) be applicable to different standard components.

Consider Different Load Scenarios
For the analysis to be complete, external loads must be taken into account. Often these are defined in the customers requirements such as the location and environmental conditions in which it must operate as well as possible payloads. As this may differ largely per project/tender, the methodology must be able to take into account these different possible load scenarios.

Compatibility
The methodology in this thesis focuses specifically on the internal loads in the deck. However, it must be compatible with other software/methods used within DAMEN. The development of this methodology does not stand on is own, as it is part of a larger project. The overall project is aimed on full analysis off jack-ups taking into account a wider range of design aspects. Among other things there are analyses of overturning moments and leg buckling.

Validity
The methodology developed must provide an alternative for the conventional FEM analysis.
Meeting the requirements of speed and considering different configurations and load cases must not interfere with the validity of the analysis. The last requirement states that through the development of this methodology, the outcome should comply with similar cases in conventional FEM analysis.

2.4. Jack-up Configuration

From the set of requirements defined above a methodology is developed and implemented into a model mainly based on the software package Matlab. In this section, by elaboration on the model, the working principle is discussed.

The starting point of the model is to create an environment in which configurations can be generated on demand. A configuration should describe the structural characteristics of the jack-up deck, providing a base for analysis. This approach is based on two main characteristics of modular construction.
First there is the repetitive nature of components. The base for modular construction is a set of standard components that is used repeatedly in a single design.

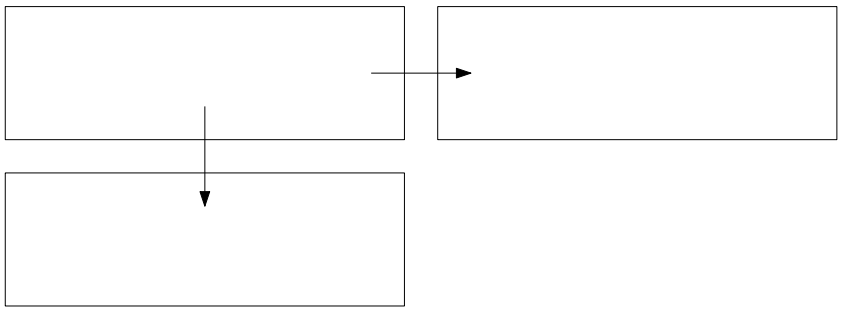

Figure 2.2: Schematic of the possible connections of DMBs

Secondly, the way these components can be combined is fixed. The connection of the DMBs is limited to two orientations, either in the transverse or in the longitudinal direction (figure 2.2).
Additionally, the jack-ups considered are four legged and rectangular. Taking into account these characteristics, the designing degrees of freedom for the deck structure are the following:

Considering the modules:
- The design of the DMB
- The design of the coupling

Considering the structure:
- The number of DMBs in the longitudinal direction
- The number of DMBs in the transverse direction
- The number of couplings used to connect them

The methodology focuses on the structure in general. As the design of the DMB and the coupling do not fall within the scope of this methodology, they are considered input for the model. As stated in the requirements however, the methodology must be able to use different DMBs and couplings in the future.
For the model to generate configurations, it must be provided with the 'building blocks' it may use to construct the deck. On the use and implementation of these blocks more elaboration will follow in chapter 3.

The base of these configurations is the Finite Element Method as it is well suited to describe the physical characteristics of complex structures. Even though this method can be slow and costly, the use of superelements should solve these issues. More elaboration on this can be found in the following section.

2.4.1. Finite Element Method

The Finite Element Method (FEM)[11], or Finite Element Analysis, is a method for numerical solutions of a field problem. A field problem in mechanics can be seen as a problem in which one seeks the distribution of one or more dependent variables in a structure. In the current case one could think of the distribution of displacements through a DMB or the complete jack-up.

In the jack-up deformations occur as a result of (external) loading. The stiffness of the structure offers resistance to these deformations resulting in counteracting (internal) loads.
The relation between stiffness and loading of a structure can often be found analytically. However, when structures become more complex in terms of geometry and material composition, this becomes very complex.

Finite elements can be seen as (small) pieces of a structure. These elements describe parts of the structure by means of stiffness. The elements are connected through nodes and all together describe the stiffness of a larger system. The arrangement of elements is called the mesh of a structure. Figure 2.3 shows an example of a plate discretized into finite elements.

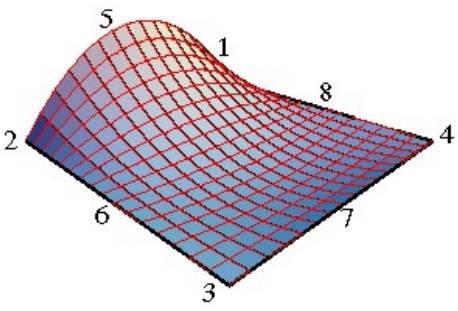

Figure 2.3: Example of a discretized plate [14]

Where the description of the overall structure may be complex, finite elements are meant to be of a more simpler nature. An element describes the stiffness relations of the nodes it contains. After combining all elements, a system of algebraic equations is attained containing the relations of all nodes in the system.
The solution of the displacements in the structure can be attained by solving this set of equations. In practice this means that the displacements throughout the structure are approximated by solving element by element. The base equation for this displacement analysis is the linear stiffness relation (equation 2.1). In this equation K represents a matrix containing the stiffness coefficients of all nodes within the system. u consists of a vector containing the nodal displacements and F_{ext} is the external load vector.

$$K_{system} \cdot \bar{u} = F_{ext} \tag{2.1}$$

Here the methodology deviates from the conventional use of FEM. The procedure of describing a structure is split up in to two main topics: *creating superelements* and *generating a configuration.*

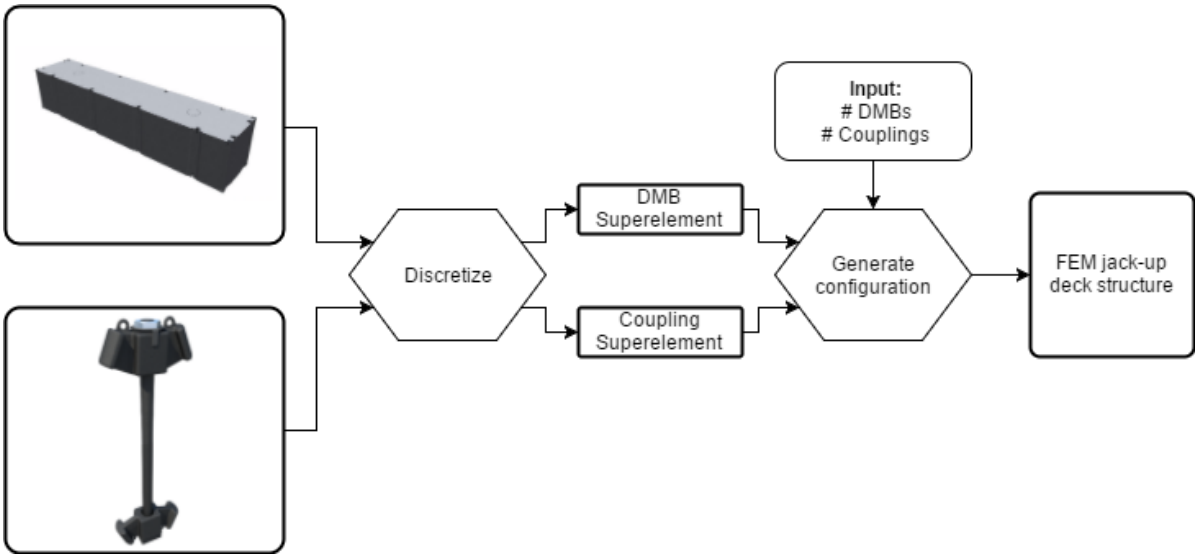

Figure 2.4: The discretizing procedure

Instead of manually creating a complete structure the discretization takes place on a component level. The DMBs and couplings are constructed and discretized into individual FEM structures. These FEM structures are the building blocks used to generate configurations (figure 2.4). For these components superelements (SE) are used. In essence the component, which consist of many finite elements is considered a single individual element.

2.4.2. Superelements

The following sections elaborates on superelements. First the concept is described followed by a segment on how these elements can be attained and used.

The Concept
When working with the Finite Element Method, superelements can be used. It can be seen as "a grouping, of finite elements that, upon assembly may be regarded as an individual element for computational purposes"[14]. These purposes may be driven by modelling or processing needs.
The term superelement is quite broad in FEM, as it comes in different ways and forms. A SE can be formed from two different approaches; "bottom up" or "top down".
In the "bottom up" context a superelement is a resulting element from grouping smaller 'simpler' elements together. In the "top down" context, superelements can be seen as large pieces of an overall structure. This distinction between different types of superelements can be defined in the following classification: Macroelements and Substructures.

Macroelements: Superelements assembled from a set of smaller elements. These elements usually resemble structural components, but are fabricated with simpler components. Main reasons for this procedure is simplification of preprocessing. Using FEM software, often a rectangular plate is meshed using quadrilateral (four-sided) elements. In reality 'behind the scenes' such mesh actually consists of several triangular elements (Figure 2.5). For the user however, this may not be important and use of quadrilaterals can be more convenient. This is an example of a macroelement.
In the same way a simple box structure, constructed from several plate elements can be defined as a SE. For larger structures with a repetitive nature, this can save time on the modelling

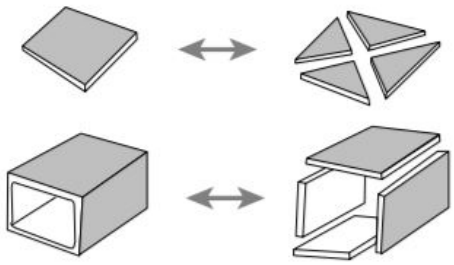

Figure 2.5: Macroelements[14]

Substructures: These are groupings of elements that together describe a well distinguished part of a structure, typically these are formed by cutting a complete structure into (if possible repetitive) components. Figure 2.6 shows a wing in the form of a substructure. Substructures can be formed on different levels of an overall system.

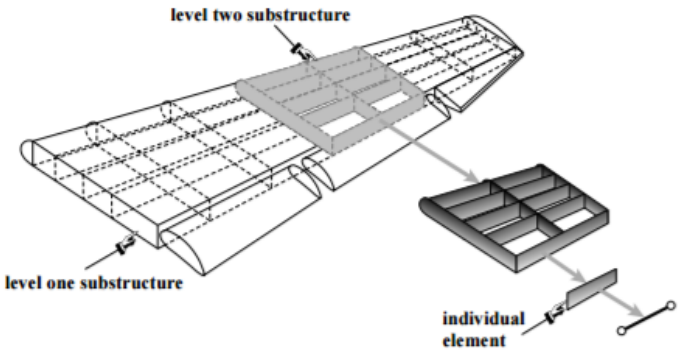

Figure 2.6: Substructuring[14]

The distinction between a macroelement or a substructure is not always straightforward. There are no precise rules for these categorizations. As mentioned above, the main difference lies in the perspective used to define it.
This unclear distinction might also be do to the fact that in practice it does not really matter. In both cases a grouping of elements is considered as one.

This idea of substructuring comes from the 1960s. At that time aerospace engineers started breaking down large structure into parts, such as complete airplanes or spacecrafts built up from stages (figure 2.7).
The base of this superelement concept was founded on three motivations. Firstly it provided more capabilities in working on different segments of a product in parallel. In aircraft design for example, a group of (specialized) engineers could focus on the wings of an airplane, while a different group covered the fuselage. These groups could separately keep improving and refining the designs of the segments as long as the interface areas where the wing and the fuselage met stayed relatively the same[14].

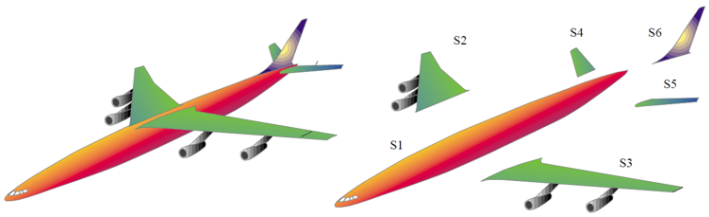

Figure 2.7: Substructuring of an airplane[14]

Secondly, the repetitive nature of certain parts of a design was used in their advantage. Considering again the airplane. Many components of the design are nearly identical to each other. Simply looking at the symmetry over the fuselage the wings on both sides are similar only mirrored. Using this repetitiveness in modelling and designing saves time.
And lastly there was the issue of computational limits. In the early days, computers were limited with respect to memory and speed, making it difficult (and very expensive) to store and analyse large complex structures.

In the methodology the building blocks are set up as superelements. The following section discusses how the FEM structures of the DMBs and couplings are modified.

Creating Superelements
To attain a SE first a distinction must be made in the degrees of freedom.
The nodes in a FEM structure describe degrees of freedom (DOF) in which displacements may occur. Considering the nodes of the original FEM structure a distinction is made between internal freedoms and boundary freedoms[14]. A node which is only connected to other nodes of the same structure describes only internal freedoms, and is therefore called an internal node. Nodes on the interface of the SE and another FEM structure also describes boundary freedoms and are therefore called boundary nodes. Figure 2.8 shows an example of the tail wing of an airplane defined by internal and boundary nodes. A superelement aims to describe a structure using only the boundary degrees of freedom. By doing so the total amount of nodes in the final structure reduces drastically, which should mean large gains on the calculation time. Taking the DMB as an example, the original FEM structure consists of more than a 100.000 nodes and elements is reduced to a single element with less than 100 nodes.

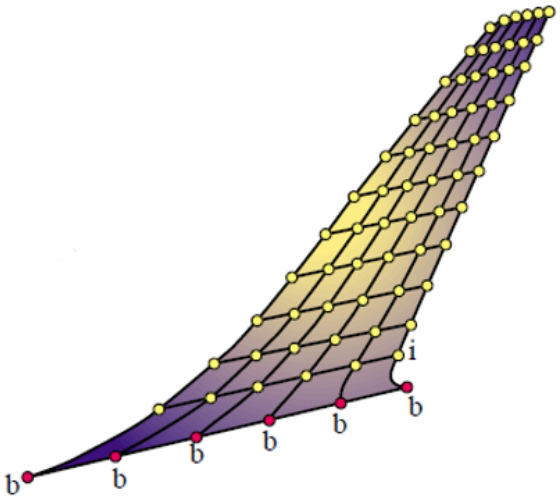

Figure 2.8: A tail wing structure defined by both boundary nodes (b) and internal nodes (i)[14]

In mathematical terms this means that a large stiffness matrix containing the relations of all nodes in the structure is replaced by a matrix containing only the external degrees of freedom.
This can be achieved in several ways. Either by modification of a full stiffness matrix or directly by constructing the superelement matrix from scratch using the unit displacement method [16].

With the full stiffness matrix as starting point, mathematical operations (such as Gaussian elimination[11]) can reduce it to the SE form.
In this study the unit displacement method is used. With the FEM structure of the DMB (and coupling) already present in the software package NX Nastran, the superelement matrix is attained directly. Using the example of a simple 1D problem (figure 2.9) this method will be discussed.

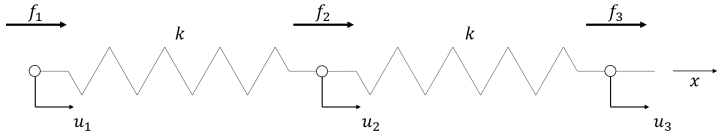

Figure 2.9: Schematic of a 1D system consisting of three boundary nodes

The force displacement relations for this system are described by the stiffness relation (eq. 2.1) in matrix form. (equation 2.2).

$$\begin{bmatrix} k_{11} & k_{12} & k_{13} \\ k_{21} & k_{22} & k_{23} \\ k_{31} & k_{32} & k_{33} \end{bmatrix} \cdot \begin{bmatrix} u_1 \\ u_2 \\ u_3 \end{bmatrix} = \begin{bmatrix} f_1 \\ f_2 \\ f_3 \end{bmatrix} \tag{2.2}$$

In equilibrium the load in a node is related to the displacement of all three nodes. Using this method one node is given a unit displacement while all others are fixed (0). This simplifies the relations to equation 2.3. From the force f_1 that is attained by this procedure one finds the value of k_{11}. As well as the values for k_{21} and k_{31} using respectively f_2 and f_3. One may consider the value of $k_{i,j}$ to be the same as the force at node i due to a unit displacement at node j while keeping all other nodes fixed.

$$\begin{aligned} k_{i,1}u_1 + k_{i,2}u_2 + k_{i,3}u_3 &= f_i \\ u_1 &= 1 \\ u_2 = u_3 &= 0 \\ k_{i,1}u_1 &= f_i \end{aligned} \tag{2.3}$$

This procedure is repeated for all nodes, attaining all coefficients of the stiffness matrix.

The DMB and coupling are formed into superelements using this method.Although these systems are more elaborate in the amount of nodes and degrees of freedom, the principle holds. Hereby noted that considering a 3D problem with all 6 DOFs one must apply the procedure for each degree of freedom. So to find all coefficients of a SE, the procedure is carried out as many times as there are nodes x 6 DOFs.
In the remainder of this thesis these DOFs per node are defined as nodal degrees of freedom. For example: an element consisting of 4 nodes contains (4 x 6) 24 nodal degrees of freedom.

2.4.3. Generation of the Configuration

A jack-up deck configuration is generated through combining (local) stiffness matrices of the elements into a global matrix describing the whole structure.
Mathematically this is firstly based on setting up a global nodal coordinate system from input parameters. This system contains the locations of all nodes in the final structure. One could think of this procedure as setting up a 'skeleton' of the jack-up.
An empty global stiffness matrix is defined based on this system. Through alignment of the local nodes in a SE with the global nodes of the system, the local stiffness matrices are implemented. When (super-)elements overlap in the system the resulting stiffness coefficients are the summation of both local coefficients in this location.

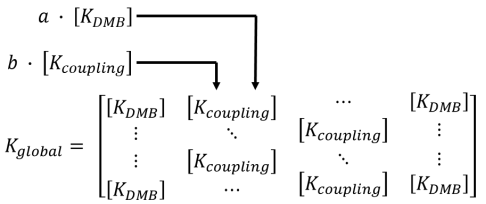

Figure 2.10: A simplified representation of the implementation of local stiffness matrices into the global stiffness matrix

Implementation of Legs
Even though the legs in a jack-up are also of repetitive nature, it is chosen not to develop these parts of the structure as superelements. The reason lies in preserving flexibility. Where the design and geometrics of the DMBs and couplings can be considered fixed, the dimensions of the legs may differ depending on the requirements of the jack-up.
Therefore the legs are constructed using beam elements. These beam elements are based on Euler-Bernoulli Beam theory [11]. This theory describes the relation of the deflection of a beam versus an externally applied load. It is applicable to situations in which the load is applied to the structure in lateral direction.

The legs of these modular structures are cylindrical with no specific spudcans. The main reason to implement legs is to take into account the effect of environmental loads on the deck. As the environmental loading from wind, waves and current is lateral to the legs, Euler-Beam theory is suitable.
This theory provides some limitations. Opposing to other theories, like the Timoshenko beam theory, Euler-Bernoulli does not take into account transverse shear strain. Because Euler-Bernoulli beam theory is based on the assumption of pure bending. However, when the length over width ratio of a beam is sufficient these shearing effects are of minor importance. In general the water depth beneath a jack-up will be enough with respect to the leg diameter to make Euler-Bernoulli beam theory valid.
Using input parameters (length, width, material) a leg is generated into a set of beam elements. The leg is discretized for the implementation of environmental loading discussed in the following section.
The generated legs are fitted into the global stiffness matrix in a similar manner as the superelements (figure 2.10). More elaboration on the implementation of this method into the model is given in chapter 3.

In this methodology influences of the P-delta and leg inclination effects are not taken into account. The P-delta effect is a destabilizing moment on the leg. As a leg experiences lateral loading it will deflect. As a result the COG of the leg is no longer in line with the legs footing, resulting in a moment of gravity times horizontal displacement of COG.
Leg inclination effects are a result of fabrication tolerances for the legs, and gaps in the leg guides.

2.5. External Loading

The methodology aims to analyse the couplings in different loadcases. The first step in this analysis is based on displacements of the structure due to external loading.
The external loads considered in this methodology are gravity, payload and environmental loading.
To define the external load vector in equation 2.1 the following must be stated for each external loading:

- The magnitude of load.
- The direction of the load.
- The node(s) it is applied on.

Gravity
A large contribution to sagging of the structure comes from gravity. Only the weight of the DMBs is taken into account as focus of the analysis lies on the deck structure.
The weight of the legs is not taken into account, as these have insignificant influence on the loading of the couplings. The weight of a DMB is evenly distributed as a downward load over the nodes describing it.

Payload
A payload is defined manually by the user. Using the weight of the payload and its footprint it is allocated to nodes present at the deck surface.

Environmental Loading
The environmental loading consists of horizontal forces exerted on the structure. Through defined weather conditions containing significant wave height, current and wind speed these loads are determined using Morrisons equations. This procedure is executed in another part of the overall jack-up project as mentioned in chapter 1 and is therefore considered an external input. This input consists of a discretized set of data of the distributed load over the legs and structure.
In addition to the static loading, the effects of inertial loading are taken into account by applying an inertial loadset[17]. This is a single point load in the centre of gravity of the structure which is determined based on the minimal and maximal loading experienced through a load cycle.

2.6. Constraints

To finalize the setup of the analysis, the system is constrained. This is done by setting certain nodal degrees of freedom to a prescribed displacement of zero. These constraint are applied on the nodes of the legs that lie at half of the penetration depth. SNAME prescribes this practice in modelling as the approximate rotation point of the legs if no detailed soil information is present[25]. By default these nodes are modelled as simple supports, constraining the translational displacements in x-, y-, and z- direction. The model also accomodates optional clamping of the legs, constraining all 6 DOFs.

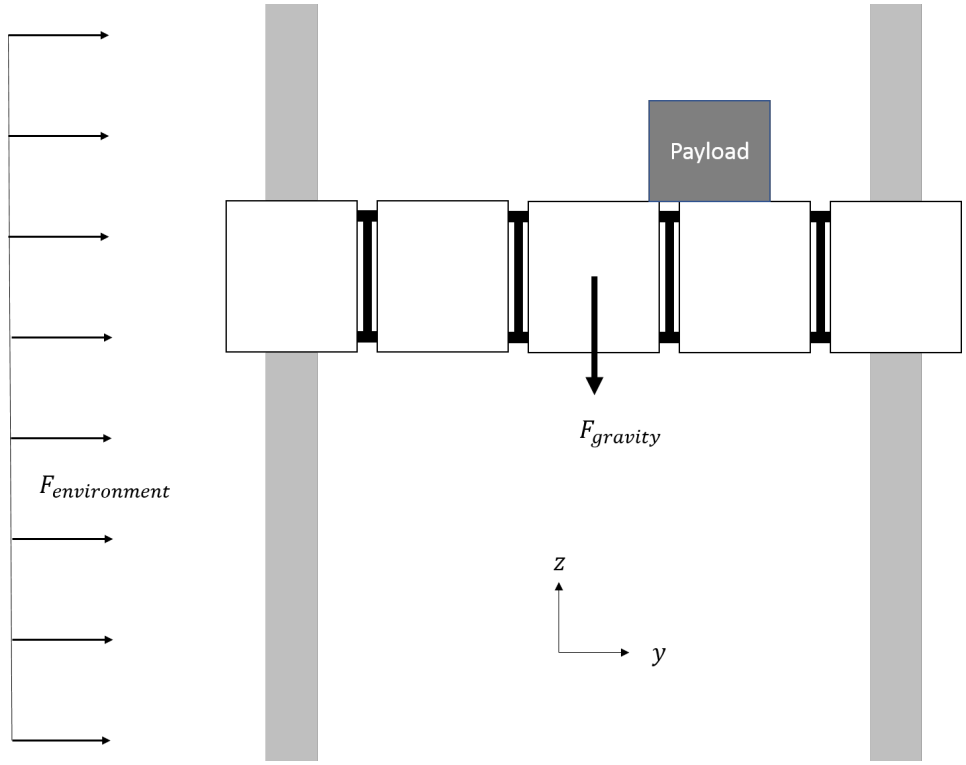

Figure 2.11: A simplified 2D representation of the complete configuration

2.7. Analysis

The aim of the methodology is to analyse the loading endured by the couplings between the DMBs. This analysis is performed in two steps.
First the full set of equations describing the system is solved for the external loading. Modification of equation 2.1 provides equation 2.4 from which the nodal displacements of the system are attained.

$$\bar{u}_{sys} = K_{sys}^{-1} \cdot F_{ext} \tag{2.4}$$

This solution shows the displacement of all nodes in the system. From this result the displacements of couplings are extracted.($u_{sys} \rightarrow u_{coupling}$). In the second step the loads endured by the couplings are determined using the coupling displacements and local stiffness matrix (equation 2.5)

$$F_{coupling} = K_{coupling} \cdot \bar{u}_{coupling} \tag{2.5}$$

2.8. Summary

The essence of this methodology is the modelling of a SE based jack-up structure, aiming to analyse the loads endured by the couplings. Using superelements, an environment is created in which deck configurations can be generated.
Through the systems stiffness matrix and defined external loading a (quasi-) static analysis is performed, providing the displacements of the structure.
These external loads consist of gravity, environmental loading and payload.
The loads endured by the couplings are determined through the linear relation between the coupling's nodal displacements and local stiffness matrix.
The creation of the environment in which one can generate load cases and configurations, whilst being sufficiently detailed, contributes to the flexibility of the methodology. Furthermore the combination of this environment and the use of superelements is expected to save a lot of time in both setting up an analysis and the calculation time.

3

The Model

3.1. Introduction

Chapter 2 elaborated on the working principle of the methodology. This is put into practice in a model. This chapter describes the outline of this model. First an overview is given of the model after which, in the paragraphs following, the different stages of the model are elaborated on in more detail.

3.2. Overview of the Model

The full process of the analysis is divided into several sections.
First there is the generation of a jack-up configuration and load case. Secondly a displacement analysis is performed based on the stiffness relation (eq: 2.1). The process ends with determining the loads endured by the couplings based on the displacements.
The layout of the model is divided in the following sections shown in figure 3.1.

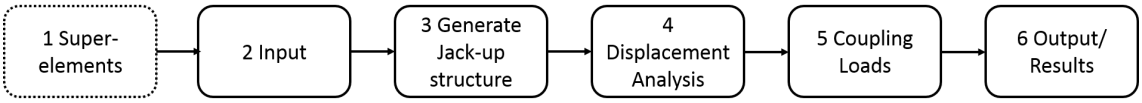

Figure 3.1: Flowchart of the model

Starting from the second section, the model is given input on the jack-up configuration and load case. Next, a basic jack-up design is generated that meets the input parameters. The fourth section consists of setting up the load case by constraining the jack-up and applying external loading. Then by solving the system the displacements of the structure are found. Using these displacements, the loading endured by the couplings is determined.

The first part of the model covers the construction of the superelements from the DMB and coupling designs. As mentioned these components are considered input for the model and their specific design does not fall within the scope of the model. Therefore, the first section in which the SEs are defined and constructed is differently connected to the overall model. As the barges and couplings are taken from a given design, modelling them into SEs is required only once. Afterwards the model can be used repeatedly.
Only when changes are made in the design of the main components, section one must be repeated, redefining the new superelements.

In the following paragraphs, the different parts of the model are elaborated on separately.

3.3. Superelements

This section elaborates on the process of developing superelements. In chapter 1.2 some insight is given on the real system and its components. The creation of SEs from the main components is discussed here.

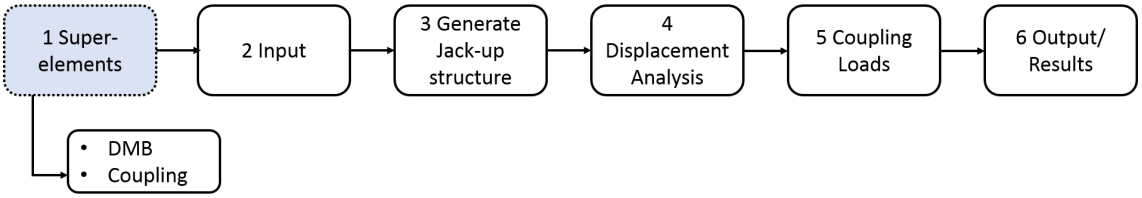

3.3.1. The DMB

Even though the DMB is a standard product, there are different in sizes. In the model the full size DMB of approximately 12 meters length and 2.4 meters height is chosen in consultation with the C&MC department (table 3.1). Optionally, in the future different DMBs can be used.
As these DMBs are the cornerstones of modular building, existing FEM drawings are acquired from the department (figure 3.2).

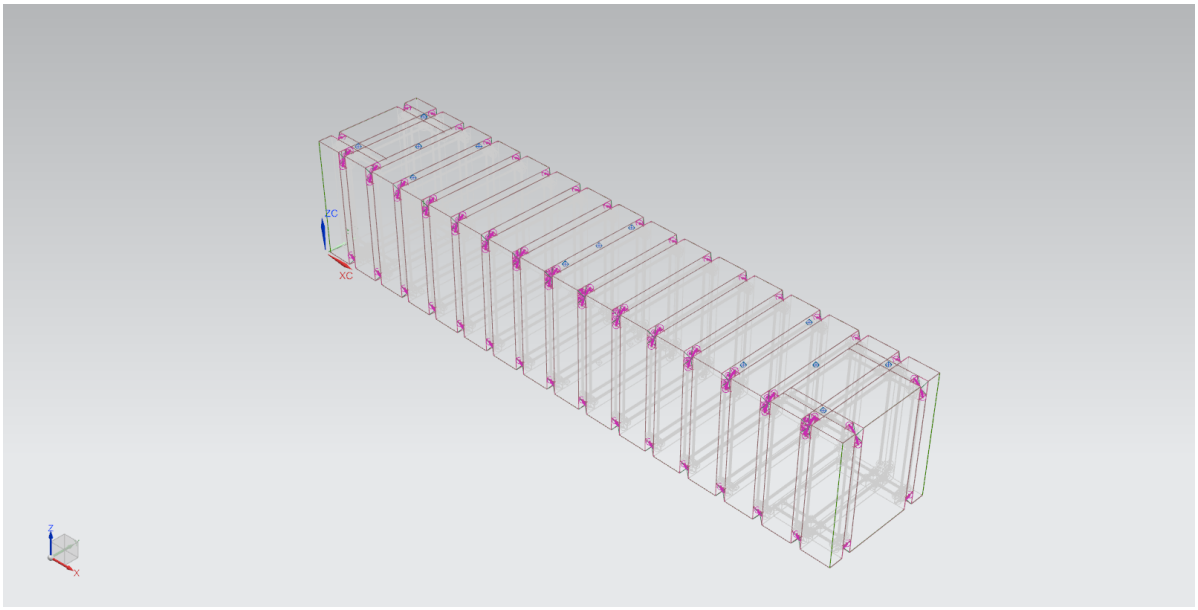

Figure 3.2: FEM Representation of a 12 meter DMB

As these barges are firstly designed for floating products some modifications are made. One of the flexibilities desired of the methodology was the use of couplings than the standard number of 4 on the long end of a barge. Therefore, modifications on the original barge design make it possible to link up to 12 couplings on the long end. This can be seen by the added locks visualised in purple in figure 3.2.
For the DMBs located at the corners of the final structure a modified DMB is used which houses additional structural components for the connection with the legs.

Table 3.1: Specifications of used DMB

DMB		
Length	12	m
Width	2.3	m
Height	2.4	m
Material	Steel	
E-modulus	$207 \cdot 10^3$	N/mm^2
Weight	18	tons

To create a superelement, the extensive DMB FEM structure is reduced to a single element with a total of 82 nodes. Most nodes correspond to the locks for the couplings (68) and an additional 26 (shown by the blue points in figure 3.2) nodes have been taken on the top and bottom of the DMB for implementation of external loading in a later stage of the process.

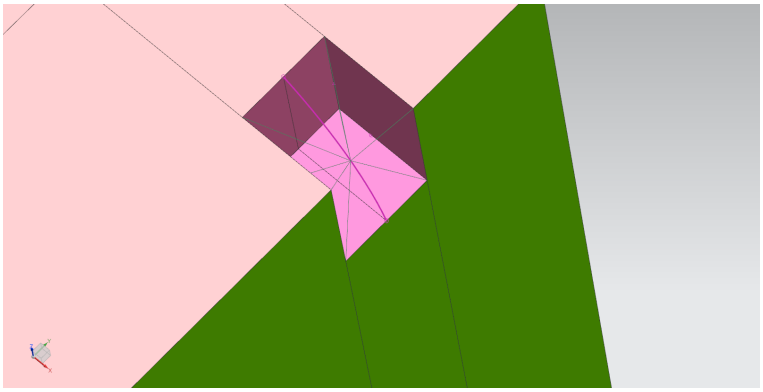

Figure 3.3: Visualisation of the RBE element implemented in a lock of the DMB (NX Nastran)

One of the challenges is defining the outline of a lock consisting of several elements into a single node in the SE. From earlier FEM studies on the couplings a point in the centre of the lock was determined where stress concentrates when the coupling is loaded. This location is defined in the original FEM structure as the single node needed. With the use of a rigid body element (RBE)[11] a relation is set up between the original elements of the lock and the (new) single node. An RBE is actually not a real element, but a constraints relation between nodes. By setting up this RBE one states that the displacements of certain nodes is dependant of the displacement of the main node. In figure 3.3 the RBE element is shown as a *web* connecting parts of the lock structure to the single SE node in the centre of the lock.

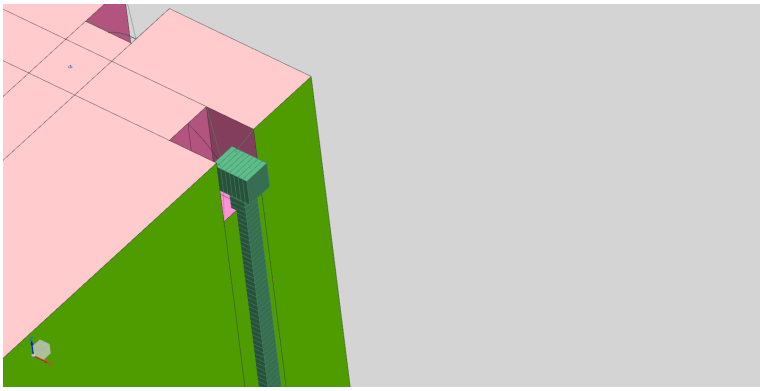

Figure 3.4: Visualisation of the connection between a coupling and DMB (NX Nastran)

A local coordinate system is attained with a numbering sequence used for the nodes in play. The system set up is visualised in figure 3.5. This sequence is used to sort the stiffness matrix. Understanding of the local coordinate system is necessary to implement the DMBs into the global stiffness matrix in a later stage.

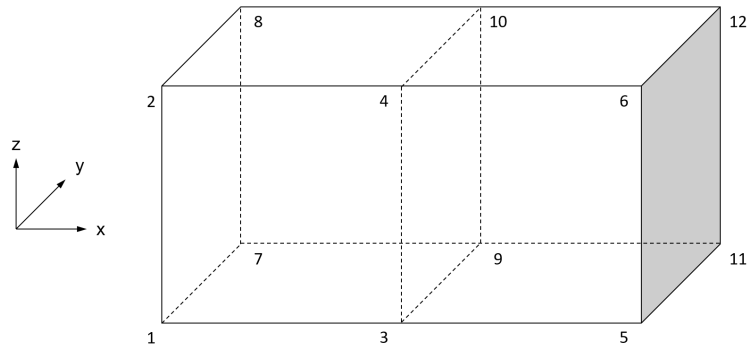

Figure 3.5: Local node numbering sequence

After defining the desired layout of the SE, the stiffness matrix describing the DMB through the defined nodes is attained. As mentioned in chapter 2 for this the unit displacement method is used. A set of simulations (# SE nodes x 6 DOF) is performed in the FEM software. In each simulation all DOFs of the 82 nodes are constrained except for one. The free DOF is given a unit displacement and the simulation is solved. With the resulting reaction forces in the constrained nodal DOFs a single column of the local stiffness matrix is attained. This is repeated for all nodal DOFs.

At the end of this stage the final output of the FEM software that is used in the Matlab model is:

- The local stiffness matrix of a DMB described by 82 SE nodes.
- An additional local stiffness matrix corresponding to the DMB that will connect to a leg.
- A nodal information file containing the coordinates and node numbering sequence used in the local coordinate system of the SE nodes.

3.3.2. Coupling

For the modelling of the coupling a simplified structure is made based on the main dimension of the original design. These main dimensions are the the length and cross section of the main rod and of the clamps at both ends. As the connection between DMB and coupling is taken as a single point the inclinations and contact area of the coupling is not taken into account. The connection between the two is modelled using a rigid body element as mentioned in the paragraph above.

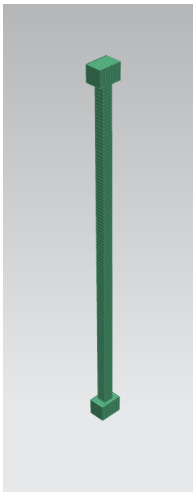

Figure 3.6: Representation of a coupling in NX Nastran

The couplings characteristics are described through 4 nodes at the outer ends of the two clamps.
The local stiffness matrix of this SE is therefore vastly smaller than for the DMB. Similar to the DMBs' local coordinate system a numbering sequence is set up for the coupling starting with local node number 1 at the left bottom to 4 at the right top.

Table 3.2: Specifications of modelled coupling

Coupling		
Length main rod	2.176	m
Crossection main rod	60 x 60	mm
Length clamp	140	mm
Crossection clamp	80 x 80	mm
Material	Steel	
E-modulus	$207 \cdot 10^3$	N/mm^2

For the stiffness coefficients corresponding to the couplings matrix the unit displacement method is used again. This way of modelling the coupling and connection provides the ability to find the loads that are transferred from the DMB to the coupling and vice versa.

At the end of this stage the final output of the FEM software that is used in the Matlab model is:

- The local stiffness matrix of a coupling described by 4 SE nodes.
- A nodal information file containing the coordinates and node numbering sequence used in the local coordinate system of the SE nodes.

3.3.3. The NX Simulations and Coding

The process of attaining stiffness coefficients described above must be carried out for all nodes and directions of freedom as mentioned. For the DMB, which consists of 82 nodes, setting up the 492 (82x6 DOF) simulations manually is time consuming. The software package of NX Nastran is able to run simulations based on code in different programming languages. One of these being *Visual Basic for Applications* (VBA) . This language was produced by Microsoft and was initially used for coding in Excel.

By using this language a code is developed. The user provides as input a list containing the node numbers of the SE nodes. For all nodal degrees of freedom (492), two scenarios are defined. A nodal DOF is either set to 0 (constrained) or 1 (unit displacement). This creates two data sets of 492 displacements of 0 or 1 (mm or rad). Secondly the simulations are set up. Each of these consists of 491 displacements of the data set containing zeros (constraints) and 1 single unit displacement. This way 492 simulations are created all with a unit displacement on a different nodal DOF keeping all others constrained. Running this code within the software program of NX Nastran sets up these simulations and solves them simultaneously.

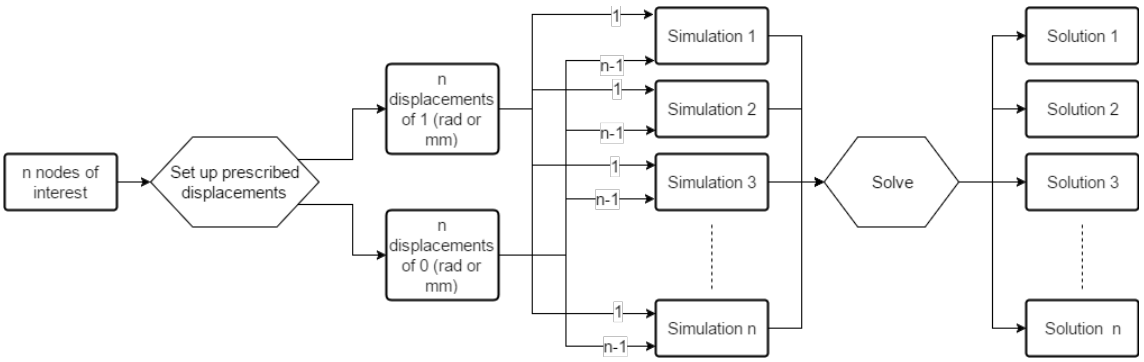

Figure 3.7: Schematic of automated NX simulations for unit displacement method

The output of each of these simulations consists of the reaction forces of all nodal degrees of freedom (but one). As a stiffness coefficient $k_{i,j}$ can be seen as the force at node i as a result of a unit displacement at node j all the reaction forces can be transformed into stiffness coefficients following equation 2.3.

This stage of the overall model produces the building blocks for the generation of a structure in later stages.

3.4. Input

Elaboration is given on the different inputs needed for the MATLAB model.

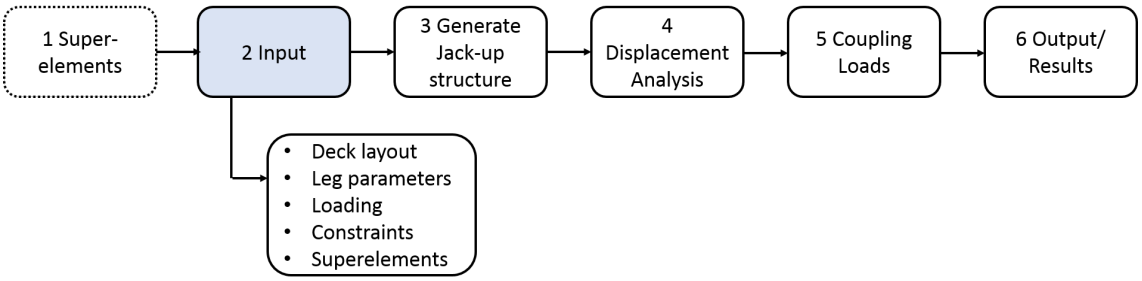

Deck Layout
A configuration must be defined by stating the amount of DMBs in each direction. The JUP2420 mentioned in chapter 1 for example consists of 2 by 8 DMBs in x- and y-direction respectively. Additionally one defines the amount of couplings used on the long end of the DMB as noted in paragraph 3.3. When it is desired to do analysis on the structure related to redundancy one can also remove specific couplings.
The input settings are:

- Number of DMBs in x-direction
- Number of DMBs in y-direction
- Number of couplings on long end of the DMB
- Couplings to be removed

Legs
The legs are constructed within the model. The input parameters needed for this process are:

- Length
- Outer diameter
- Wall thickness
- Youngs' modulus
- Poisson ratio
- Leg mesh size

Loading
The model distinguishes three types of loading; *gravity*, *environmental loading* and *applied loading*. Each of these loads can be switched on or off in this part of the model.
For the gravity input is required on the weight of the DMBs.
The environmental loading is attained from external software. Input for this software is a specified weather type and the angle of attack. More elaboration follows the loading section of the model.
Payload is added as an applied load. The input for an applied load consists of a magnitude, direction and the location(s) on the deck where it is applied

- DMB weight (deck weight)
- Weather type
- Weather angle
- Magnitude of applied force
- Direction of applied force
- Location of applied load

Constraints
The user defines the constraint of the structure as being fully clamped at the seabed or simply supported. By doing so the footings of the legs at the seabed will either be constrained in translational and rotational degrees of freedom, or in translational directions only.

- Definition of either clamped or simply supported at seabed

Superelements
Additional to the input parameters mentioned above, one could state that the building blocks created in section 3.3 are also input.

- The local stiffness matrix of the DMB
- An additional local stiffness matrix corresponding to the DMB that will connect to a leg
- A nodal information file containing the coordinates and node numbering sequence used in the local coordinate system of the SE nodes.
- The local stiffness matrix of a coupling
- A nodal information file containing the coordinates and node numbering sequence used in the local coordinate system of the SE nodes.

3.5. Generate Jack-up Structure

The third section of the model consists of creating a configuration. This section gives insight in the approach followed, developing this part of the model. Starting with construction of the legs, the procedure of implementing the building blocks into a structure is discussed.

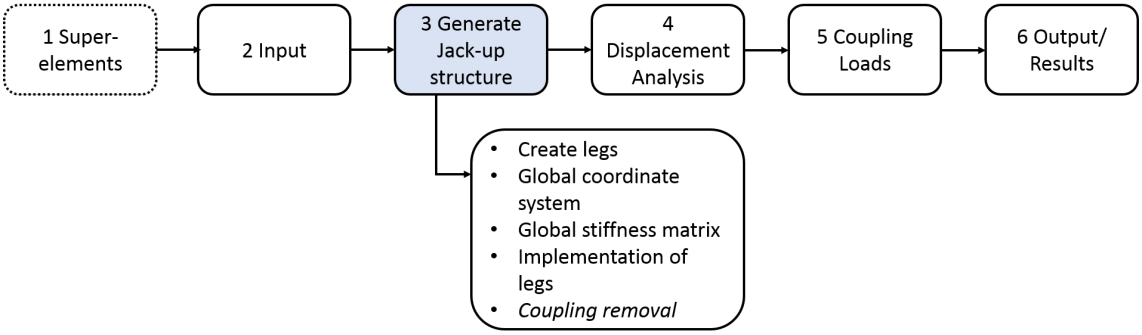

3.5.1. Legs

The leg is chosen to be constructed as a set of Euler-beam elements within the model for flexibility reasons mentioned in chapter 2.
The main parameters of the leg are defined by the user. For now the parameters based on the JUP2420 design are used (table 3.3).

Table 3.3: Specifications of modelled coupling

Leg		
Length	46	m
Diameter	1400	mm
Thickness	25	mm
Material	Steel	
E-modulus	$207 \cdot 10^3$	N/mm^2

Based on these parameters and the mesh size chosen, a local coordinate system and nodal numbering sequence is set up. Taking a leg of 46 meters and a mesh size of 1000 mm results in a leg consisting of 46 elements and a corresponding 47 nodes.
In this automated process it is taken into account that certain nodes need to align with nodes in the DMB structure for the connection in a later stage. Elaboration on this connection follows later in this section.

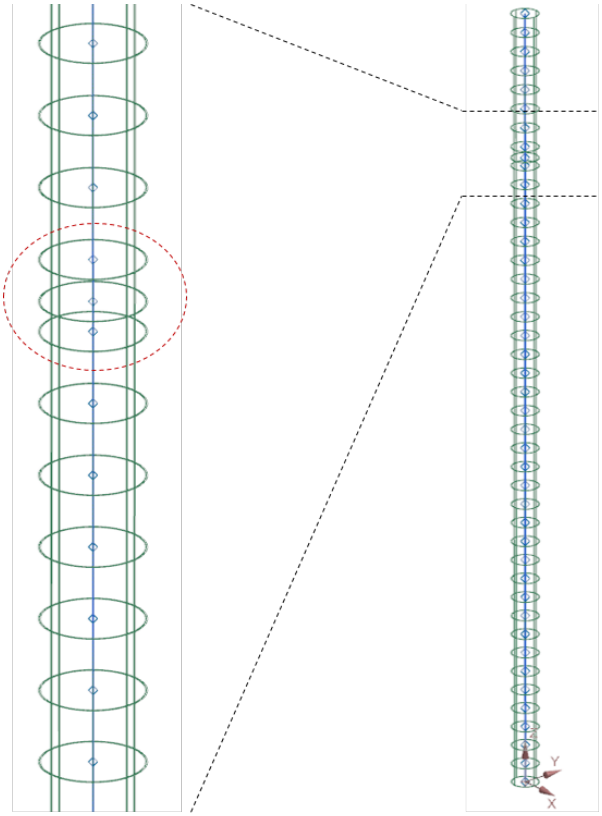

Figure 3.8: Representation of discretized leg (NX Nastran)

The stiffness of each of these elements is set up using Euler Beam Theory as mentioned in chapter 2. From a single beam element described by two local nodes ($\bar{u}_1$ and $\bar{u}_2$), the overall leg can be described combining the beam element stiffness matrices into an overall leg matrix. A representation of the construction of this stiffness matrix of the total leg is shown in equation 3.1. Where most nodes belong to two beam elements, overlapping stiffness coefficients are summed

$$K_{BeamElement} = \begin{bmatrix} k_{1,1} & k_{1,2} \\ k_{2,1} & k_{2,2} \end{bmatrix} \begin{bmatrix} u_1 \\ u_2 \end{bmatrix} \rightarrow K_{Leg} = \begin{bmatrix} \ddots & \ddots & 0 & 0 & 0 & 0 \\ \ddots & k_{1,1} & k_{1,2} & 0 & 0 & 0 \\ 0 & k_{2,1} & k_{2,2}+k_{1,1} & k_{1,2} & 0 & 0 \\ 0 & 0 & k_{2,1} & k_{2,2}+k_{1,1} & k_{1,2} & 0 \\ 0 & 0 & 0 & k_{2,1} & k_{2,2} & \ddots \\ 0 & 0 & 0 & 0 & \ddots & \ddots \end{bmatrix} \begin{bmatrix} \vdots \\ u_i \\ u_{i+1} \\ u_{i+2} \\ u_{i+3} \\ \vdots \end{bmatrix} \tag{3.1}$$

The outcome of this procedure is similar to the other building blocks:

- The local stiffness matrix of the discretized leg.
- A nodal information file containing the coordinates and node numbering sequence used in the local coordinate system of the leg nodes.

3.5.2. Global Coordinate System

With all the necessary components defined the overall configuration is made. First a 'skeleton' is created of the eventual structure. Using the input parameters and the composition of the different components, the outline of the global structure is defined.

A global coordinate system is set up with a corresponding node numbering sequence for the overall structure. The sequence is similar to the one used for the local coordinate systems of the components described earlier

(figure 3.9). The (additional) nodes describing the legs follow after the nodes of the deck. So from a deck consisting of n nodes, the numbering sequence of the legs starts at n+1.

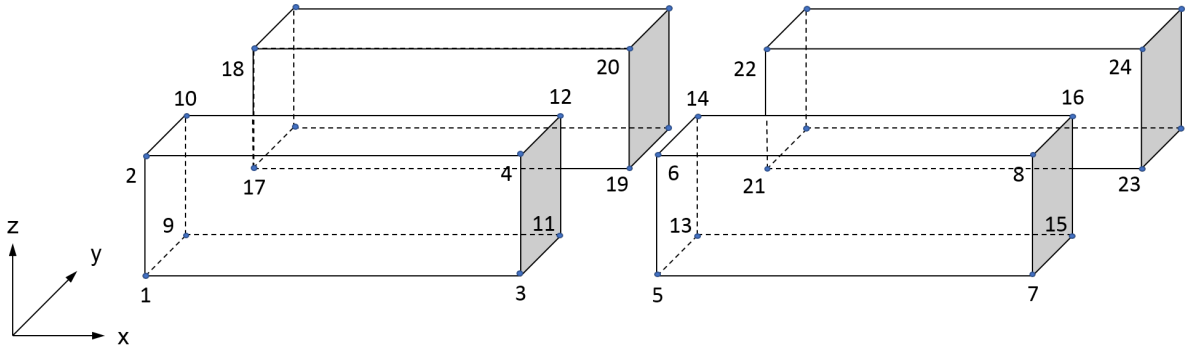

Figure 3.9: Schematic of the numbering sequence in global system

By doing so, each node attains a global node number (node ID). As each node is described by 6 DOFs one could also define global nodal degree of freedom numbers (node DOF ID).
A structure is described using a certain amount of nodes that can be listed in a *nodal ID* vector running from 1 to n nodes. Considering a full 3D configuration with 6 degrees of freedom is described by $n \cdot 6$ nodal degrees of freedom. So corresponding to a nodal ID vector one can construct a *nodal DOF ID* vector of length $n \cdot 6$ (equation 3.2). This mapping of nodes is used to organize the final structure in a proper way into the global stiffness matrix.
In the following section the use of these labels (Node ID and Node DOF ID) is discussed.

$$u_{Node} = \begin{bmatrix} u_1 \\ \vdots \\ u_n \end{bmatrix} \rightarrow u_{NodeDOF} = \begin{bmatrix} u_{x_1} \\ u_{y_1} \\ u_{z_1} \\ u_{\phi_1} \\ u_{\theta_1} \\ u_{\psi_1} \\ \vdots \\ u_{x_n} \\ u_{y_n} \\ u_{z_n} \\ u_{\phi_n} \\ u_{\theta_n} \\ u_{\psi_n} \end{bmatrix} \tag{3.2}$$

3.5.3. Global Stiffness Matrix

With the outline of the final structure, a global stiffness matrix is created. The size of this matrix is based on the nodal DOF ID vector (equation 3.4).

The local stiffness matrices of the couplings, DMBs and legs must be implemented in this global stiffness matrix. These 3 components can be seen as 3 types of elements (table 3.4).

Table 3.4: Element types

Type	# of nodes
DMB	82
Coupling	4
Leg element	2

This procedure of implementation is the same for each of these building blocks and is performed in 3 steps. The main objective is finding the relation between the local and global nodes in respectively the components and the overall system. For the coupling some elaboration is done:

Within a configuration a certain amount of couplings is used. These are described by four nodes ($\bar{u}$). In the first step the location of each coupling in the system is determined. In the second step the relations are set up between the local nodes and their corresponding global nodes at that location (Local node → Node ID). Finally using the relation between the nodal ID and the nodal DOF ID in equation 3.2 is used to place the local stiffness matrices into the global matrix (equation 3.3)

$$K_{coupling} = \begin{bmatrix} k_{1,1} & k_{1,2} & k_{1,3} & k_{1,4} \\ k_{2,1} & k_{2,2} & k_{2,3} & k_{2,4} \\ k_{3,1} & k_{3,2} & k_{3,3} & k_{3,4} \\ k_{4,1} & k_{4,2} & k_{4,3} & k_{4,4} \end{bmatrix} \begin{bmatrix} u_1 \\ u_2 \\ u_3 \\ u_4 \end{bmatrix} \xrightarrow{Implement} K_{global} = \begin{bmatrix} k_{1,1} & k_{1,2} & \dots & k_{1,3} & k_{1,4} & \dots \\ k_{2,1} & k_{2,2} & \dots & k_{2,3} & k_{2,4} & \dots \\ \vdots & \vdots & \ddots & \vdots & \vdots & \ddots \\ k_{3,1} & k_{3,2} & \dots & k_{3,3} & k_{3,4} & \dots \\ k_{4,1} & k_{4,2} & \dots & k_{4,3} & k_{4,4} & \dots \\ \vdots & \vdots & \ddots & \vdots & \vdots & \ddots \end{bmatrix} \begin{bmatrix} u_1 \\ u_2 \\ \vdots \\ u_5 \\ u_6 \\ \vdots \end{bmatrix} \tag{3.3}$$

Note that the representation in equation 3.3 is given on a level of Node ID. In the model this procedure is performed on the level of Nodal DOF ID where local degrees of freedom are related to a global degrees of freedom (e.g. $u_{3_x} = u_{5_x}$) resulting in a matrix as shown in equation 3.3. For ease of reading the visualization in equation 3.3 is shown on a nodal level.

$$K_{global} \cdot \bar{u}_{nodalDOF} = \begin{bmatrix} k_{x_1x_1} & k_{x_1y_1} & k_{x_1z_1} & \cdots & k_{x_1\phi_n} & k_{x_1\theta_n} & k_{x_1\psi_n} \\ k_{y_1x_1} & k_{y_1y_1} & k_{y_1z_1} & \cdots & k_{y_1\phi_n} & k_{y_1\theta_n} & k_{y_1\psi_n} \\ k_{z_1x_1} & k_{z_1y_1} & k_{z_1z_1} & \cdots & k_{z_1\phi_n} & k_{z_1\theta_n} & k_{z_1\psi_n} \\ k_{\phi_1x_1} & k_{\phi_1y_1} & k_{\phi_1z_1} & \cdots & k_{\phi_1\phi_n} & k_{\phi_1\theta_n} & k_{\phi_1\psi_n} \\ k_{\theta_1x_1} & k_{\theta_1y_1} & k_{\theta_1z_1} & \cdots & k_{\theta_1\phi_n} & k_{\theta_1\theta_n} & k_{\theta_1\psi_n} \\ k_{\psi_1x_1} & k_{\psi_1y_1} & k_{\psi_1z_1} & \cdots & k_{\psi_1\phi_n} & k_{\psi_1\theta_n} & k_{\psi_1\psi_n} \\ \vdots & \vdots & \vdots & \ddots & \vdots & \vdots & \vdots \\ k_{x_nx_1} & k_{x_ny_1} & k_{x_nz_1} & \cdots & k_{x_n\phi_n} & k_{x_n\theta_n} & k_{x_n\psi_n} \\ k_{y_nx_1} & k_{y_ny_1} & k_{y_nz_1} & \cdots & k_{y_n\phi_n} & k_{y_n\theta_n} & k_{y_n\psi_n} \\ k_{z_nx_1} & k_{z_ny_1} & k_{z_nz_1} & \cdots & k_{z_n\phi_n} & k_{z_n\theta_n} & k_{z_n\psi_n} \\ k_{\phi_nx_1} & k_{\phi_ny_1} & k_{\phi_nz_1} & \cdots & k_{\phi_n\phi_n} & k_{\phi_n\theta_n} & k_{\phi_n\psi_n} \\ k_{\theta_nx_1} & k_{\theta_ny_1} & k_{\theta_nz_1} & \cdots & k_{\theta_n\phi_n} & k_{\theta_n\theta_n} & k_{\theta_n\psi_n} \\ k_{\psi_nx_1} & k_{\psi_ny_1} & k_{\psi_nz_1} & \cdots & k_{\psi_n\phi_n} & k_{\psi_n\theta_n} & k_{\psi_n\psi_n} \end{bmatrix} \begin{bmatrix} u_{x_1} \\ u_{y_1} \\ u_{z_1} \\ u_{\phi_1} \\ u_{\theta_1} \\ u_{\psi_1} \\ \vdots \\ u_{x_n} \\ u_{y_n} \\ u_{z_n} \\ u_{\phi_n} \\ u_{\theta_n} \\ u_{\psi_n} \end{bmatrix} \tag{3.4}$$

At the connection points of the DMBs and couplings different local stiffness coefficients overlap. At these locations the stiffness of both the coupling and DMB are summed creating a connection between the elements (figure 3.4).

In addition the coordinates of the nodes are defined. These are used for visualisation purposes later in the results section.

Leg Implementation

The legs are implemented into the structure using the Master Slave method [14]. This differs from the implementation of the DMBs and couplings elements due to the way a leg is fitted.

As the legs run through the deck, from a nodal perspective, there are two possible connection points at the top and the bottom of the deck (see figure 3.10).

Using the same method as for the other components, summation of the overlapping coefficients results in the complete merging of two nodes. This would result in a leg fixed to the DMB in all six degrees of freedom both at the top and the bottom of the deck. However, at the bottom of the deck this is not a realistic representation. In the jack-up a leg is fixed to the DMB at the top but 'only' guided through the structure at the bottom (blue circle in figure 3.10). Therefore, at the bottom vertical and rotational movements of the leg should not be translated into the jack-up.

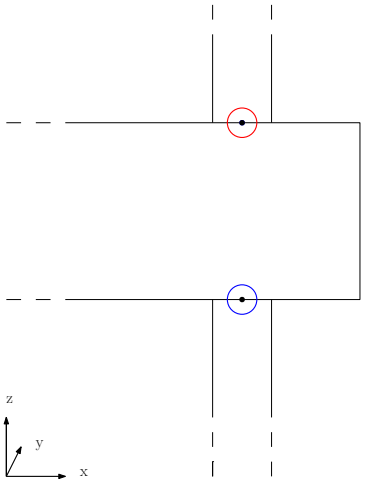

Figure 3.10: Schematic of leg hull interaction

With the Master Slave method these type of multifreedom constraints between nodes are defined.
In essence this method makes a distinction between nodes in the same location describes their displacement relations for all degrees of freedom separately.
For the nodes at the bottom of the deck the nodal translational displacements of the leg and DMB in the horizontal plane are coupled. The remaining degrees of freedom remain uncoupled. These boundary conditions are shown in table 3.5.
It must be noted that in the implementation of this method, spacing between the leg and guide of the structure is not taken into account. This is elaborated on in section 5.7.

Table 3.5: displacement relations for the Master Slave method at the leg hull connection

Top node displacement relations	Bottom node displacement relations
$u_{x_{leg}} = u_{x_{DMB}}$	$u_{x_{leg}} = u_{x_{DMB}}$
$u_{y_{leg}} = u_{y_{DMB}}$	$u_{y_{leg}} = u_{y_{DMB}}$
$u_{z_{leg}} = u_{z_{DMB}}$	
$u_{\phi_{leg}} = u_{\phi_{DMB}}$	
$u_{\theta_{leg}} = u_{\theta_{DMB}}$	
$u_{\psi_{leg}} = u_{\psi_{DMB}}$	

Removal of Couplings
An additional feature is implemented in the model providing the user the ability to remove specific couplings. This can be useful for redundancy related analyses. In a conceptual design it can be of interest to know how load is redistributed over the set of couplings in a configuration when a single coupling has failed or is faulty. This is done by removal of the local stiffness matrix of a coupling eliminating the connection between DMBs at that location.

3.6. Displacement Analysis

After the configuration is created, in this section the additional requirements are defined and the displacement analysis is solved. Firstly the external loading applied on the structure is defined. Afterwards the constraints of the structure are set up. Finally the displacement analysis is solved using equation 2.1.

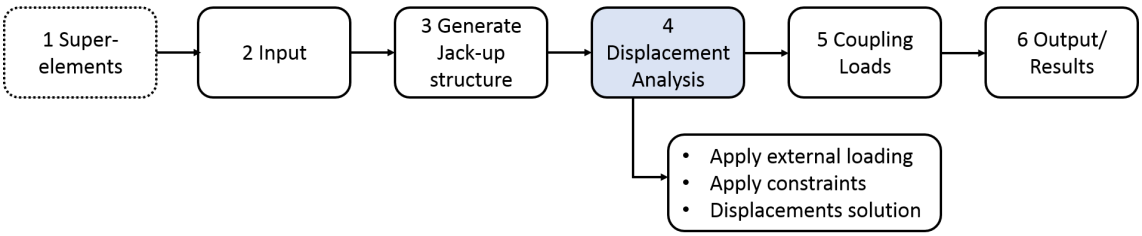

3.6.1. External Loading

As mentioned in the methodology the external loads that are taken into account are *gravity*, *environmental loading*, and *applied loading*. All of these forces are applied on the nodes describing the structure. Mathematically this means that the force vector (eq. 3.5) is defined in this section.

$$F_{global} = \begin{bmatrix} f_{x_1} \\ f_{y_1} \\ f_{z_1} \\ f_{\phi_1} \\ f_{\theta_1} \\ f_{\psi_1} \\ \vdots \\ f_{x_n} \\ f_{y_n} \\ f_{z_n} \\ f_{\phi_n} \\ f_{\theta_n} \\ f_{\psi_n} \end{bmatrix} \tag{3.5}$$

Gravity

For the gravity of the structure the total weight of the deck is defined and evenly distributed over all nodes in the deck. The weight of additional components like the legs are not taken into account. This is decided as the aim of the methodology is the analysis of the deck. As the weight of the structure is eventually carried by the legs, the weight of the legs themselves do not have influence on the loading between DMBs.

The empty weight of a single DMB is 18 tons. Additional items installed on the deck like e.g. a wooden deck also need to be accounted for. From the specifications of the JUP2420 it was found that the weight of the total base structure is approximately 570 tons. Excluding the legs which together make up for 170 tons, a deck structure of 16 DMBs has a total weight of 400 tons. The total installed weight per DMB is approximately 25 tons. As the nodes within a DMB are quite evenly spread throughout the superelement the weight of 25 tons is evenly distributed over the 82 nodes.

Environmental Loading

The environmental loading taken into account are wind, waves and current. At this stage in the model a connection is made between other software within the general jack-up project. As mentioned in one of the requirements the methodology at hand is made compatible with other software in the project. From this standpoint, as this model is to be part of a larger overall jack-up model, it is chosen to use the same forms of environmental loading.

In the external software the loading on the structure in a specified weather type is attained. The output from this external software (and the input for the current model) are given below and will shortly be elaborated on.

- A distributed load over each separate leg due to wind, waves and current
- The wind load experienced by the deck structure
- An inertial loadset

Firstly from the input of wind velocity, Morison's equation[21] is used to determine the load experienced by the legs due to wind. This same procedure is used to calculate the load experienced by the deck structure.
Similarly the load from a combination of waves and current is calculated from an input of current velocity and significant wave height. Using the stream function[21] the water particle velocities and accelerations over the height of the leg are determined. Implementing these velocities and accelerations in Morison's equation provide the loads experienced by each leg.

These environmental loadings are of an oscillatory nature in time. However, the analysis is time independent. This makes that a form of static load needs to be taken from a single point in time. For this the timestep is taken at which the overturning moment from the environmental loading is at its maximum. This combination of loading is provided to the model in the form of a dataset describing the distributed load over each leg as a horizontal load per length.

An inertial loadset is added to the environmental loading to account for the dynamic effect of the waves on the structure. "The inertial load set is an additional static load which, when combined with the quasi-static extreme storm wind, wave and current loading, results in global levels of response which reflect the inclusion of dynamic effects." [17]. Based on 1 DOF calculations, the magnitude of this load is calculated. It is applied on the structure on a set of nodes in the middle of the deck representing the centre of gravity figure 3.12.
The same nodal implementation is used for the wind force on the deck. It is noted that the implementation of these forces in this manner may influence the loading on the couplings surrounding it. However, as the magnitude of these loadings (deck wind and inertial loadset) is marginal with respect to other forms of loading, these influences are not considered critical for the outcome of the analysis.

The implementation of the distributed loading over the legs starts with the dataset attained from external software. As the model is based on nodal loading, the distributed load is divided over the nodes describing the legs. This is done using element-by-element load lumping[14]. From the dataset load per unit length at the nodes is attained (q_i and q_j in figure 3.11). By doing so, the distributed load on each element between two nodes of the leg is approximated as a trapezoid.

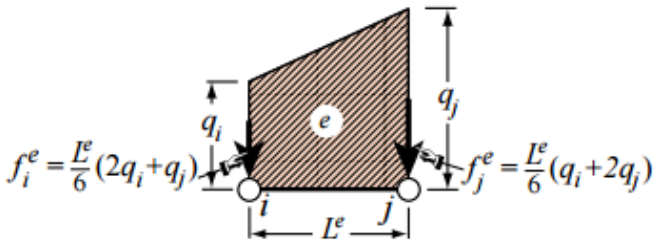

Figure 3.11: Element-by-element load lumping method[14]

Integration of the load over this element results in a single downward force at the centroid of the trapezoid. This load can be replaced by two loads acting on the nodes the element (f_i^e and f_j^e). The values of these loads are defined using the moment equilibrium around the centroid. Apart from the nodes at the end of the leg, each node has two adjacent elements on which the method is applicable. The resulting force on each node is the sum of the lumped forces from both adjacent elements.

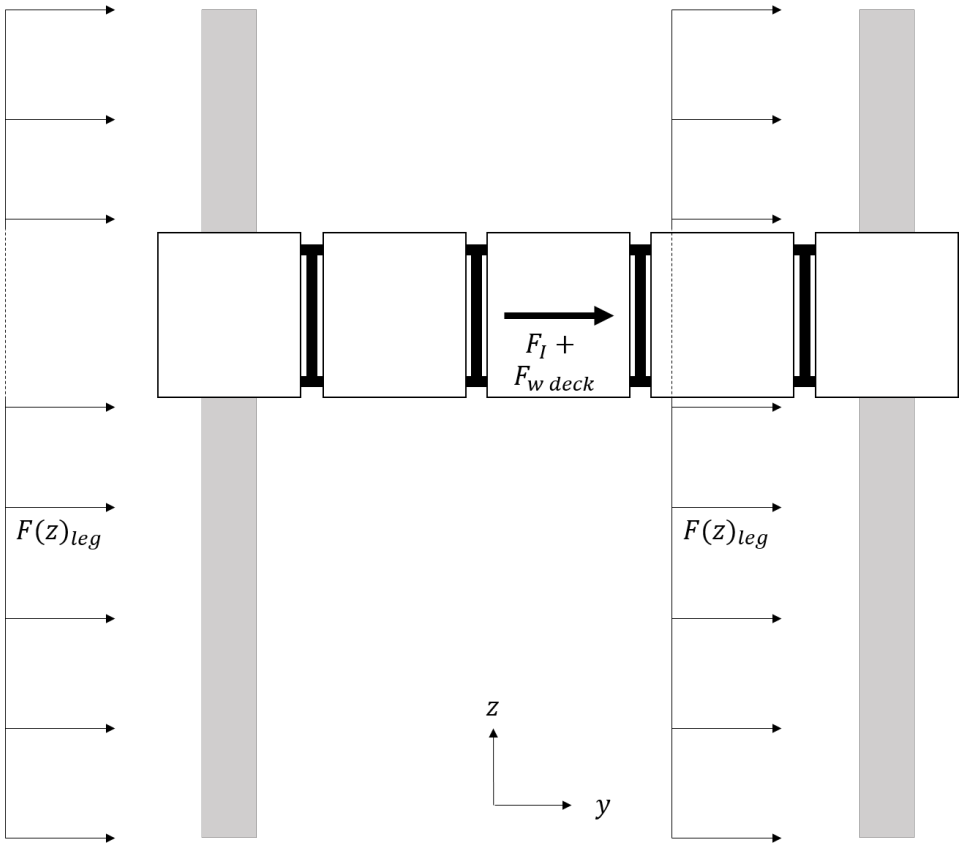

Figure 3.12: A simplified 2D representation of the environmental loading

Applied Loading
The possibility of an applied load is primarily meant for payload on the structure. In this part of the model the user can apply any kind of static load onto the structure at any nodal location. For this load the user defines:

- The magnitude of the applied load (payload)
- The nodes in the structure on which it acts
- The degree of freedom in which the load works (downward for payload analysis)

Combining all loads defined above provides the global force vector (eq: 3.5).

3.6.2. Constraints

When installed, the legs penetrate the soil to a certain until they reach equilibrium, turning the jack-up into a bottom founded structure.
In the analysis of the finite element based jack-up configuration this form of constraints need to be implemented. For this model, the use of simple supports is most conservative as it will result in the largest bending moments in the deck. This entails that the structure is fixed in translational movements (x-, y- and z-direction).
This is achieved by attaining these nodal degrees of freedom in the global coordinate system and setting their displacements to zero in the global displacement vector ($u_{nodalDOF}$). Class prescribes that this constraint is applied on the legs of the structure at approximately half the penetration depth. If detailed information about the soil and possible spudcan footings is not at hand this point is seen as the location where the combined moment due to the reaction forces from the soil and the environmental forces are zero. One could also select a constraint in all 6 degrees of freedom (also constraining the legs in rotational movement). This is explained by the fact that this is the more conservative approach. As the structure is more free to move, higher displacements can occur. As one of the key features of jack-ups is that can be used in varying locations, this conservative approach is most suited.

3.6.3. Displacements Solution

The output of this section consists of the vector containing all nodal DOF displacements of the system due to external loading. As in the former sections the global stiffness matrix (K_{global}) of the structure is attained and all external loads have been defined (F_{global}), the stiffness relation can be used to attain the unknown displacements (u) (apart from the displacements that are constrained).

$$K_{global} \cdot u_{nodalDOF} = F_{global} \rightarrow \begin{bmatrix} k_{x_1x_1} & k_{x_1y_1} & k_{x_1z_1} & \cdots & k_{x_1\phi_n} & k_{x_1\theta_n} & k_{x_1\psi_n} \\ k_{y_1x_1} & k_{y_1y_1} & k_{y_1z_1} & \cdots & k_{y_1\phi_n} & k_{y_1\theta_n} & k_{y_1\psi_n} \\ k_{z_1x_1} & k_{z_1y_1} & k_{z_1z_1} & \cdots & k_{z_1\phi_n} & k_{z_1\theta_n} & k_{z_1\psi_n} \\ k_{\phi_1x_1} & k_{\phi_1y_1} & k_{\phi_1z_1} & \cdots & k_{\phi_1\phi_n} & k_{\phi_1\theta_n} & k_{\phi_1\psi_n} \\ k_{\theta_1x_1} & k_{\theta_1y_1} & k_{\theta_1z_1} & \cdots & k_{\theta_1\phi_n} & k_{\theta_1\theta_n} & k_{\theta_1\psi_n} \\ k_{\psi_1x_1} & k_{\psi_1y_1} & k_{\psi_1z_1} & \cdots & k_{\psi_1\phi_n} & k_{\psi_1\theta_n} & k_{\psi_1\psi_n} \\ \vdots & \vdots & \vdots & \ddots & \vdots & \vdots & \vdots \\ k_{x_nx_1} & k_{x_ny_1} & k_{x_nz_1} & \cdots & k_{x_n\phi_n} & k_{x_n\theta_n} & k_{x_n\psi_n} \\ k_{y_nx_1} & k_{y_ny_1} & k_{y_nz_1} & \cdots & k_{y_n\phi_n} & k_{y_n\theta_n} & k_{y_n\psi_n} \\ k_{z_nx_1} & k_{z_ny_1} & k_{z_nz_1} & \cdots & k_{z_n\phi_n} & k_{z_n\theta_n} & k_{z_n\psi_n} \\ k_{\phi_nx_1} & k_{\phi_ny_1} & k_{\phi_nz_1} & \cdots & k_{\phi_n\phi_n} & k_{\phi_n\theta_n} & k_{\phi_n\psi_n} \\ k_{\theta_nx_1} & k_{\theta_ny_1} & k_{\theta_nz_1} & \cdots & k_{\theta_n\phi_n} & k_{\theta_n\theta_n} & k_{\theta_n\psi_n} \\ k_{\psi_nx_1} & k_{\psi_ny_1} & k_{\psi_nz_1} & \cdots & k_{\psi_n\phi_n} & k_{\psi_n\theta_n} & k_{\psi_n\psi_n} \end{bmatrix} \begin{bmatrix} u_{x_1} \\ u_{y_1} \\ u_{z_1} \\ u_{\phi_1} \\ u_{\theta_1} \\ u_{\psi_1} \\ \vdots \\ u_{x_n} \\ u_{y_n} \\ u_{z_n} \\ u_{\phi_n} \\ u_{\theta_n} \\ u_{\psi_n} \end{bmatrix} = \begin{bmatrix} F_{x_1} \\ F_{y_1} \\ F_{z_1} \\ M_{\phi_1} \\ M_{\theta_1} \\ M_{\psi_1} \\ \vdots \\ F_{x_n} \\ F_{y_n} \\ F_{z_n} \\ M_{\phi_n} \\ M_{\theta_n} \\ M_{\psi_n} \end{bmatrix} \tag{3.6}$$

Equation 3.6 describes the full static elastic relation between the nodal displacements, the stiffness of the structure and external loading. The solution of the displacements is found by solving the set of equations for u, which is done by multiplication of the inverse stiffness matrix with the external load vector (equation 3.7)

$$u_{nodalDOF} = K_{global}^{-1} \cdot F_{global} \tag{3.7}$$

3.7. Coupling Loads

The fifth section of the model is focussed on attaining the loadings that occur at the connections between the DMBs.

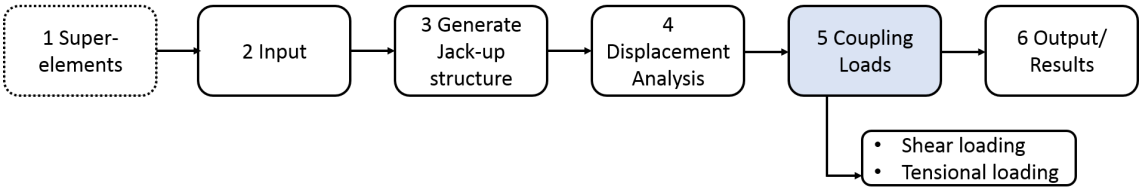

The relation between global and local nodes is used to extract the displacements of each coupling from the overall displacement vector attained in the former section (equation 3.8).
With the displacements of each coupling known, the stiffness relations are used again to attain the internal forces between the couplings and the DMBs. This is done through multiplication of the couplings displacements with the coupling's local stiffness matrix as shown in equation 2.5. Through this procedure the nodal forces and moments are attained as depicted in figure 2.1b.

$$u_{nodalDOF} \xrightarrow[local]{global} u_{coup_i} \tag{3.8}$$

As seen in the representation of the coupling capacity in figure 1.8 the final results for a single coupling consist of two values: A single value for tension and a single value for shear loading. These values are attained by using the same procedure as performed in the coupling studies done by DAMEN [23].

Shear
The single shear value for a coupling is found through summation of the vertical nodal forces on both sides of the coupling. From a static equilibrium point of view the sum of the loads on both side are equal, providing a single value for the shear of a coupling. This is checked in the code.

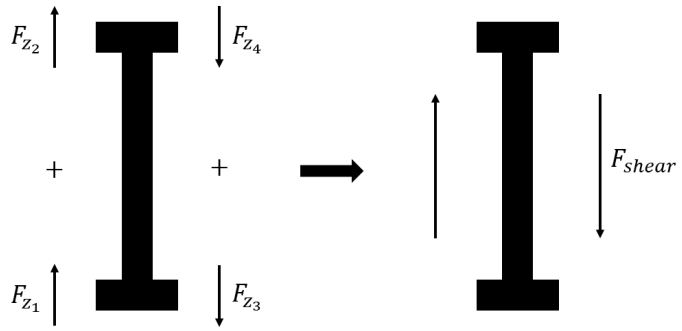

Figure 3.13: Attaining the shear value of a coupling

$$F_{z_1} + F_{z_2} = F_{z_3} + F_{z_4} = F_{shear} \tag{3.9}$$

Tension
For the tensional value the nodal forces on both sides of the coupling are first described as moments around the centroid of the coupling. Again from static equilibrium the moments on both sides of the coupling are the same. This is checked in the code In the coupling capacity format used by the DAMEN this moment is replaced by a representation of an equal force (inward or outward) at each node resulting in the same moment. This moment can also be described by an axial force that is equal for each node. This force is taken as the tensional force on the overall coupling.

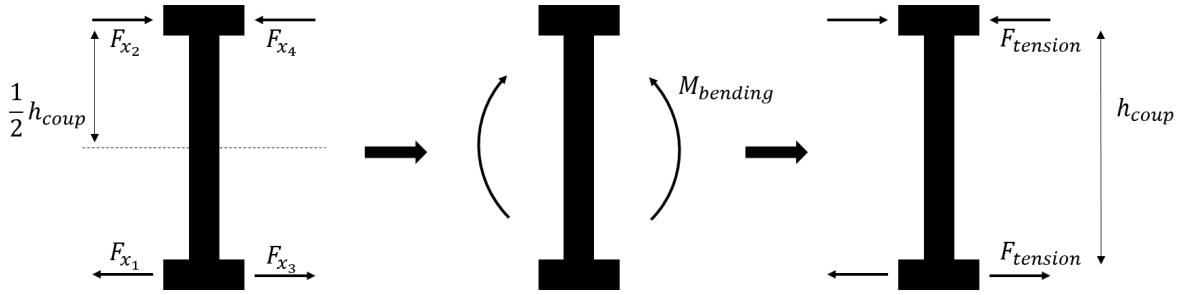

Figure 3.14: attaining the tensional value of a coupling

$$(F_{x_1} + F_{x_2}) \cdot \frac{1}{2} h_{coup} = (F_{x_3} + F_{x_4}) \cdot \frac{1}{2} h_{coup} = M_{bending} = F_{tension} \cdot h_{coup} \tag{3.10}$$

3.8. Output and Results

In the final section the results are processed and provided in several forms of output. The following examples of output are based on the JUP2420 design mentioned earlier in chapter 1.

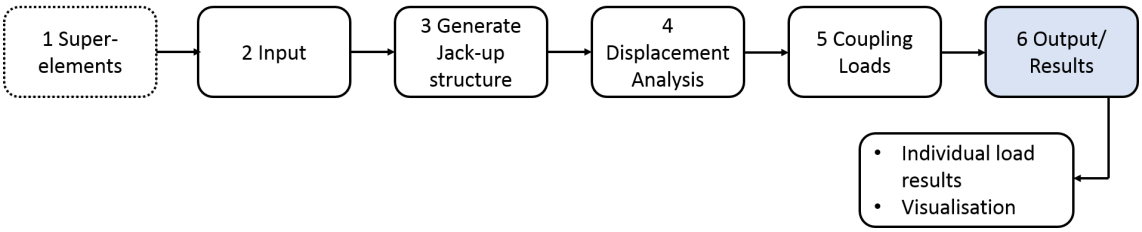

In this analysis only gravity is taken into account (no payload or environmental loading) and a total of 72 couplings is used. Firstly the main output is the results of the loading on each coupling combined in a graph of the same format as the capacity graphs used in former studies. [redacted]

[redacted]

Figure 3.15: Results on loading of couplings on a JUP2420 under gravitational loading (confidential)

In addition, a simplified top view of the deck layout is plotted to visualize which couplings in the structure are most highly loaded. This is done twice so a distinction can be made between couplings that are highly loaded in shear and couplings highly loaded in tension (figure 3.16 and 3.17). In these plots the colour scheme shows the difference between the highest (red) and lowest (green) loaded couplings in the simulation.

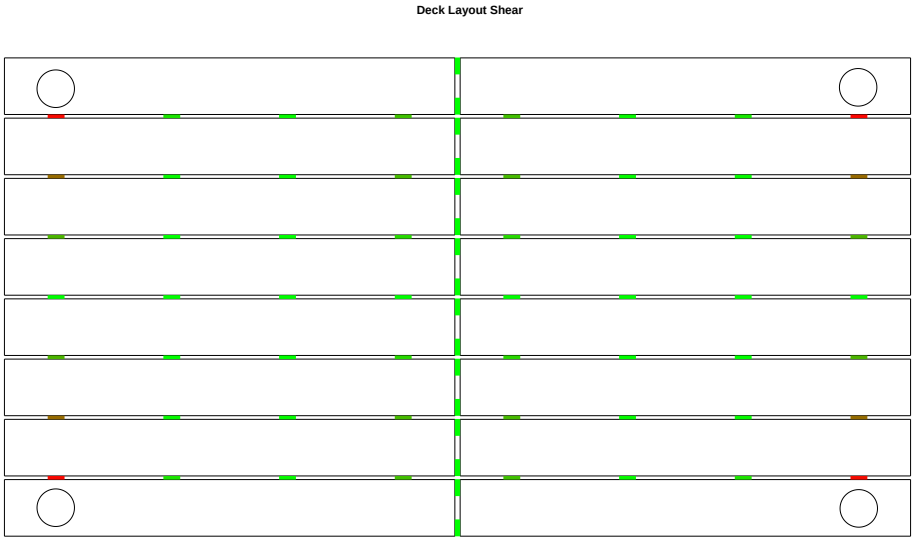

Figure 3.16: Visualisation of coupling loading in shear

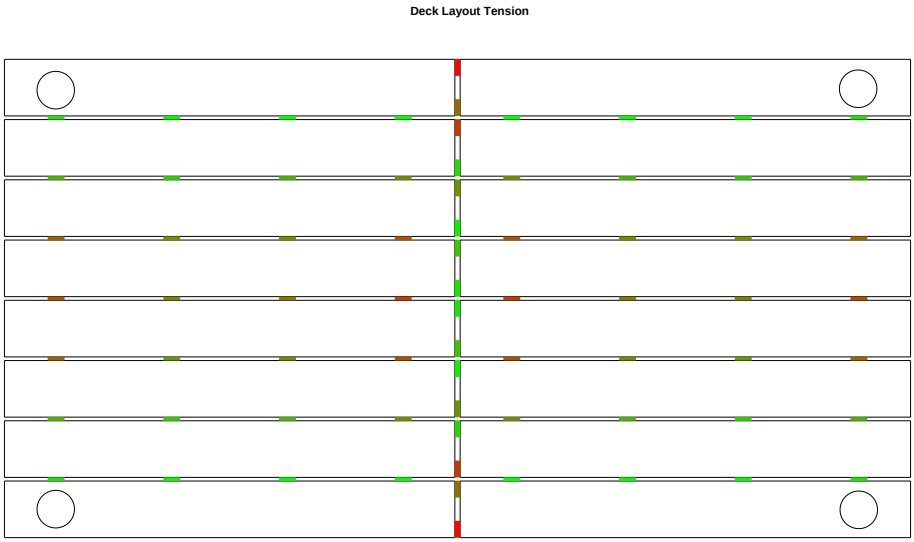

Figure 3.17: Visualisation of coupling loading in tension

A visualisation of the deck is formed showing the overall deformation of the structure (figure 3.18). In the plot a DMB is shown as two planes corresponding to the top and bottom of the original barge. The implementation of a coupling is visualized by two green lines (top and bottom) above each other connecting the different planes.
To make the deformations more visible the displacement results can be scaled up in this plot. In the figure below this scaling up results in translational displacements multiplied by a factor of 40 in the final representation.

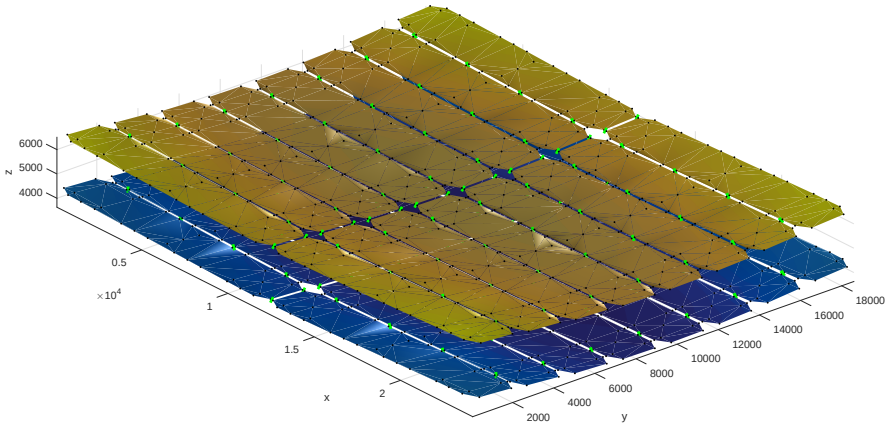

Figure 3.18: A scaled visualisation of the deformations in the deck structure

Coupling Removal
If the option is used to analyse a configuration and removing specific couplings, each of the outputs defined above is given twice. Once providing results of the original configuration and once giving the results from the modified configuration.

3.9. Limits and Improvements

Every model comes with its limitations. As the developed methodology is based on linear analysis, the accuracy of its results is also limited to the linear regime. To preserve the accuracy of the model some considerations should be taken into account.

From the analysis considering transverse loading (e.g. environmental conditions), non-linear effects can become significant as the structure experiences an overall horizontal displacement. Due to this displacement, the centre of gravity of the jack-up becomes eccentric. This creates an additional moment in the same direction as the original overturning moment due to the external loading. The magnitude of this additional moment is approximated by the weight of the structure times the horizontal displacement of the COG with respect to the seabed. This phenomenon is known as the P-Δ effect. In this static analysis model this moment is not taken into account. From the first results on the environmental cases in section 5.4, it is concluded that these additional moments become significant as they are exceeding 20 % (x-direction) and 9 % (y-direction) of the overturning moment from external loading. So as these moments can be significant, the results of analysis will provide larger displacements. As a result the loadings of the couplings will further increase. In further improvement of the model the implementation of this effect would be a natural next step. Either by use of class guidelines or based on first principle calculations.

Another note is made with respect to non-linearity. In this methodology and model the calculations are based on the linear elastic region. It is dependent on the design of the coupling whether plastic deformation occurs. For the calculations on coupling loading it is stated that while remaining under de coupling capacity curves (e.g. figure 3.15) the coupling operates in its elastic regime. Therefore, no non-linearity regarding plastic deformation is taken into account. However, this does entail that for couplings loaded beyond these curves the load results become inaccurate.

In further development of the model improvements can be made on the following aspects:

- For the gravitational loading in the model the weight of the legs is not taken into account. Adding these weights into the model can improve the accuracy of the results with respect to the (vertical) leg displacement. However, this does not affect the coupling loading.

- In the current model the leg is connected to the structure via two nodes. More detailed implementation of these legs and taking into account effects on possible leg inclinations and the spacing between the guides of the structure and the leg will probably result in less load transfer between the leg and the DMB.

- Implementation of the P-Δ effect as discussed above.

- Regarding material non-linearities, the current superelements for the couplings consist of constant stiffness matrix. An improvement would be to develop non-linear stiffness matrices for these couplings to take into account plasticity effects.

- The structure is constrained using simple or clamped supports at the seabed. Improvements can be made in the model by replacing these supports by a set of (non-linear) springs (rotational and translational). This would provide the ability to use site specific soil data improving the accuracy on the displacements of the structure.

- The loading due to wind and inertial loadset are currently implemented at the centre of the structure around the centre of gravity. The distribution of this loading throughout the structure can be improved by the implementation of the deck wind loads on the side of the structure.

- For the inertial loadset it can be considered to not focus this load as a single point load in the centre of the structure but evenly divide it over all nodes within the deck.

- The implementation of payload is currently done by equally dividing the weight of the specified payload over the deck nodes beneath it. Considering an operating crane with the boom hoisting a load outside of the structure it might be more accurate to differently spread the gravitational loading over the footprint of the crane.

3.10. Summary

The model consists of several stages. In the first section building blocks to form the deck are created as superelements using a combination of conventional FEM software and Matlab.
Next the user provides input on a desired deck configuration and load case.
From the input, the superelements are combined into a jack-up deck structure to which legs are added.
After generation of the load case, a displacement analysis is performed on the structure.
The results of this analysis consists of the displacements of all nodes within the structure. Using the displacements of the nodes describing the couplings and their local stiffness matrix, the loadings on the couplings are determined. Hereby focus lies on the vertical shear and bending moment.
In the final section different forms of output are created.

4

Validation of the Model

4.1. Introduction

In chapter 3 the development of the model is discussed. This chapter focuses on the validation. When validating a model, checks are performed on whether the outcome corresponds to reality.
In addition to validation, a model must also be verified. When verifying a model checks are performed on whether no mistakes have been made in the development of the code and equations. Throughout the development of the model in chapter 3 verification measures are continuously performed. It is assumed that the combination of these verification measures and the validation study performed in this chapter are sufficient for the model.

Considering the set up of the model, the main goal is to predict the load that will occur in the connections. These loads are described by the linear relation of $K \cdot \bar{u} = F$. A validation study is carried out containing four different structures. These four structures are chosen such that all variables in the relation are examined.
In the end a final check is performed on a full jack-up structure loaded under a horizontal external loading.

4.2. Validation through Displacements and Loads

Ideally, when modelling a system the results are compared to real life data. Often this is not possible as the actual system is too large or doing experiments on it is too risky. Another possibility is that it does not exist. This is the case for these modular jack-ups.
As real life data is unavailable, another way must be found to validate. The solution here is found in the software programme of NX Nastran. Within the company of DAMEN, NX Nastran is widely used for structural analysis of designs [24]. Results produced by NX Nastran are used as the baseline for the validation study.

During the development of the model simplified block structures are used instead of the more elaborate DMB configurations. These same blocks are used for the validation study approaching it as a proof of concept. It is assumed that if the validation holds for these blocks this will be the same for the DMBs.

The comparison is based on displacements and loads. In a load case analysis, all nodes within the structure are displaced corresponding to their stiffness by the linear formula of equation 2.1. For the validation, the displacements and loads in NX Nastran and the Matlab model must match.

4.2.1. Approach

Four cases are set up to investigate. These cases are based on certain validity interests. The main difference between them is their deck layout.

- The first case consists of just a single block. With this comparison the construction of the stiffness matrix of a single barge is examined.
- In the second case two blocks are linked together. This comparison gives insight in the implementation of couplings in the structure in the longitudinal direction.
- The third case consists of two blocks linked in the other direction. This comparison gives insight in the implementation of couplings in the structure in the transverse direction.
- In the fourth case a two-by-two barge deck structure is linked together. This can validate the outcome of a combined structure consisting of several barges and couplings in both directions.

Each case emphasises a single validation topic as described above. The topics are separated over different cases to prevent possible mistakes or errors in one topic to be palliated by another. Table 4.1 provides an overview of the main specifications per case. A note on the main dimensions; the implementation of couplings adds 140 mm between two blocks.

Table 4.1: Validation case specification overview

Case	# Blocks	L x W x H [m]	# Nodes	# Couplings
1	1	2 x 1.5 x 1	40	0
2	2	4.14 x 1.5 x 1	80	2
3	2	2 x 3.14 x 1	80	3
4	4	4.14 x 3.14 x 1	160	10

Where the deck layouts differ, the loading of each case is similar. In all cases the bottom corners of the structure are constrained in all six degrees of freedom to simulate the legs. Furthermore, an external loading, consisting of a single downward vertical load, is applied on one of the nodes. The load has a magnitude of a 1000 kN. This value is chosen to create significant displacements in the structure. In the following sections each case will be elaborated on. The figures 4.1a,4.3a,4.6a and 4.9a visualize the loading and constraining of each structure. Constraints and loads are shown using blue and red markers respectively. Possible couplings are represented by green lines. The deformations have been scaled up to make them more visible. The corresponding graphs that follow provide correct numerical values.

During the execution of the comparisons, each node is reviewed separately.
For each node all displacements are included:

- Translations: u_x, u_y and u_z
- Rotations: u_ϕ, u_θ and u_ψ

When a node is part of a connection, the corresponding forces and moments on the node are included as well. The following are included:

- The axial force F_{xx} and shear forces (F_{xy}, F_{xz})
- Torsion M_{xx} and bending moments (M_{yy}, M_{zz})

For each of the points above four values are determined providing a possible base for a comparison:

- The value in NX Nastran
- The value in the Matlab model
- The difference between these values
- The relative error

The relative error is calculated as the percentage difference of the models outcome with respect to the outcome of NX Nastran. The displacement errors are not calculated for nodes that were constrained as these values were set to be zero in both models. Additionally, for nodes having a displacement of less that 10 micrometer or micro-radian, no error was calculated as these displacements are considered insignificant.

In the following sections the four cases are shown. The focus lies on the magnitude of the calculated errors and their distribution. The results are shown and analysed using probability histograms. Afterwards an overall analysis is performed using the data of the four cases. This analysis is aimed on finding a possible relation between the errors of a certain data point and its original value (for both displacements and load).
As a final check a full jack-up structure using DMBs and couplings is analysed using horizontal external loading.

4.2.2. Case 1: A Single Block

Case 1 consists of a single steel plated block. The structure's main dimensions are given in table 4.1. There are no couplings included and the load is applied on the middle top node on the long end of the block (figure 4.1).

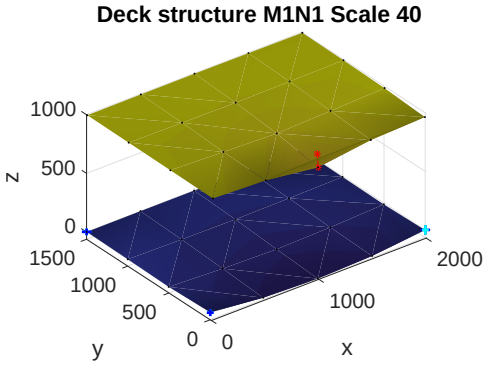

(a) Matlab model

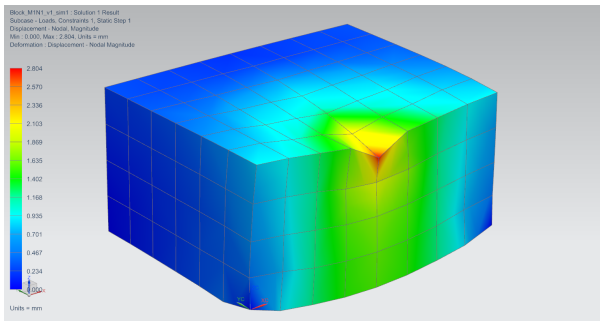

(b) NX Nastran

Figure 4.1: Visualization case M1N1 with the external load is visualized by a red point

Histograms of the calculated relative errors in the x-, y- and z-direction (figure 4.2a) and the ϕ-, θ-, and ψ-direction (figure 4.2b) are set up. By doing so, a distinction is made between the translational and rotational displacements of nodes.
As the block consists of 40 nodes (20 on the top surface and 20 on the bottom), the histogram is composed of 120 data points coming from the three concerning degrees of freedom.
The horizontal axis shows the magnitude of the errors. On the vertical axis the probability of occurrence is given as the number of times an error occurred divided by the total amount of datapoints.

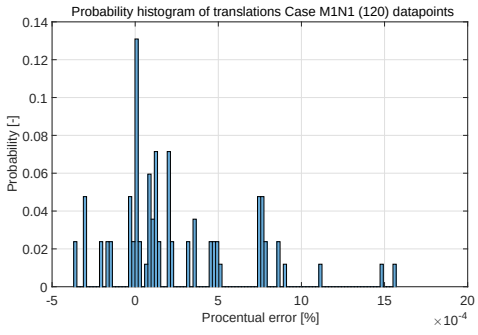

(a) Translations

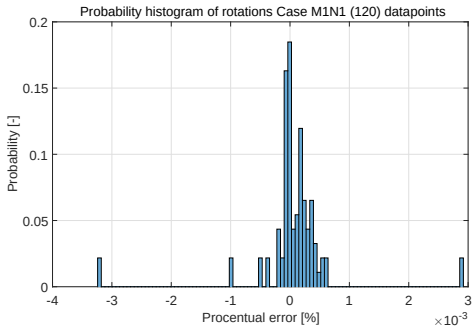

(b) Rotations

Figure 4.2: Error distribution of all data points with respect to the displacements of case M1N1

For both translations and rotations the majority of the errors is (close to) zero. Note that it seems as if the errors of the rotations are grouped closer together but this is a misperception due to the different axes. In fact, considering the outliers, the errors of the translations stay within an absolute value of 0.002 % and those of the rotations go up to 0.003 %.
Table 4.2 provides some numerical insight in the distribution of the different errors. Considering for example

the rotations, it can be seen that despite the presence of these outliers, 95 % of the errors are smaller or equal to 0.001 %.
From these results it is considered that the modelling of the stiffness of a block is valid.

Table 4.2: Maximum errors Case M1N1

	Translations	Rotations
90 % of data	≤ 0.0008 %	≤ 0.0005 %
95 % of data	≤ 0.0009 %	≤ 0.0010 %
100 % of data	0.002 %	0.003 %

For this case, the maximum error found is 0.003 %. As the cases in this validation study are representative for the load cases the model is meant for, these errors are considered reasonable and the results valid.

4.2.3. Case 2: Two Blocks in Longitudinal Direction

The second case consists of two blocks connected in x-direction by two couplings over the short end (see figure 4.3). This results in main dimensions of 4.14 x 1.5 x 1 meters (L x W x H) and a total amount of 80 nodes. The 1000 kN downward load is applied on the short end of the second block.

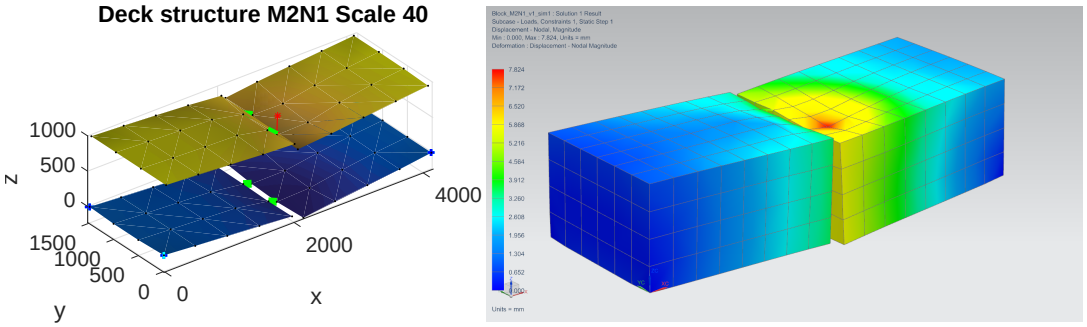

(a) Matlab model (b) NX Nastran

Figure 4.3: Visualization case M2N1 with the external load is visualized by a red point

In figures 4.4a and 4.4b the distribution of the displacement errors is shown. The data is constructed from (80 nodes times 3 degrees of freedom) 240 calculated errors for both translations and displacements. The majority of errors is found close to the zero value again. The outliers have increased with respect to case 1 to 0.023 and 0.043 percent for the translations and rotations respectively. Table 4.3 shows that over 95 % of all calculated displacement errors has a magnitude smaller or equal to 0.005 %.

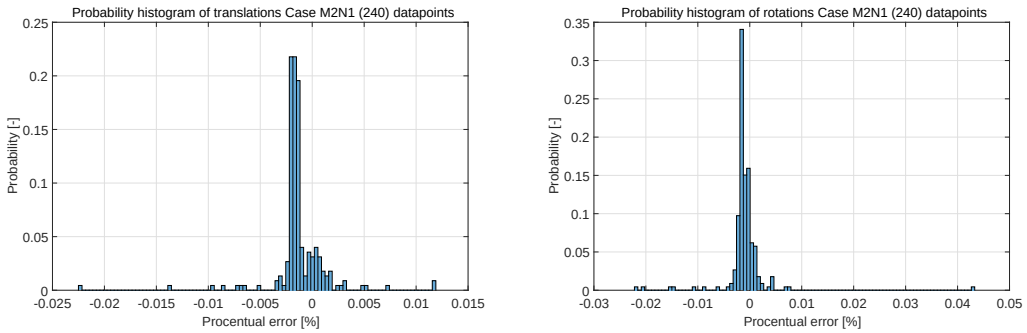

(a) Translations (b) Rotations

Figure 4.4: Error distribution of all data points with respect to displacements of case M2N1

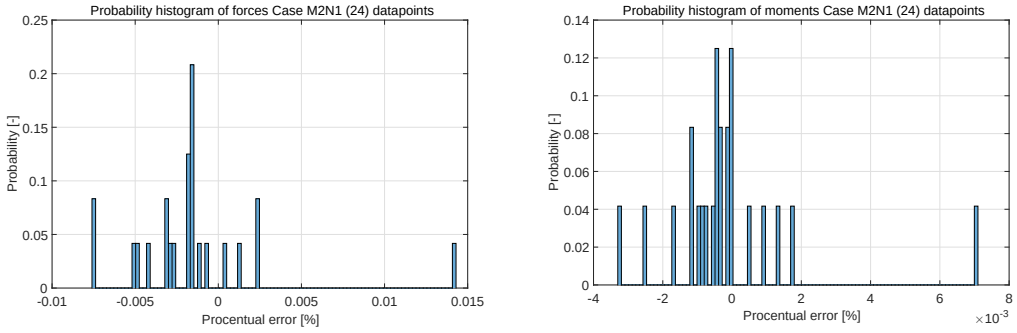

(a) Forces (b) Moments

Figure 4.5: Error distribution of all data points with respect to loads of case M2N1

The structure includes a set of two couplings. As described in chapter 3, a single coupling consists of four nodes, resulting in 12 forces and 12 moments. For two couplings this gives a total of 48 error calculations (figure 4.5a and 4.5b).
As well as for the displacements, the majority of errors is found around the zero percent value. The largest outlier has a value of 0.014 % (in the forces). Table 4.3 shows that 95 % of the calculated errors has an absolute value of less than (or equal to) 0.008 and 0.003 % for the forces and moments respectively.
From these results it is found that the modelling of the stiffness of several blocks connected by couplings in longitudinal direction is valid.

Table 4.3: Maximum errors Case M2N1

	Translations	Rotations	Forces	Moments
90 % of data	≤ 0.003 %	≤ 0.003 %	≤ 0.005 %	≤ 0.0017 %
95 % of data	≤ 0.005 %	≤ 0.004 %	≤ 0.008 %	≤ 0.0025 %
100 % of data	0.023 %	0.043 %	0.014 %	0.007 %

For this case, the maximum load error found is 0.014 %. As the cases in this validation study are representative for the load cases the model is meant for, these errors are considered reasonable and the results valid.

4.2.4. Case 3: Two Blocks in Transverse Direction

The third case consists of two blocks in y-direction, linked together by three couplings over the long end (see figure 4.6). The load is applied on the first block near the most left coupling. The structure has main dimensions of 2 x 3.14 x 1 meters (L x W x H) and consists of 80 nodes.

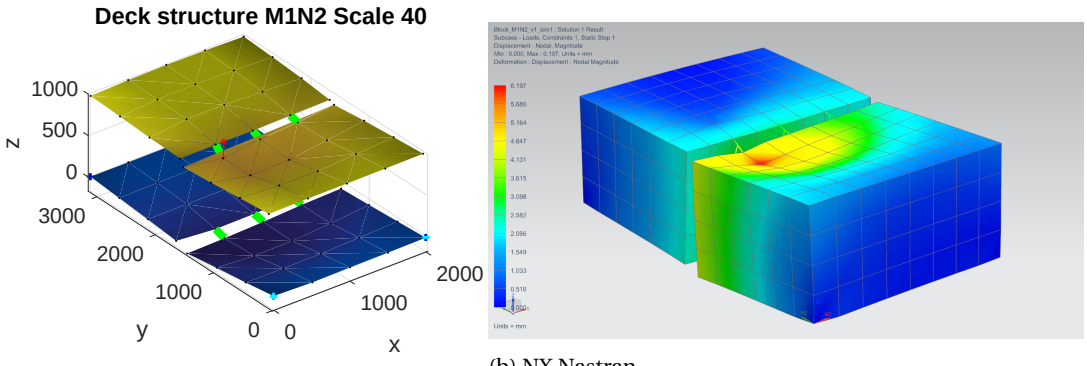

(a) Matlab model (b) NX Nastran

Figure 4.6: Visualization case M1N2 with the external load is visualized by a red point

Figures 4.7a and 4.7b show the distribution of the displacement errors of the 240 data points On a first view these histograms seem quite similar to case two having the highest probabilities a little below zero percent.

Table 4.3 shows the outliers for the displacements remaining under 0.04 % and 95 % of all relative displacement errors being less than 0.005 %.

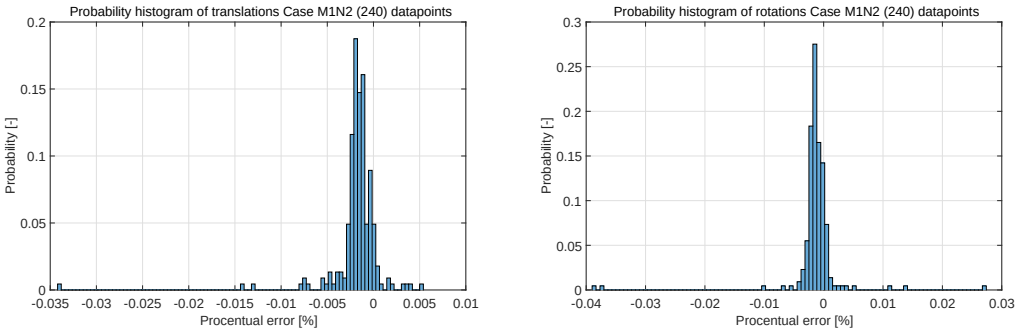

(a) Translations (b) Rotations

Figure 4.7: Error distribution of all data points with respect to displacements of case M1N2

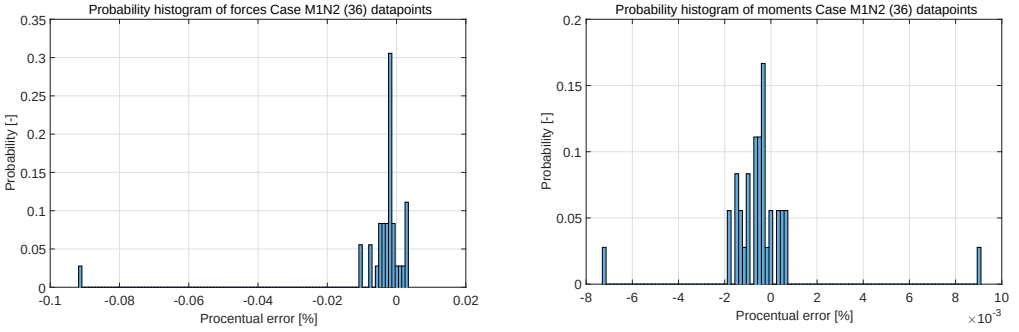

(a) Forces (b) Moments

Figure 4.8: Error distribution of all data points with respect to loads of case M1N2

The three included couplings provide 36 errors calculations for both forces and moments in figure 4.8a and 4.8b). Compared to case two these result are quite different. Reason for this appears to be the larger outliers of around 0.09 %. However, considering the gross part of the data, the cases are comparable with 95 % of the errors being smaller than 0.01 and 0.002 percent for the forces and moments respectively (table 4.4).
From these results it is found that the modelling of the stiffness of several blocks connected by couplings in transverse direction is valid.

Table 4.4: Maximum errors Case M1N2

	Translations	Rotations	Forces	Moments
90 % of data	≤ 0.003 %	≤ 0.003 %	≤ 0.007 %	≤ 0.0015 %
95 % of data	≤ 0.005 %	≤ 0.004 %	≤ 0.010 %	≤ 0.0019 %
100 % of data	0.034 %	0.039 %	0.092 %	0.009 %

For this case, the maximum load error found is 0.092 %. As the cases in this validation study are representative for the load cases the model is meant for, these errors are considered reasonable and the results valid.

4.2.5. Case 4: A two-by-two Deck Structure

The fourth case resembles more of an actual deck structure containing four blocks, linked up in a two-by-two fashion. A combination of couplings is implemented working in both directions (see figure 4.9a). The main dimensions of the structure are 4.14 x 3.14 x 1 meter (L x W x H) and consists of 160 nodes.
The load of a 1000 kN downward is applied on the second block near the middle of the structure.

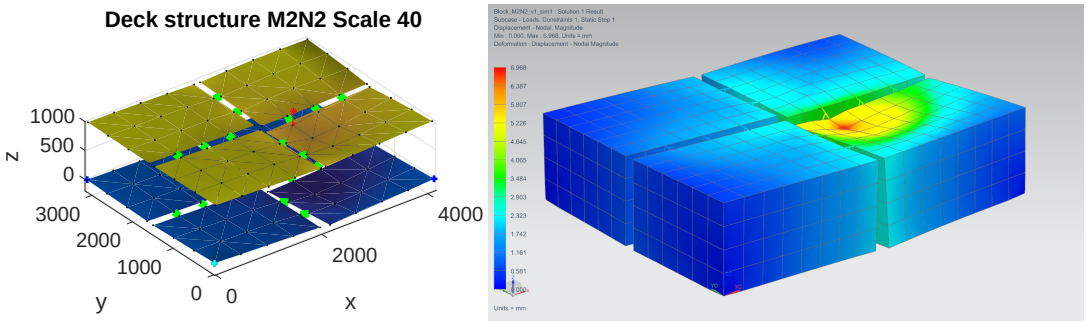

(a) Matlab model

(b) NX Nastran

Figure 4.9: Visualization case M2N2 with the external load is visualized by a red point

The 160 nodes provide for 960 calculated displacement errors. These are shown in figure 4.10a and 4.10b. Table 4.5) shows the displacement outliers going up to approximately 0.084 % and 0.088 %. However, the vast majority of 90 % of the relative errors remains below the 0.01 percent.

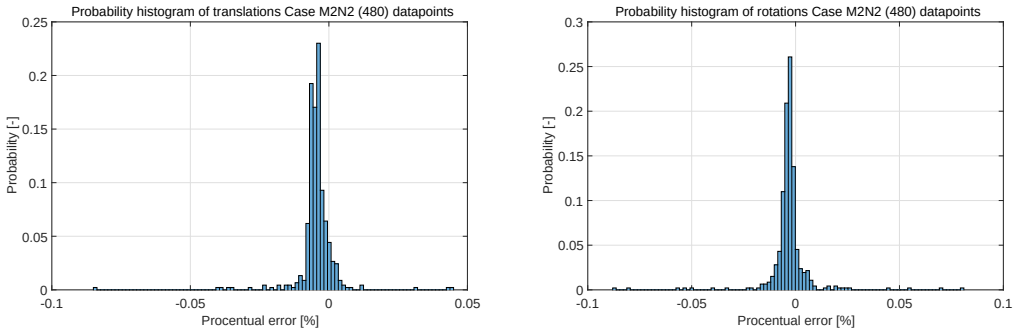

(a) Translations

(b) Rotations

Figure 4.10: Error distribution of all data points with respect to displacements of case M2N2

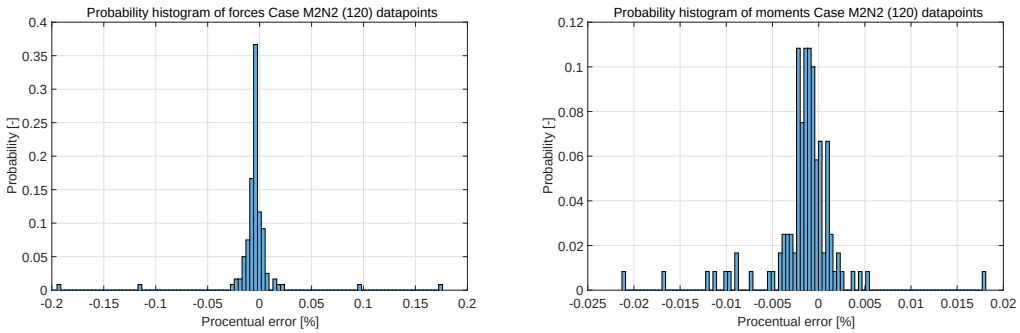

(a) Forces

(b) Moments

Figure 4.11: Error distribution of all data points with respect to loads of case M2N2

With the configuration built up in both directions, the number of couplings increases to ten in both x- and y-directions. The calculated load errors corresponding to these 40 nodes are shown in figures 4.8a and 4.8b). The vast majority of the loads has an absolute value of less than 0.02% (table 4.5).
From these results it is found that the modelling of the stiffness of several blocks connected by a combination of couplings in both directions is valid.

Table 4.5: Maximum errors Case M2N2

	Translations	Rotations	Forces	Moments
90 % of data	≤ 0.008 %	≤ 0.009 %	≤ 0.016 %	≤ 0.0049 %
95 % of data	≤ 0.011 %	≤ 0.016 %	≤ 0.023 %	≤ 0.0095 %
100 % of data	0.084 %	0.088 %	0.200 %	0.021 %

For this case, the maximum load error found is 0.2 %. As the cases in this validation study are representative for the load cases the model is meant for, these errors are considered reasonable and the results valid.

4.2.6. Analysis of Error versus Initial Value

To finalize the validation, an analysis is performed on the relations between errors, their corresponding actual values and the absolute difference. By doing so, it becomes clear whether the outliers mentioned in the cases above are significant.
Taking in consideration that the interest of the tool lies in defining the loading on the couplings, the following may be stated; the interest in an error decreases with decreasing initial displacement/load.

In figure 4.12 all cases are combined providing a three dimensional representation of the calculated errors, absolute differences and actual values.
In a perfect model all values would lie on the absolute displacement axis, meaning that there would be no difference and therefore an error of zero percent.
Where the outliers of both translations and rotations go up to approximately 0.1 percent, these values seem to correspond to small initial values.
It can also be seen that the overall displacements range over 6.7 millimetres for the translations, with differences staying within a range of 15 micrometers.
The rotations went up to values of approximately 0.02 radians, with differences smaller than 12 micro-radian.

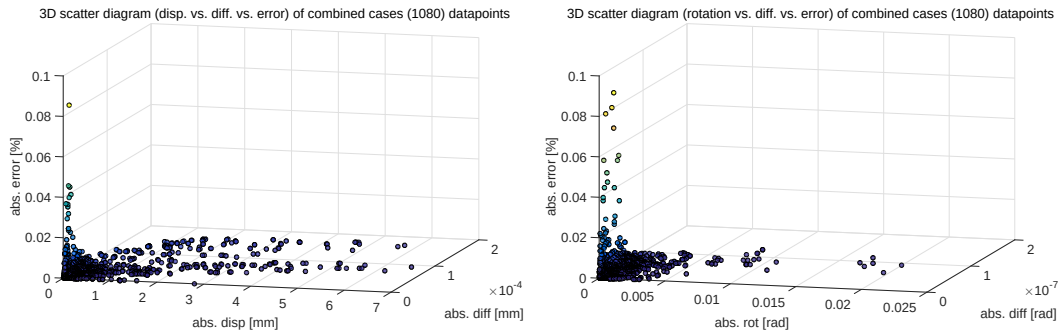

(a) Translations (b) Rotations

Figure 4.12: Nodal calculated error versus displacement and absolute difference

The same representation is shown in figure 4.13 for the load comparisons.
Outliers of the forces reached almost 0.2 percent. Again these errors belong to small initial values. As for the moments, these maximum errors were smaller near 0.02 percent.
Overall, with forces ranging up to 530 kN the absolute differences remained within 9.5 N. A similar pattern is seen in the moments with differences of less than 2.1 Nmm over moments up to approximately 355 kNmm. It is concluded that the error is highest with very low loading.

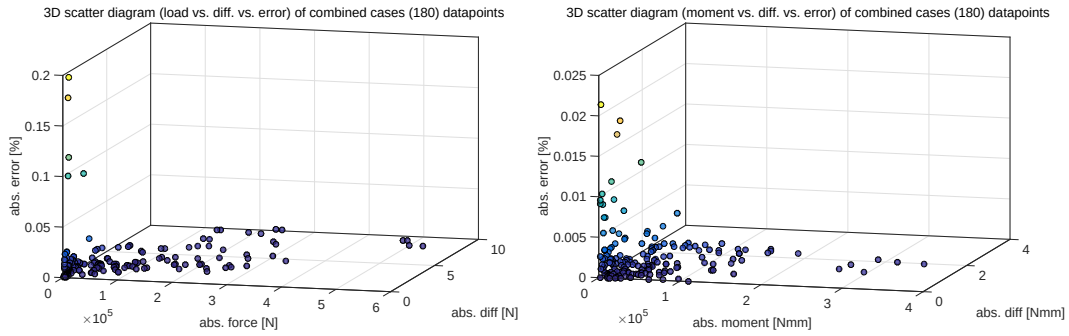

(a) Forces (b) Moments

Figure 4.13: Nodal calculated error versus load and absolute difference

4.3. Validation of Leg Implementation

The last part of the validation study focusses on the leg implementation. In NX Nastran, the full jack-up structure corresponding to the conceptual design of the JUP2420 is created as shown in figure 4.14.

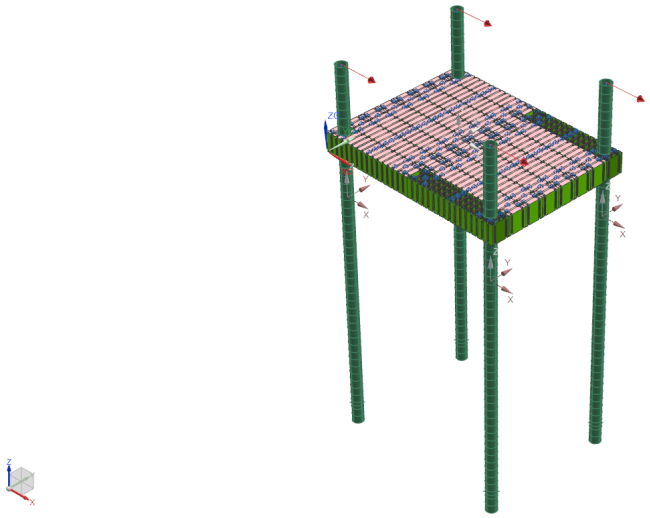

Figure 4.14: NX Nastran representation of the full jack-up

After externally loading this structure horizontally, the displacements of NX Nastran and the model are compared. It is chosen to consider the horizontal displacement of the nodal point(s) connecting the legs to the structure as shown in figure 4.15. The red arrow visualizes the displacement of the node considered. In addition also the node at the bottom of the DMB is analysed.

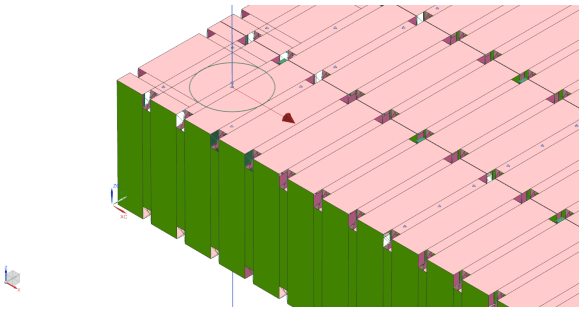

Figure 4.15: NX Nastran representation of the considered displacement at the leg implementation

From applying a horizontal load of 500kN on the top of each legs, the results of the simulations of both models are shown in table 4.6. The differences are considered sufficiently small being less than 2 percent for this external loading.

Table 4.6: Horizontal displacements of leg connection nodes from external loading of 4 x 500 kN

Node	NX Nastran [mm]	Matlab model [mm]	% difference
Top deck	571.69	562.51	-1.61
Bottom deck	548.51	538.65	-1.80

4.4. Possible Reasons for Error

Throughout the study the differences between the models are marginal. A possible explanation of these differences lies in rounding errors. As mentioned in chapter 3, the stiffness matrices of the blocks (and DMBs) are set up using the unit displacement method in FEM simulations. These FEM results are implemented in the model via a text file. In this file the results are shown in a 7 digits scientific notation. Due to this, the model is restricted to an accuracy of 7 digits in the construction of the stiffness matrix. This might result in numerical rounding errors. This is supported by the fact that the error is largest at small values.

4.5. Conclusions

Overall the validation shows all errors staying within 0.1 percent for the displacements and 0.2 percent for the loading. Additionally it is found that the absolute error is inversely related to the initial value of displacement/load. From the final check on horizontal external loading, the error of the model with respect to the leg implementation is less than 2 percent. From these findings it is concluded that the model is valid.

5

Case Study

5.1. Introduction

In this chapter case studies are performed on different load cases considering a predetermined conceptual modular jack-up design of DAMEN. The details of this JUP2420 have been discussed in chapter 1 and can be found in appendix B. The case studies focus on the following aspects:

Gravity
The first part of the study (section 5.2) focuses on the case in which the structure is only loaded under its self-weight. By doing so insight is attained on the distribution of load through the structure and the effects of using different amounts of couplings.

Payload Shift
Section 5.3 of the case study focuses on the location of a specified payload on the modular deck. These jack-ups are often equipped with a mobile crane for lifting operations. The location of this payload may differ during operations which raises the question about the effects on the couplings.
It is of interest for the designers of these structures to get insight in the influence of the payload location on the loading of couplings.

Environmental Loading
Section 5.4 of the case study considers the influences of environmental loading on the couplings within the structure. The presence of environmental conditions introduces horizontal external loading into the structure. These loadings occur in different magnitudes and at different angles of attack.
The case examines the influence of the angle of attack of the loading with respect to the loading on the couplings. Secondly different lengths of waves are applied on the structure to examine the possible influences.

Punch-through
Section 5.5 of the study focuses on the phenomenon of a *punch-through*. With the model at hand a simulation of a punch-through is simulated in an attempt to attain knowledge on the effects of the sagging of a leg on the internal forces between DMBs. As this study may reach the limits of the model a discussion is opened on the results at hand and the validity of modelling such a phenomenon using this model.

Overall Feasibility
In this section the results from the studies mentioned above are combined into an overall result (section 5.6). These overall results can be used to specify the feasibility of developing a JUP2420 using the current coupling design.

In the first parts of the studies focus lies on change of the magnitude of loading in the couplings as a result of the specified case. As noted in section 3.9 the analysis is based on linear calculations and deformations. As no coupling capacity curves are considered in these case studies all results are based on the assumption of linear elastic behaviour of the structure. Not taking into account the capacity of the coupling the accuracy of

these results should be handled with care considering non-linearities due to plastic deformation.
In the last part on the feasibility it is investigated how these loadings compare to the capacity of the coupling designs.

Additional Research on Leg Implementation
From the case studies performed, one of the findings is that the legs and leg-hull connection appears to have significant influence on the couplings surrounding it. For this reason the chosen leg implementation method is examined.

5.2. Gravity

In the development of these jack-ups it is expected that the loading endured by the couplings will be higher in comparison to other modular floating products as mentioned in chapter 3. For this reason it is considered to use more than the original 4 couplings on the long end of the barge (figure 5.1).
The following study is performed to attain answers to the following research questions:

- *What is the influence of the number of couplings on the loading of the structure?*
- *How is the load distributed over the set of couplings in the configuration?*

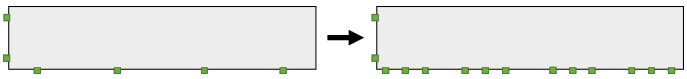

Figure 5.1: Schematic of DMB with 4 or 12 couplings on long end

Before executing the payload shift cases an analysis is run on the structure without payload merely considering gravity on the self-weight of approximately 400 tons. From here insight is attained on the critical couplings within the structure and the difference when considering DMBs with layouts of 4 or 12 couplings on the long end. In figure 5.2 the results of this analysis are visualised. Each coupling within the structure is represented as a mark on the plot.

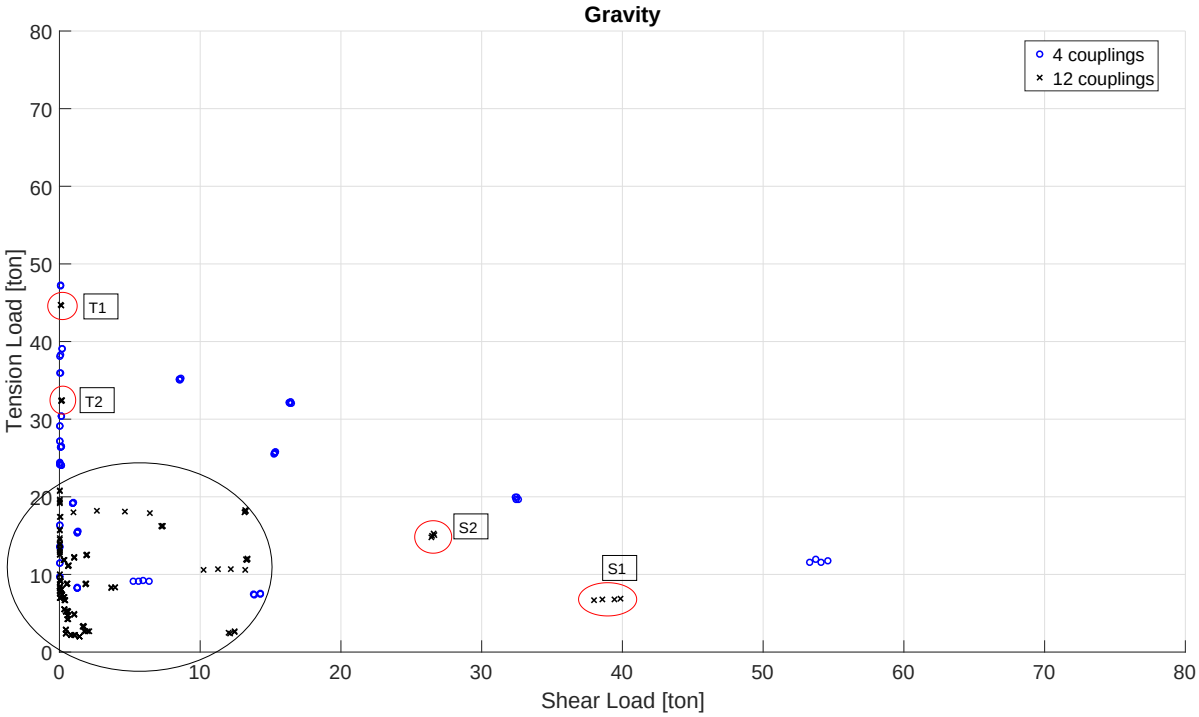

Figure 5.2: Coupling load result for gravity case considering either 4 or 12 couplings on the long end of the DMBs

5.2.1. 4 Coupling Configuration

Considering the configuration with 4 couplings (blue markers), the majority of the couplings is loaded within the region of 20 tons shear and 40 tons tension. Outliers in the direction of tension are not very extreme. One set of couplings is maximally loaded at 47.2 with 0 shearing force. When focussing on shear, the outliers are more extreme and go up to 54.6 tons of shear.

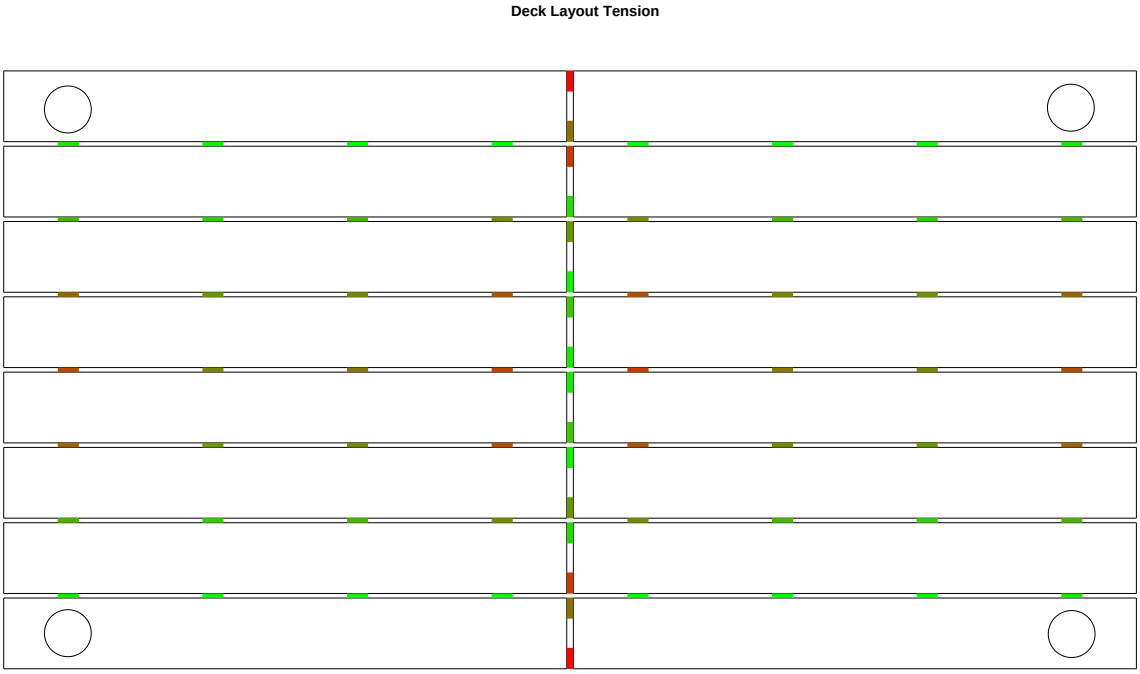

Figure 5.3: Coloured representations of tensional loading for gravity case (4 couplings)

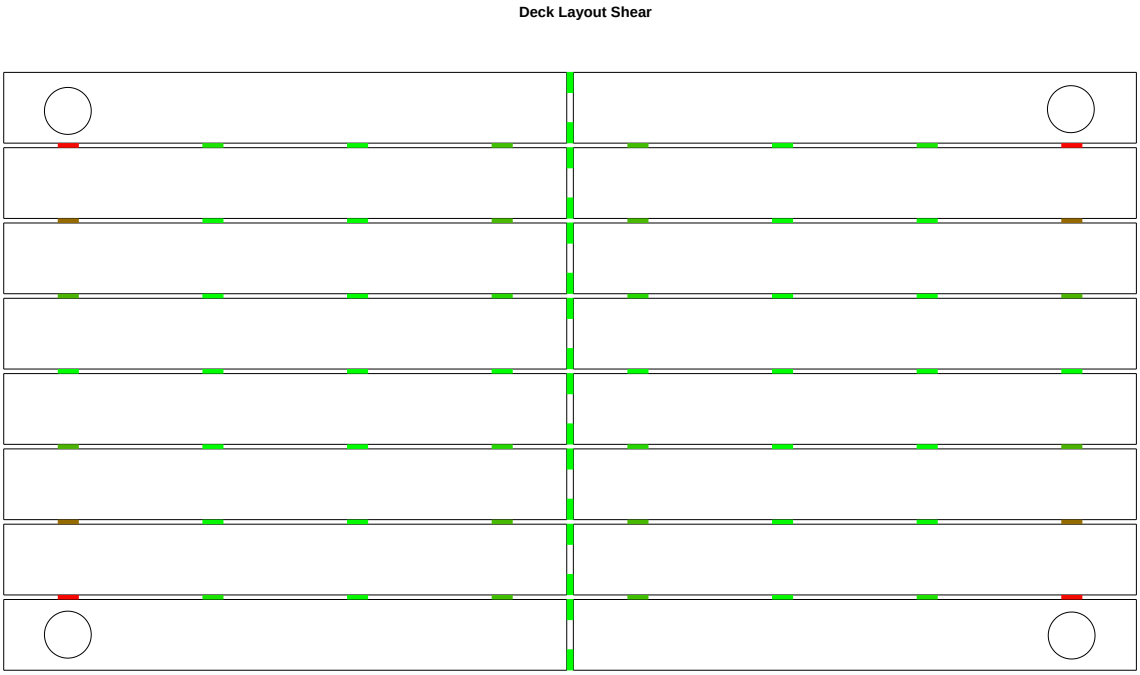

Figure 5.4: Colour visualisation of tensional loading for gravity case (4 couplings)

In figures 5.3 and 5.4 a coloured representation is shown of the distribution of loading in respectively tension and shear. Red markers indicate maximal loading and green minimal loading.

This shows that the outliers in tension are found at the edge of the structure over the short end of the DMBs, whereas the highest shear is found at the couplings closest to the leg.

This can be explained by considering the (simplified) situation from a side view as in figure 5.5. The downward distributed load is to be counteracted by the legs holding up the deck. Considering the shear lines it is expected that the largest shearing will occur close to these leg supports.
In the same way, as the tensional loads are a result of bending on the structure, the largest bending moments are found halfway between the legs.

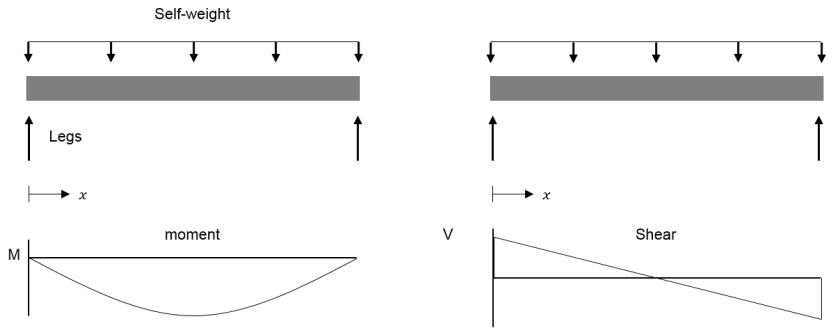

Figure 5.5: 2D schematic of self-weight on shear and moment

5.2.2. 12 Coupling Configuration

The main reason to increase the number of couplings is to redistribute the overall load over a larger set of couplings reducing the extremes. In an ideal structure every coupling would take on the same amount of loading which would mean that there would be no outliers.
Considering figure 5.2 it shows that the loading on all couplings is reduced. The majority of the couplings is now located in the region of 15 and 20 tons shear and tension, respectively. However it can also be seen that the outliers are relatively more extreme. Four groups of outliers can be distinguished.

For the tension the highest loading can be found in locations T1 and secondly in T2 (figure 5.6). As the couplings are added on the long ends of the DMBs the loading on these couplings is divided more evenly. However, in the longitudinal direction the amount of couplings did not change and therefore not significantly decreasing the high loads on the outer couplings.

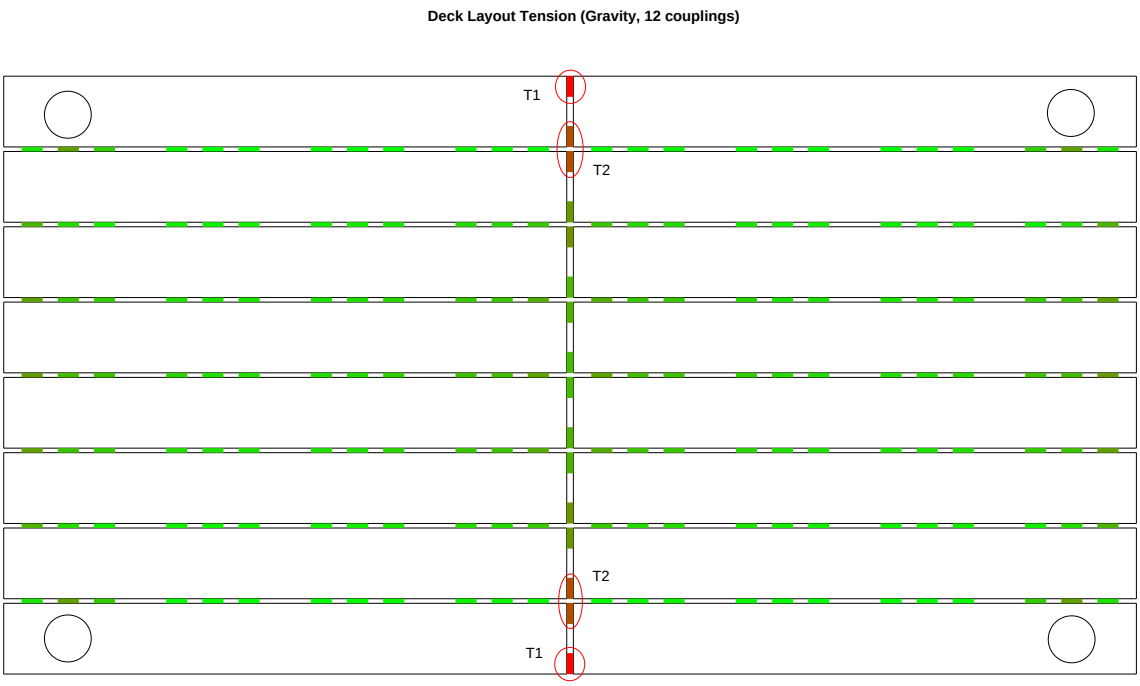

Figure 5.6: Colour visualisation of tensional loading for gravity case (12 couplings)

Considering the shear outliers seen at locations S1 and S2 (figure 5.8), the original outliers using 4 couplings were found in the transverse direction. As this is also the direction in which couplings are added it was expected that the maximum load in the structure would decrease rapidly. Focussing on the corners, a single coupling (that was loaded at 54.6 tons of shear) was replaced by a set of three. Ideally the load would be equally divided resulting in three couplings with a loading of 54.6/3 tons maximum. However, this is not the case: From the 54.6 tons still about 40 tons is taken on by the outer coupling.
The maximum shear loading using 12 couplings is 39.9 tons. Comparing to the 4 coupling configuration this corresponds to a decrease of 26.9 %

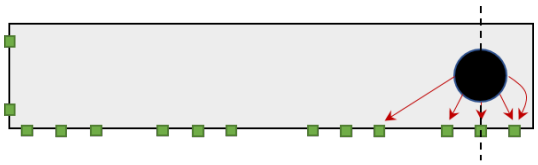

Figure 5.7: Shear load concentration at end of DMB

This might be explained by the layout of the structure as the outer couplings are close to the end of the DMB. The upward reaction force at the legs introduces high shear that gradually decreases (corresponding to equilibrium equations) away from the leg. As the end of the DMB is close to the leg a discontinuity in the structure arises and the shearing may concentrate into the outer coupling (figure 5.7). However, for full understanding of this phenomenon a more detailed FEM analysis of the structure is needed considering also the stresses within the structure. The current methodology is not suitable for this purpose.

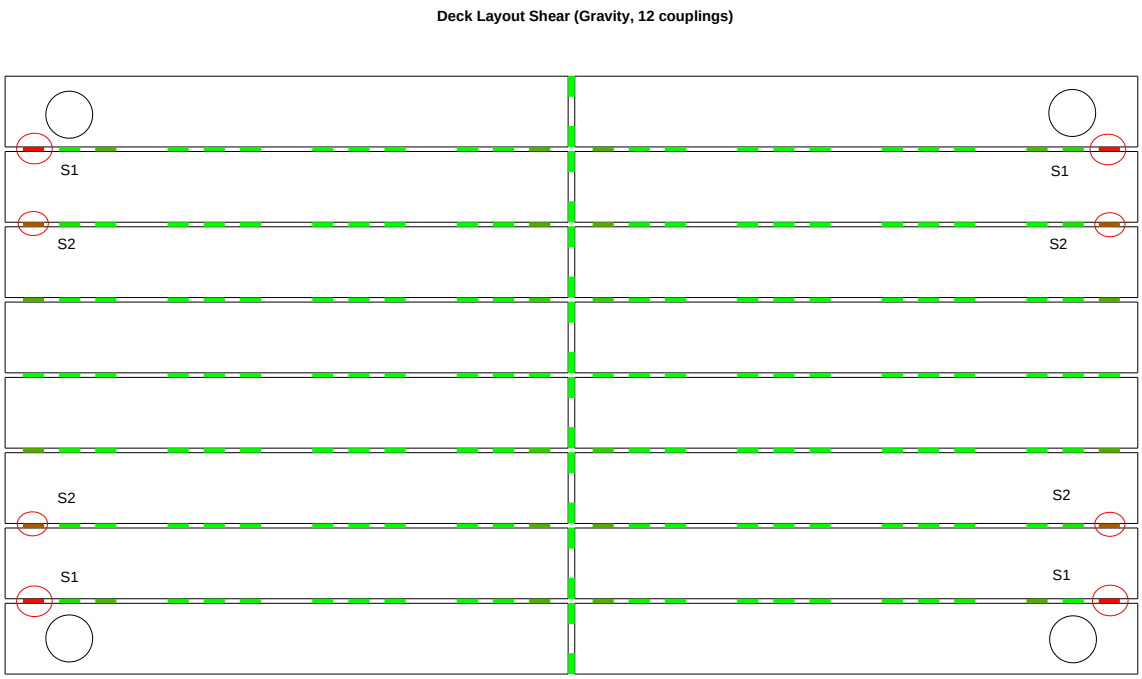

Figure 5.8: Colour visualisation of shear loading for gravity case (12 couplings)

Considering the tensional loading of the structure initially in the configuration using 4 couplings these high loadings were located in the longitudinal direction of the structure on the short en of the DMB. As no couplings are added in this direction the change in tensional loading is not significant. In the configuration using 12 couplings on the long end of the barge the maximum tensional loading in the structure is found to be 44.7 tons. This corresponds to a decrease of 5.3 % with respect to the configuration using 4 couplings.

A summary of the results of the case is shown in table 5.1.

Table 5.1: Summary of maximum loadings for number of couplings case

Case	max. Shear [tons]	difference [%]	max. Tension [tons]	difference [%]
4 couplings	54.6	-	47.2	-
12 couplings	39.9	-26.9 %	44.7	-5.3 %

5.2.3. Discussion

Coming back to the questions set up at the start of this study the following is concluded:

- *What is the influence of the number of couplings on the loading of the structure?*

  The implementation of extra couplings in the transverse direction leads to a significant decrease in the maximum shear loading in the structure.
  Considering a JUP2420 under gravitational loading leads to a decrease of 26.9 %. In tension the changes are less significant mostly due to the fact that the highest tensional loads are found in the longitudinal direction. In this direction no couplings are added leading to a decrease in tensional loading of only 5.3 %.

- *How is the load distributed over the set of couplings in the configuration?*

  Considering the distribution of loading over the full set of couplings it can be concluded that the vast majority is loaded up to a comparable degree. However, it is seen that both in the 4 and 12 couplings configuration high concentrations of loading are found at the couplings near the legs (shear) and at the edges of the structure in the longitudinal direction (tension). These locations are visualised in figures 5.6 and 5.8

5.3. Payload Shift

For the study on payload five locations on the structure are considered most relevant to investigate. It is expected that placement of the payload at these locations results in the highest loading of couplings. In figure 5.9 a schematic shows the five locations mentioned.
This study aims to find answers to the following questions:

- *What is the influence of the location of payload on the loading of the structure?*
- *How is the load distributed over the set of couplings in the configuration?*

Location 1 can be seen as the base case, corresponding to the location where the crane isw stored when not in operation. Location 2 and 3 are defined as the locations in which the couplings surrounding the payload are expected to encounter high tensional loads due to the bending of the structure. Considering a 2D simplification of the situation in figure 5.10 placement of the load in the middle between the supports (the legs) should provide the largest bending moment.
Similarly the highest shear loading is expected in by placement of the payload at locations 4 and 5.

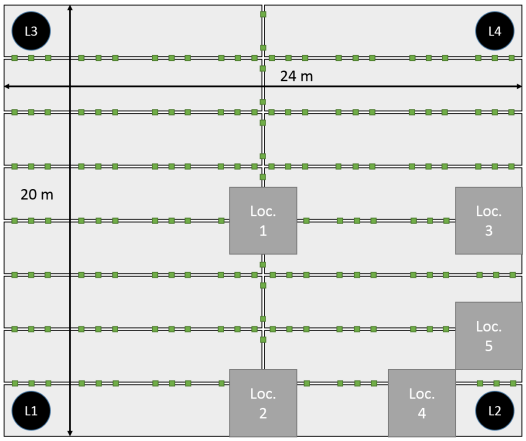

Figure 5.9: Schematic of payload locations of interest

From there two movements have been defined that are further examined.
The first movement is the shifting of the payload from the centre (loc. 1) to the edge (loc. 2). Location 2 was chosen over 3 as the span between the legs on this end is larger resulting in larger moments (see figure 5.10).
The second movement is focussed on the shearing effects as one moves the payload towards the leg. This is examined by movement of the payload from location 3 to 5. The reason for doing this on the short end of the jack-up has to do with the orientation of the DMBs. In this direction couplings are mounted closest to the leg where large shear is expected (see figure 5.10).

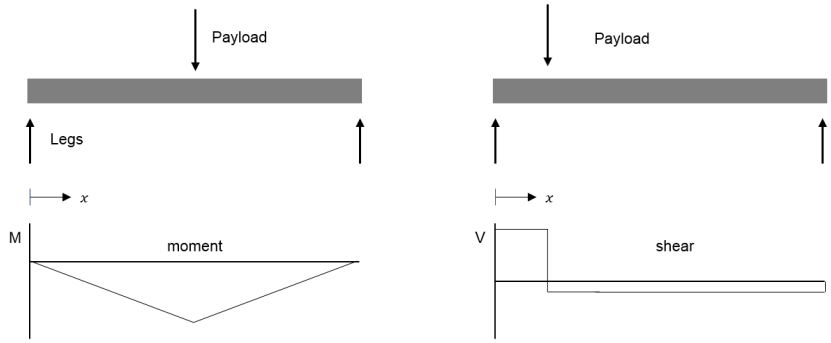

Figure 5.10: 2D schematic of the effect of payload locations on shear and moment lines

Next to the payload other loadings are taken into account such as the weight of the deck structure itself. As the focus lies on the influences of the payload, it is chosen not to take into account environmental loads. Furthermore, the construction is constrained at the seabed using simple supports. This constrains the footings of the structure in the three translational directions (x, y, and z).

Mobile Crane
For the case study a payload is taken as a mobile crane. More specifically, the crane considered is the *Hitachi Sumitomo SCX900-2* [2] hydraulic crawler crane (figure 5.11). This crane was opted for by the department of Civil & Modular Construction as it is considered for the design of these jack-ups. Due to this, the specifications of this crane were also readily available for this study.
The crane has a footprint of two tracks of approximately 0.8 meters wide and 5.5 meters long. From the specifications a crane is considered for digging operations using a clamshell. The weight of the crane is around 90 tons. Combining this with the weight of the bucket, being approximately 5 tons, and an additional maximum of 10 tons lifted load makes a total of 105 tons.
The load is applied evenly over the footprint of the crane as a downward force on the structure. As mentioned, the structure consists of superelements with a limited amount of nodes at the deck surface. The forcing of this footprint is implemented as accurate as possible in the nodes that fall within the track dimensions.
Dynamic effects that may occur on the bucket during digging operations have not been taken into account.

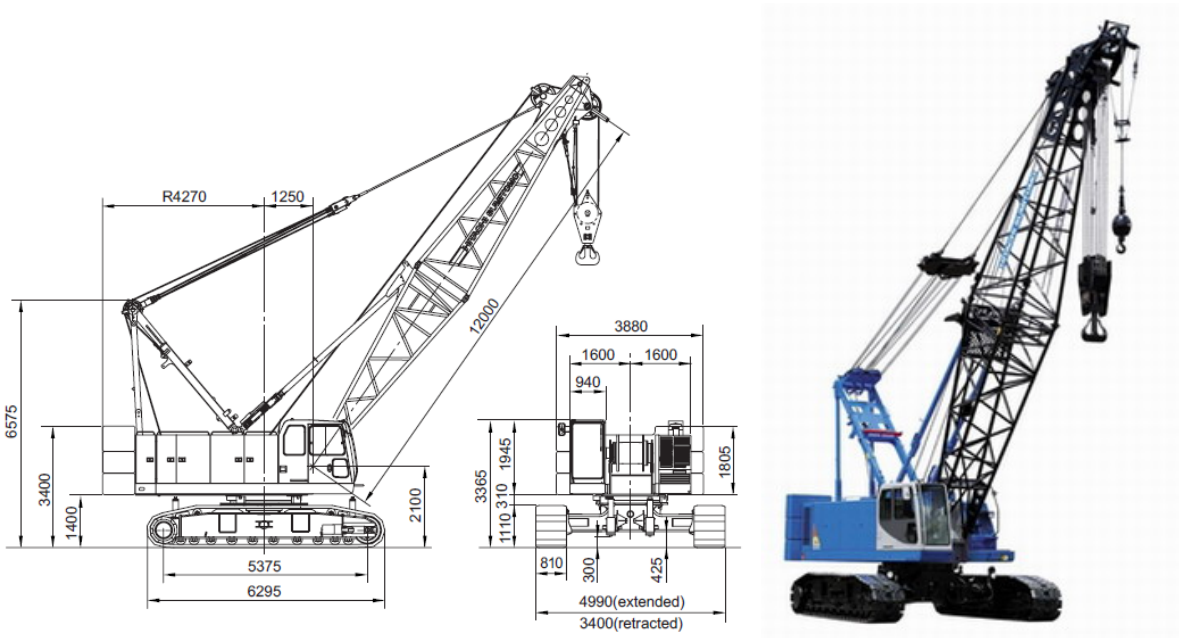

Figure 5.11: The Hitachi Sumitomo SCX900-2 (dimension in mm)[2]

Summarizing the input for the case study:

- A payload of a 105 tons is equally distributed over the footprint of the crane
- This load is shifted from the centre of the structure to the edge (case 1) and along the edge of the structure towards a leg (case 2)
- The self weight (400 tons) of the deck structure is taken into account and evenly distributed over the deck
- Loads due to environmental conditions are not taken into account
- The structure is constrained at the seabed using simple supports

5.3.1. Centre-to-edge

Considering figure 5.9 the payload is shifted from location 1 to location 2. This shift is performed in four steps from location A to D in figure 5.12. With the overall dimensions of the deck structure being approximately 20 x 24 meters, the payload is shifted over a total distance of 7 meters.

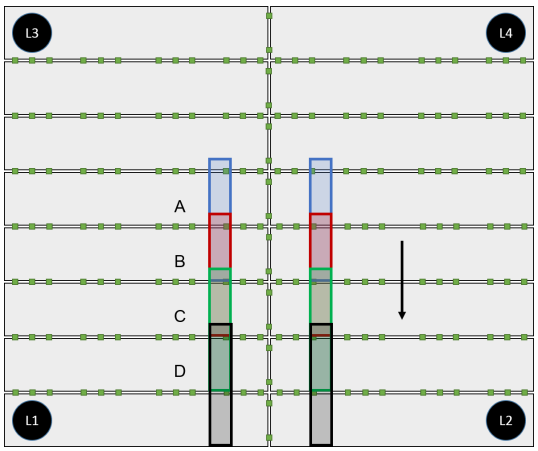

Figure 5.12: Locations considered for the center-to-edge payload shift

The results of the four analyses are combined into an overall graph in appendix C.1. In figure 5.13 the two outer locations A and D are shown.
The full structure considered houses a total of 184 couplings. 16 of them are located on the short ends of the DMBs in the centreline between the tracks of the payload. The other 168 are placed in the perpendicular direction over the long ends of the DMBs. From a first glance at the results it can already be noted that the difference in loading per coupling is considerable. The majority of the couplings is located in the lower regions of loading, where only a few of them are located at the extremes of shear and tension.

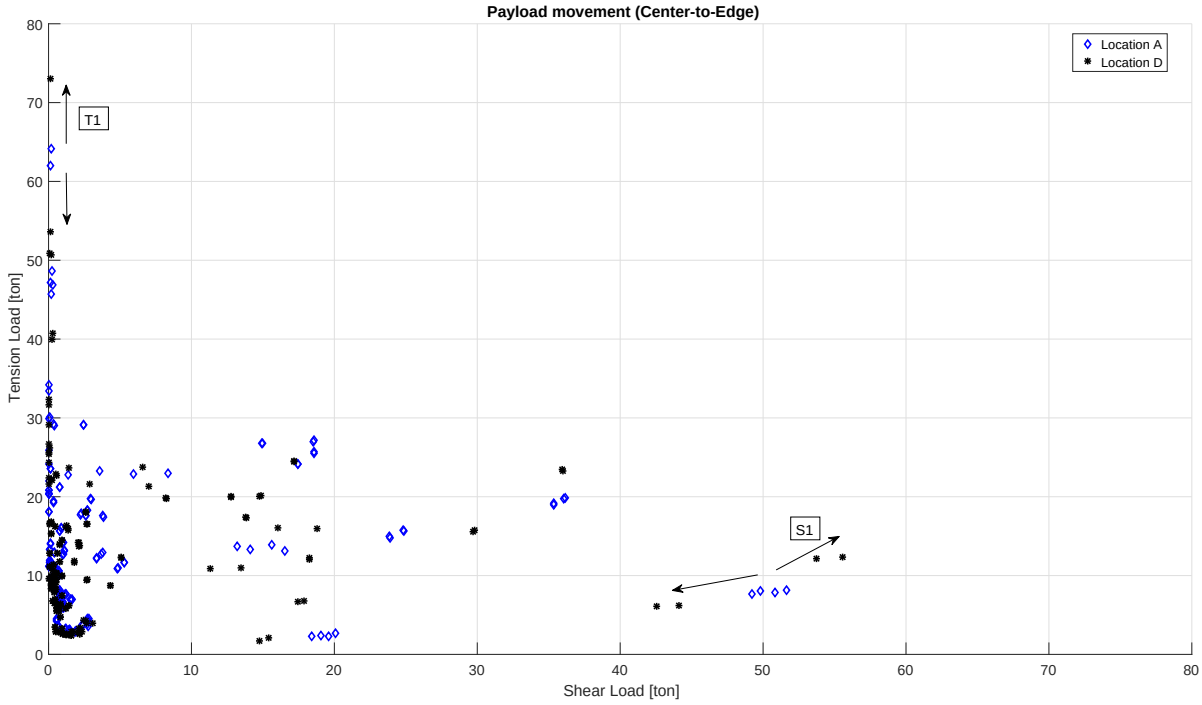

Figure 5.13: Coupling loading for cases Center-to-Edge

Shear Loading
Considering the scenario of a jack-up without payload resulted in a maximum shear load of 39.9 tons. Adding the payload and shifting it to the side resulted in a maximum shear value going from 51.6 tons at the centre to 55.6 tons at the edge (S1). Correspondingly the shear at the far end of the structure lowers.

Shifting the load from centre to edge increases the maximum shear values with approximately 7.8 % to 55.6 tons with respect to the payload in the centre.

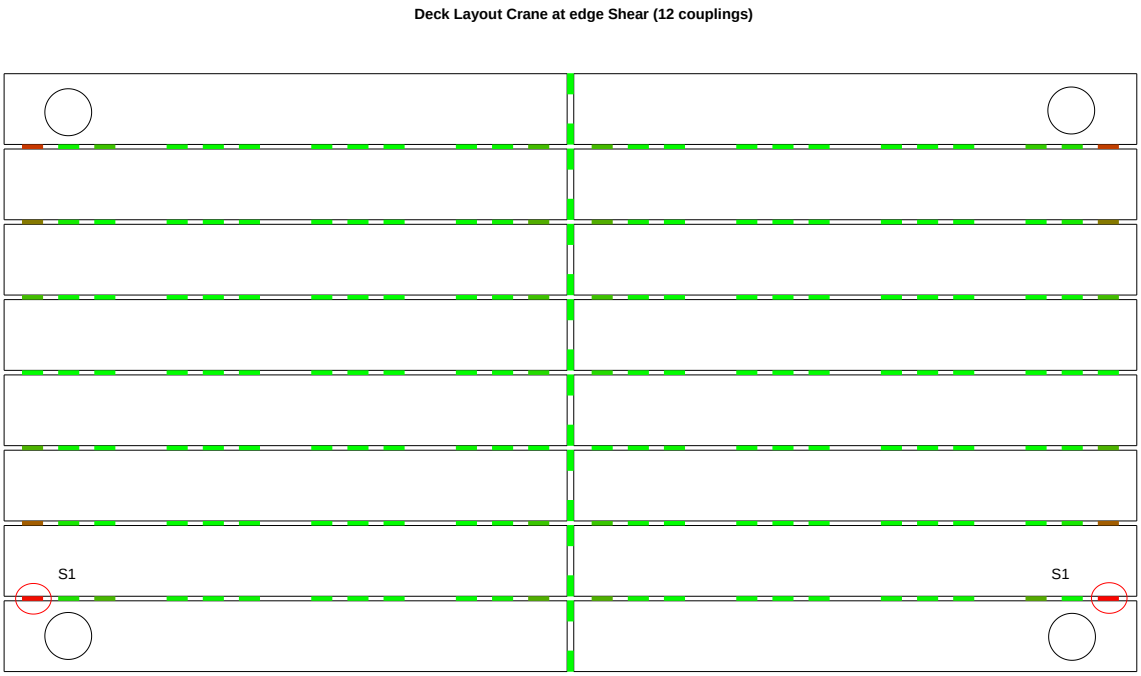

Figure 5.14: Colour visualisation of shear loading for Center-to-Edge case (12 couplings)

Tensional Loading
Again considering the scenario of a jack-up without payload resulted in a maximum tension load of 44.7 tons. Adding the payload and shifting it to the side increases the tension from 64.2 tons at the centre to 73.0 tons at the edge (T1). Correspondingly the tension at the far end of the structure lowers.

Shifting the load from centre to edge increases the maximum tension values with approximately 13.7 % to 73.0 tons with respect to the payload in the centre

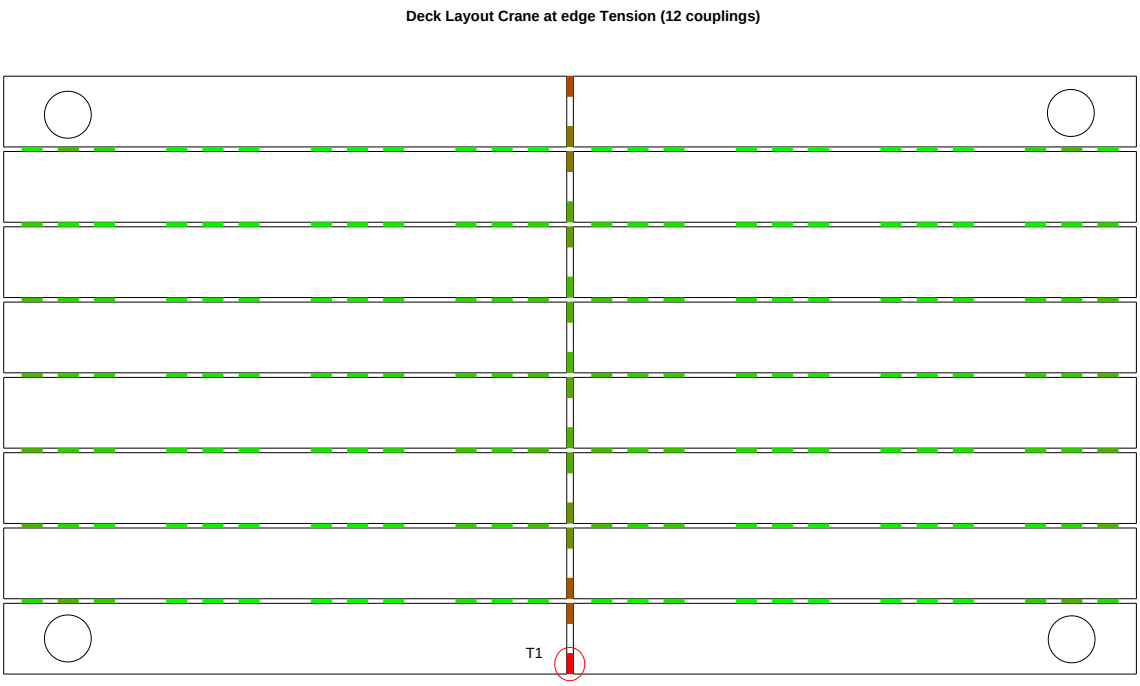

Figure 5.15: Colour visualisation of tensional loading for Center-to-Edge case (12 couplings)

As mentioned the distribution of the loads over the full set of couplings is poor. The vast majority of the 184 couplings is loaded beneath approximately 20 tons shear and 30 tons tension.

Table 5.2: Summary of maximum loadings for center-to-edge case

Case	max. Shear [tons]	difference [%]	max. Tension [tons]	difference [%]
No payload	*39.9*		*44.7*	
A	51.6	-	64.2	-
D	55.6	7.8 %	73.0	13.7 %

5.3.2. Edge-to-leg

Shown in figure 5.9, the payload is shifted from location 3 to location 5. This shift is performed in four steps from location E to H in figure 5.16. With the overall dimensions of the deck structure being approximately 20 x 24 meters, the payload is shifted over a total distance of 4 meters.

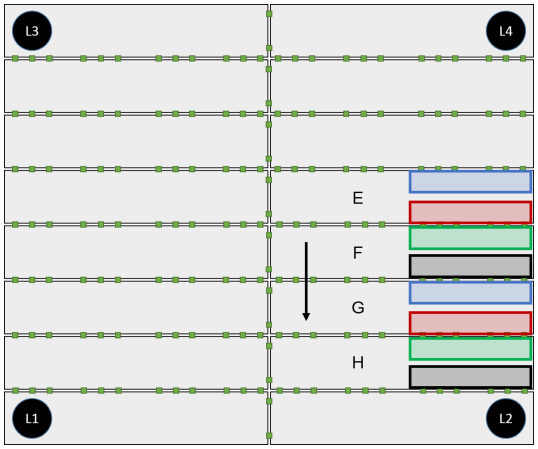

Figure 5.16: Locations considered for the edge-to-leg payload shift

The results of the four analyses are combined into an overall graph that can be found in appendix C.1. Figure 5.17 shows the two outer locations E and H.

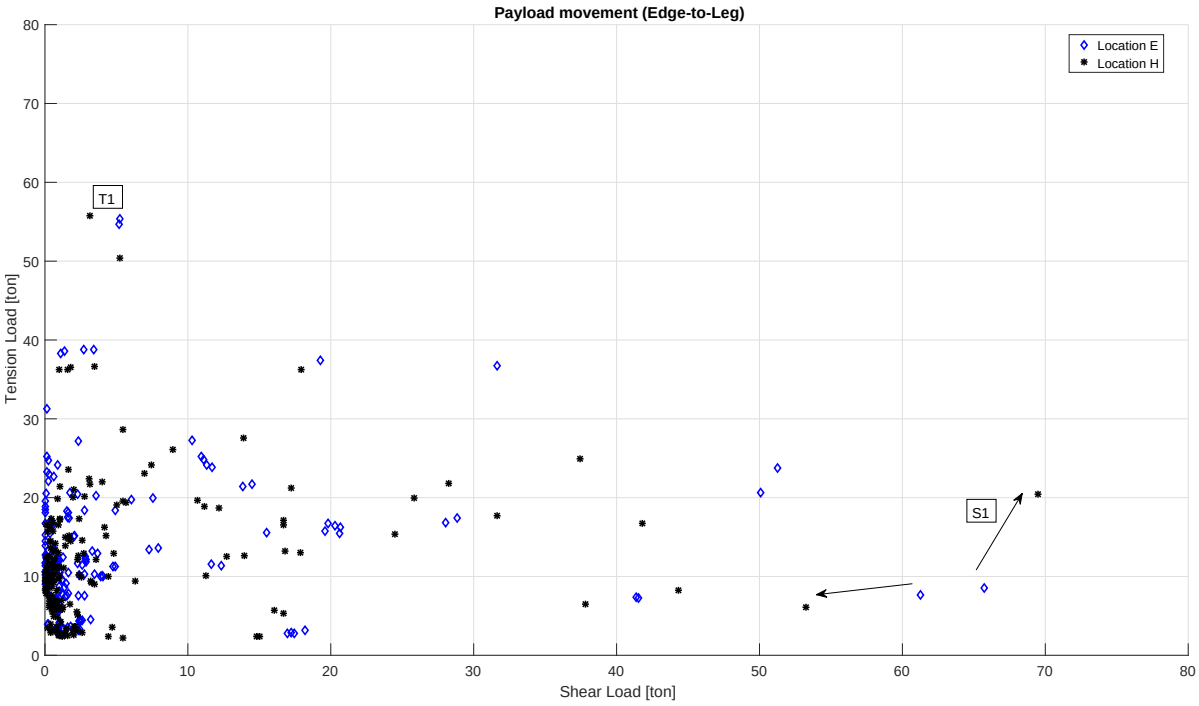

Figure 5.17: Coupling loading for cases Edge-to-Leg

Shear Loading

Considering the scenario of a jack-up without payload resulted in a maximum shear load of 39.9 tons. Adding the payload at the centre of the edge resulted in a maximum shear value of 65.8 tons. It must be noted that the starting position of the crane is already slightly closer to leg 2 than leg 4 (figure 5.16). This explains why in the initial results in blue the maximum shear that occurs at the couplings close to leg 2 and 4 is not the same. Shifting the payload towards leg 2 results in a maximum shear of 69.5 tons (S1). These couplings do not only increase in shear but also in tension. Considering a schematic cross-section of the structure between leg 2 and for this can be explained. By moving the payload, not only the highest shear is shifted towards the leg, but also the maximum bending moment (figure 5.18).

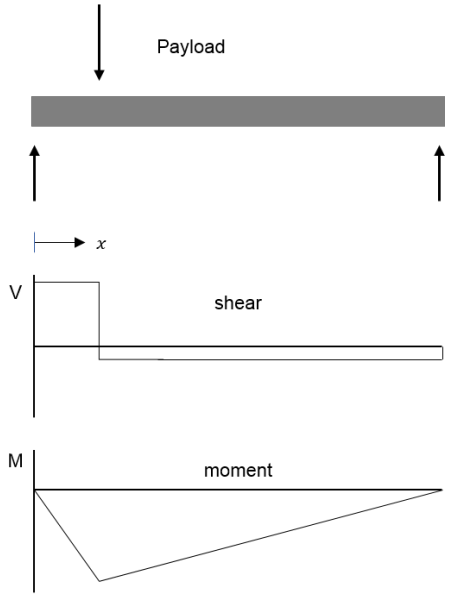

Figure 5.18: 2D schematic of the effect of payload near leg on shear and moment

Shifting the load along the edge towards the leg increases the maximum shear values with approximately 5.6 % to 69.5 tons with respect to the payload in the centre of the edge.

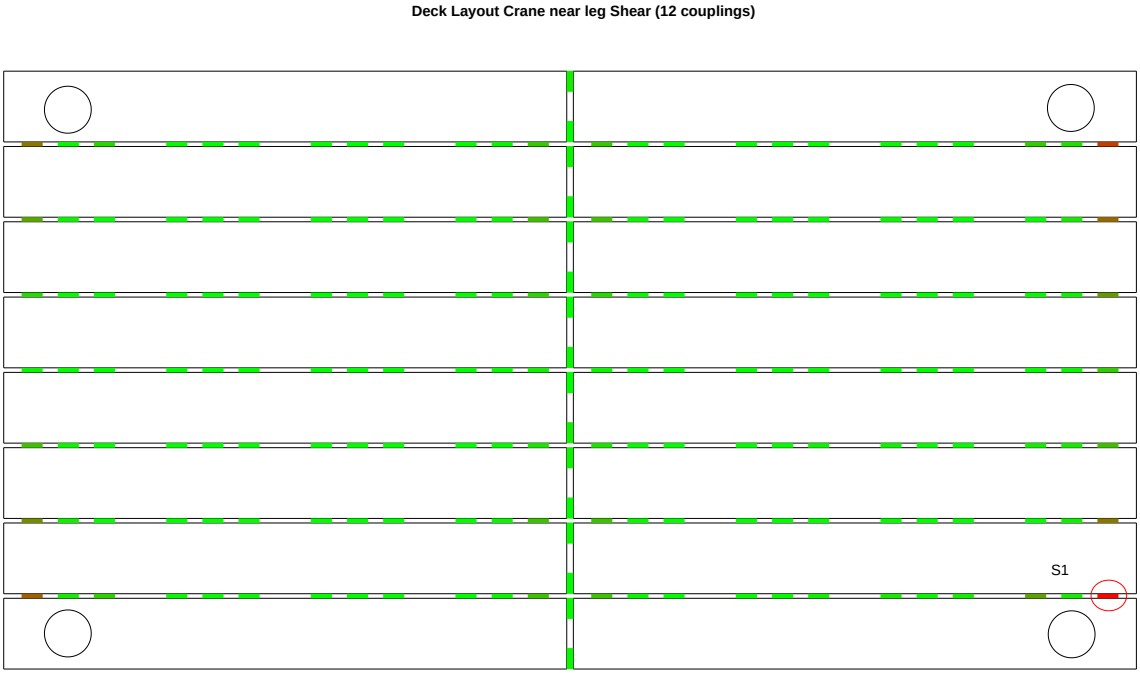

Figure 5.19: Colour visualisation of shear loading for Edge-to-Leg case (12 couplings)

Tensional Loading

Looking at the maximum loaded couplings with respect to tension. No real changes occur as the highest loaded coupling is still located at T1 between leg 1 and 2 which is far from the location(s) of the payload the effects on this coupling are not significant. Some of the couplings between legs 2 and 4 beneath the payload do increase in tension, however this tensional loading still remains significantly lower than the maximum value.

Again considering the scenario of a jack-up without payload resulting in a maximum tension load of 44.7 tons. Adding the payload on the edge and shifting it towards the leg increases the tension from 55.4 tons at

the centre of the edge to 55.7 tons towards the leg (T1).
Shifting the load towards the legs increases the maximum tension values with approximately 0.5 % to 55.7 tons with respect to the payload in the centre

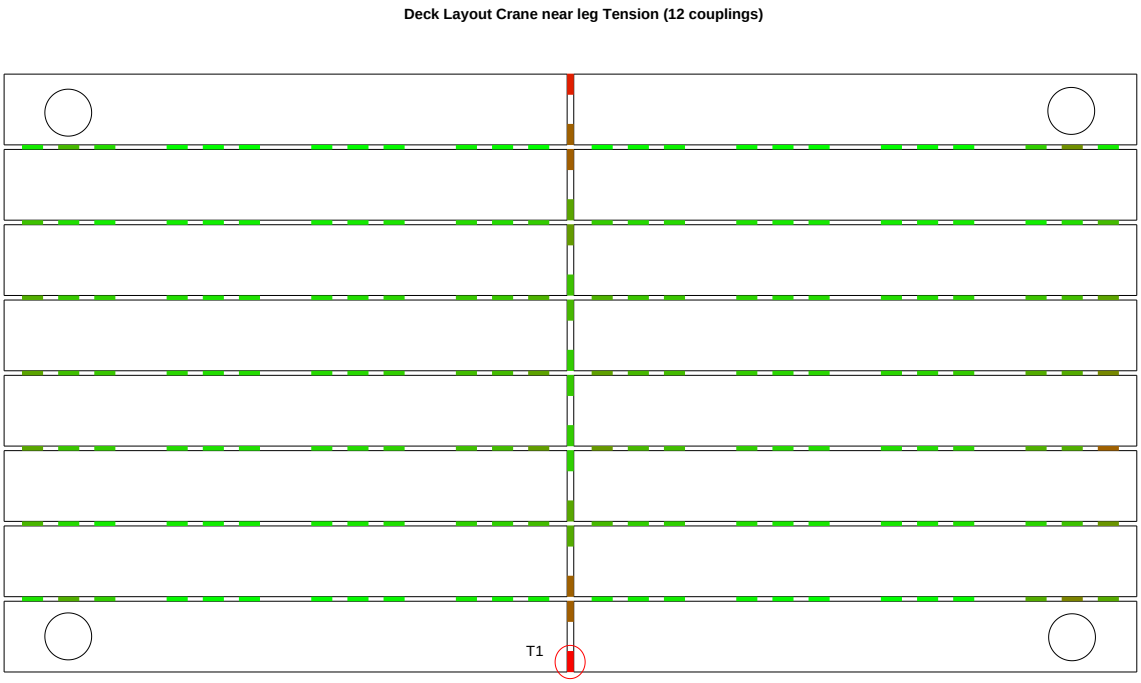

Figure 5.20: Colour visualisation of tensional loading for Edge-to-Leg case (12 couplings)

A summary of the findings on the maximum loading in tension and shear is found in table 5.3

Table 5.3: Summary of maximum loadings for center-to-edge case

Case	max. Shear [tons]	difference [%]	max. Tension [tons]	difference [%]
No payload	*39.9*		*44.7*	
E	65.8	-	55.4	-
H	69.5	5.6 %	55.7	0.5 %

5.3.3. Discussion

Considering the questions set up at the start of this study the following is concluded:

- *What is the influence of the location of payload on the loading of the structure?*

  The use of a mobile crane as defined above has significant influence on the maximum loading within the structure. The base case with the crane located at the centre of the structure results in an increase of approximately 10 and 20 tons in maximum shear and tensional loading respectively with respect to structure without payload.
  The movement of payload towards the edge of the deck mostly influences the tensional loading. The maximum loading reaches a value of 73.0 tons at the couplings beneath the payload corresponding to an increase of 13.7 % with respect to the base case.
  The second movement going towards the leg mostly influences the shear loading. Placement of the payload close to the leg leads to a maximum shear loading of 69.5 tons. The movement along the edge of the structure towards the leg results in an increase of 5.6 %. In comparison to the crane at the centre of the structure this load increases with approximately 18 tons (34.7 %).

- *How is the load distributed over the set of couplings in the configuration?*

  From the overall results it is concluded that the majority of the couplings is loaded within the region of 20 and 30 tons shear and tension respectively. It is found that loading in both tension and shear concentrates at the couplings near the legs and at the middle of the edges of the structure in longitudinal direction. Movement of the payload towards the edge significantly increases the outliers in tensional direction where movement towards the leg increases the outliers most significantly in shear loading.

5.4. Environmentals

This part of the case study investigates the influence of environmental conditions on the loading endured by the couplings. In this study research is performed on two aspects of environmental loading. In the first part the influence of the angle of attack is examined, where in the second part the influence of a different wave period is examined.
This study aims to find answers to the following questions:

- *What is the influence of the angle of attack of environmental conditions on the loading of the structure?*
- *How is the load distributed over the set of couplings in the configuration?*
- *What is the optimal environmental angle of attack for a JUP2420?*
- *How does the wavelength influence the loading of the structure?*

5.4.1. Angle of Attack of Environmental Loading

From design specifications of the JUP2420, a weather condition is defined in which the structure should be able to operate. This environmental condition forms the load case for the study on the weather angle.

Table 5.4: Environmental conditions for study on weather angles (confidential)

As mentioned in chapter 3, the loads applied on the structure due to these environmental conditions are attained from DAMEN software, using the specified wave height, period and the depth which is stated at 25 metres.

Three simulations are performed in which the environmental conditions as described above hit the structure at an angle of 0, 37.5 and 90 degrees respectively. An angle of attack of 0 degrees corresponds to the environmental conditions going over the x-axis of the overall structure. Or in other words along the longitudinal direction of the DMBs as shown in figure 5.21. the 37.5 angle corresponds to a loading over the diagonal of the structure.

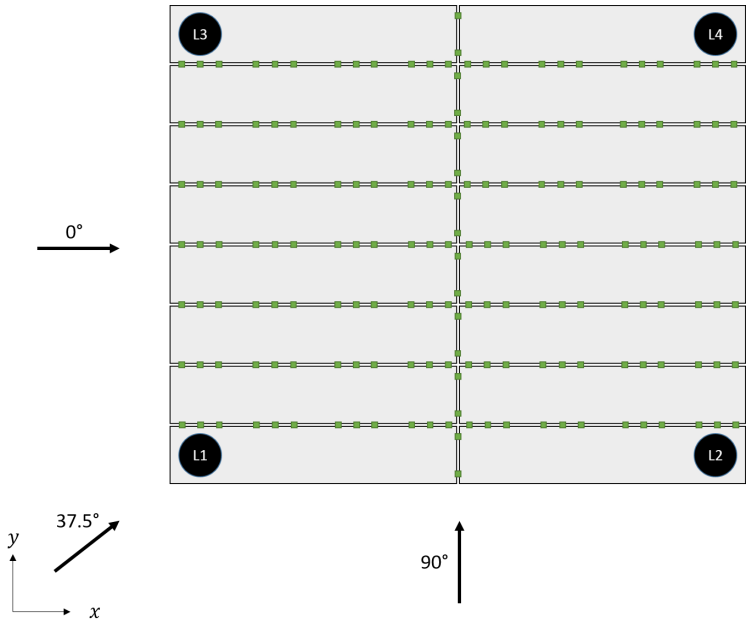

Figure 5.21: The three angles of attack for the case study on environmental loading

In these simulations the gravitational loading of the structure itself is taken into account. Furthermore, no additional loading in the form of a payload is present.

The results of these simulations are combined in figure 5.22. The lines in this graph show some load path that specific couplings follow throughout the simulations with different angles of attack. These loadpaths are discussed seperately in the following sections.

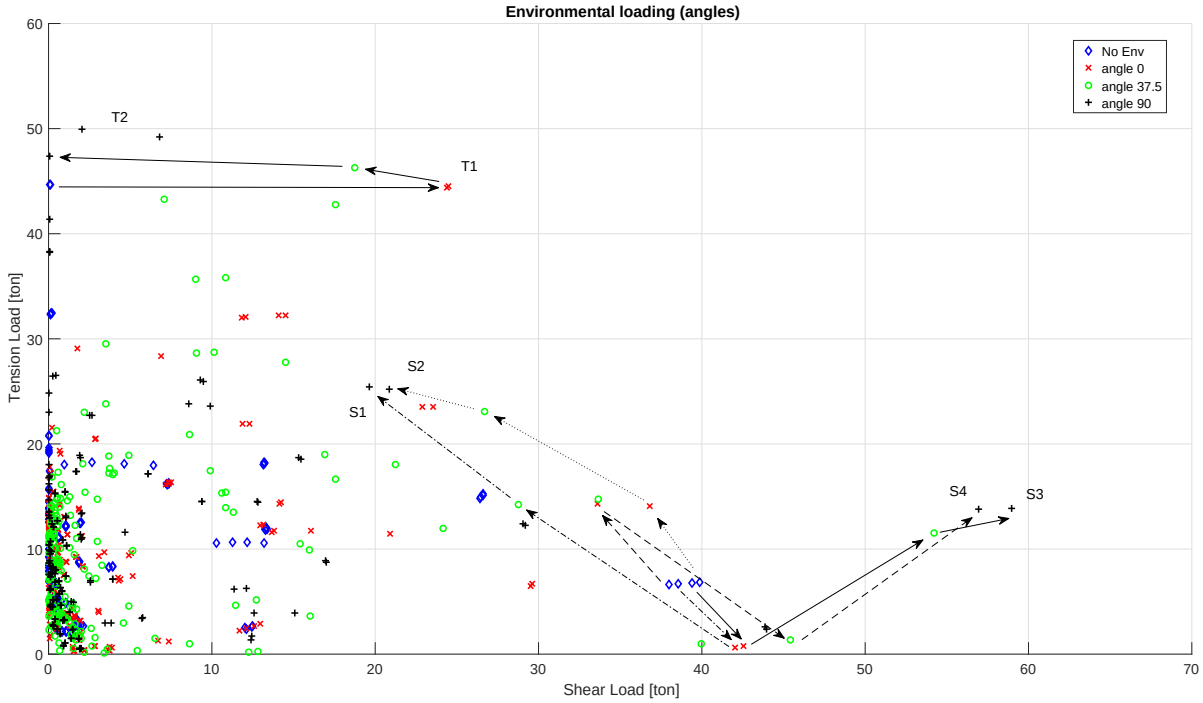

Figure 5.22: Results of the three angles of attack focussing on the load paths of the highest tensional and shear loaded couplings

From the overall results the focus lies on three locations in the deck structure shown in figure 5.23:
The first set of couplings described by T1 correspond to the outer couplings on the short ends of the DMBs in the longitudinal direction of the structure, as these couplings are loaded significantly in tension.
The second set consists of the outer couplings located near the legs experiencing the highest loading in shear (S1 to S4).
A third set of couplings described by T2 is found at leeward legs (when considering the 90° load case) as these are also highly loaded in tension.

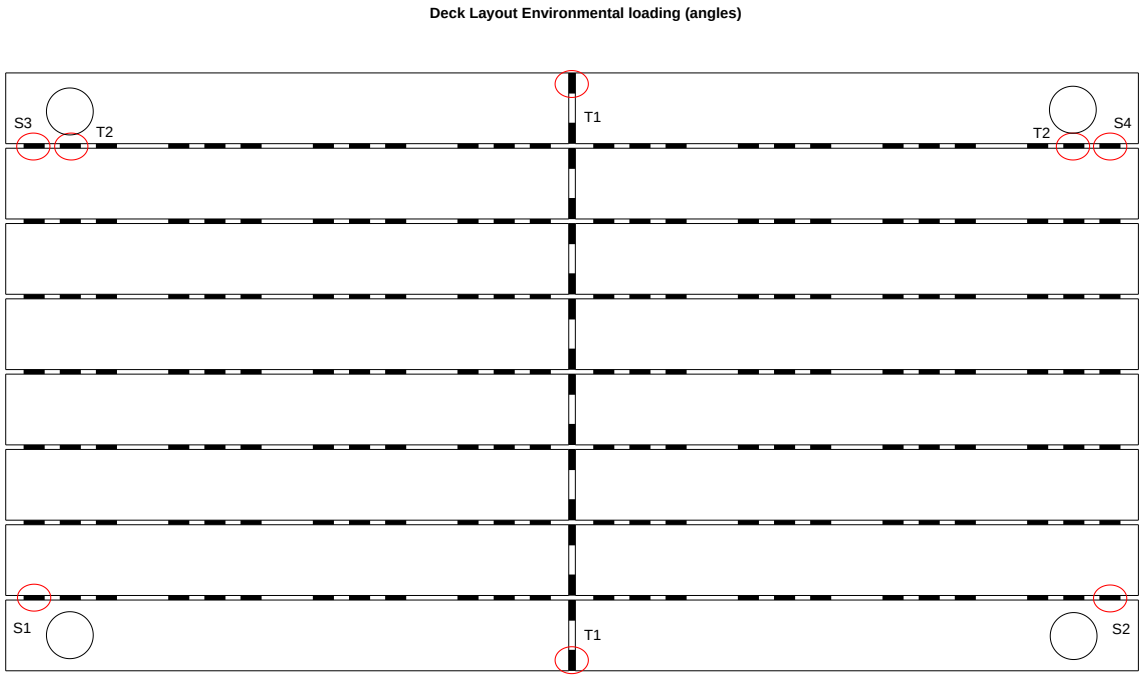

Figure 5.23: Locations of couplings which are loaded highly in shear or tensional loading

Shear Loading
The maximum shear loading in the structure is found near the legs at the outer couplings comparable to the load cases considering only gravity. The load paths these four couplings follow are discussed alongside the angle of attack changing from 0° to 90°.

In the case considering only gravity the four outer couplings (S1 to S4) are all loaded around 40 tons of tension. As the loading comes in at an angle of 0° the load distribution of these four couplings changes in the sense that the couplings S1 and S3 at the windward side of the structure decrease in shear loading where the couplings at the leeward side (S2 and S4) have an increase resulting in a maximum shear loading of 42.6 tons. This corresponds to an increase of maximum loading of 6.8 % with respect to the environmentally unloaded structure.

With the environmental loading coming in at an angle of 37.5° the maximum shear load increases up to 54.2 tons and is now located at S3.
As the angle is rotated over 0 to 37.5° the shear load in the couplings near the windward legs (S1 and S2) gradually decreases where the leeward located couplings gradually increases (S3 and S4).
The maximum shear load is found at 54.2 tons corresponding to an increase of 35.8 % with respect to the unloaded situation.

In the final situation the weather angle is set to 90°. This results in the highest shear loading. The maximum is now located at the leeward side of the structure at S3 and S4 with a value of 59.0 tons. This corresponds to an increase of 47.9 % with respect to the unloaded situation.

An explanation for the increase and decrease of the load at the couplings S1 to S4 is found in the combination of shear loading due to gravitational loading and environmental loading. In figure 5.24 a simplified schematic is shown in which the structure endures environmental loading. As it starts tilting towards the leeward end the rotational movement of the DMBs (that is imposed by the bending/tilting legs) is counteracted by the couplings in the transverse direction. The direction of this shear loading is the same for each coupling in the transverse direction (represented by the black arrows in the figure). The total shear loading of these couplings is a combination of both environmental and gravitational loading. On the leeward end these shear loadings will enforce each other where they will counteract each other on the windward end.

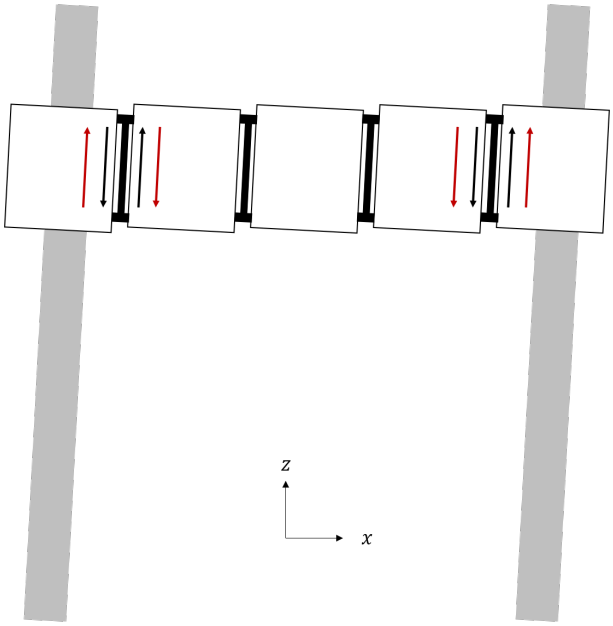

Figure 5.24: Shear load effects due to environmental loading (black) and due to gravitational loading (red)

Overall considering shear loading, the structure can withstand environmental conditions best at 0° angle of attack.

Tensional loading
Initially the highest tensional loading is found at locations presented by T1 in figure 5.23 similar to the gravitational case study.

At an angle of 0° the tensional loading on these couplings does not change significantly and even drops slightly to a value of 44.5 tons corresponding to a decrease in tension of 0.4 % with respect to the unloading condition. The horizontal loading due to weather conditions does not have a significant effect on the downward bending moments in the structure. The shear loading on these couplings does increase significantly, however it remains less than the shear concentrations found near the legs discussed above.

As the angle of attack increases to 37.5 % the tensional loading at T1 still remain approximately the same but the shearing load decreases. IT does appear that the tensional loading on the T1 coupling at the leeward side of the structure increases somewhat in comparison to the T1 coupling at the windward side.
The highest tensional loading in this case is 46.3 tons which corresponds to an increase of 3.6 % to the unloaded condition.

With the angle of attack at 90° the shear on the outer couplings at T1 has decreased to its original value of 0 tons in the unloaded case.
Again the changes in tension in these couplings is small. Comparing to the unloaded state the T1 coupling at the leeward side has increased with a few tons to a value of approximately 47 tons.
However, in the case of the 90° angle the highest tensional loading is found at a different location represented by T2. The couplings at T2 are found near the corners of the structure at the windward side. If one would draw a line from the centre of the windward leg to the leeward leg, the couplings located at T2 are on this line. The loads on these couplings increase significantly to 50.0 tons, corresponding to a 11.3 % increase with respect to the unloaded condition.

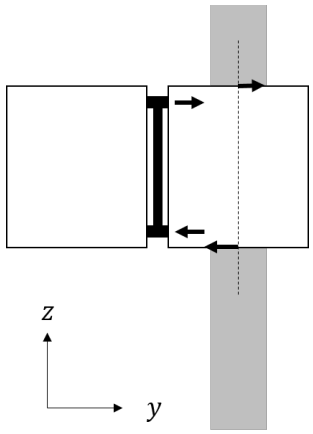

Figure 5.25: Bending moment introduced by the leg

A possible reason for the increase in tensional loading of these couplings is found in modelling the legs. In the model these are connected to the deck structure through two nodes at the top and bottom of the DMB. Due to the environmental loading these legs exert a bending moment into the DMB. As the coupling is located in line with the legs, a substantial part of this bending moment is transferred to these couplings creating high tension loads. This is shown in a simplified representation in figure 5.25.

Table 5.5 shows an overall summary of the maximum loading. It is concluded that the ability to withstand environmental loading changes significantly with changes of the angle of attack.
Loads from a 90° angle of attack result in the highest loading of couplings in both shear and tension. When this type of modular jack-up is located at a site where there is a predominant direction for the environmental conditions it is preferable to install the structure at an angle of attack of 0°.

Table 5.5: Summary of maximum loadings for different angles of attack

Case	max. Shear [tons]	difference [%]	max. Tension [tons]	difference [%]
No Env.	*39.9*	-	*44.7*	-
0°	42.6	6.8 %	44.5	-0.4 %
37.5°	54.2	35.8 %	46.3	3.6 %
90°	59.0	47.9 %	50.0	11.9 %

5.4.2. Wavelength

In the second part of this study the influence of a different wave period and corresponding wavelength is examined. It appears that the loading on the legs of the structure has significant influence on the loading endured by the couplings. Therefore it is investigated what the effects are when different types of waves are exerted on the structure. Two waves are identified as relevant for this study. These are visualised in figure 5.26.

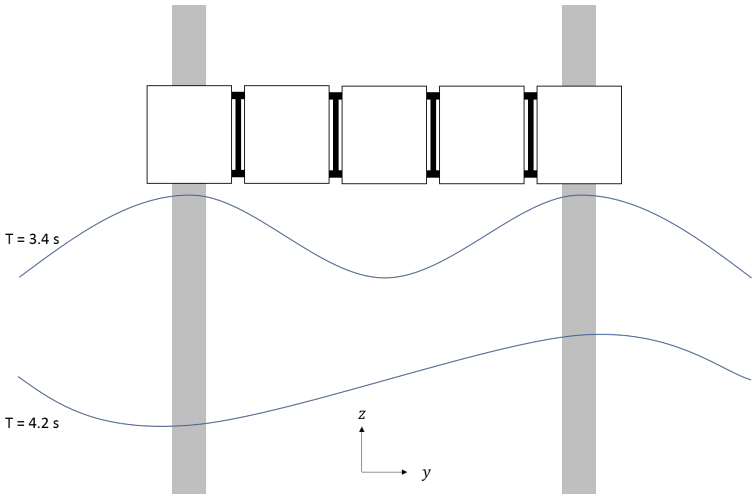

Figure 5.26: The two different wave periods considered for the study

The first wave has a wave length of 18 metres (approximately the distance between the windward and leeward legs). Using the dispersion relation[18] (equation 5.1) describing the relation between the length of a wave and its period this results in wave period of 3.4 seconds. With this wavelength the legs of the structure are loaded to a similar degree as both wind- and leeward legs can encounter the crest of a wave at the same time.

$$\lambda = \frac{g}{2\pi} T^2 \tanh(\frac{2\pi h}{\lambda}) \tag{5.1}$$

The second wave is set up to create the largest difference in loading on the front and rear legs of the structure. As visualized in figure 5.26 this corresponds to a situation in which two legs encounter the through of a wave at the same time as the other legs experience a crest. This correspond to a wave length of 1.5 times the distance between the legs (27 metres). From the dispersion relation this corresponds two a wave period of approximately 4.2 seconds.

In both simulations the structure is loaded in the 90° angle of attack taking into account only wave loading and gravity. Due to limitations of the external software with respect to these desired wavelengths (and periods) the wave height is limited to 1 metre (significant wave height). This is sufficient to investigate the difference in load patterns between these two wave conditions.
The results are combined in figure 5.27 in which the red and green data correspond to the different wavelengths of 18 and 27 metres respectively.

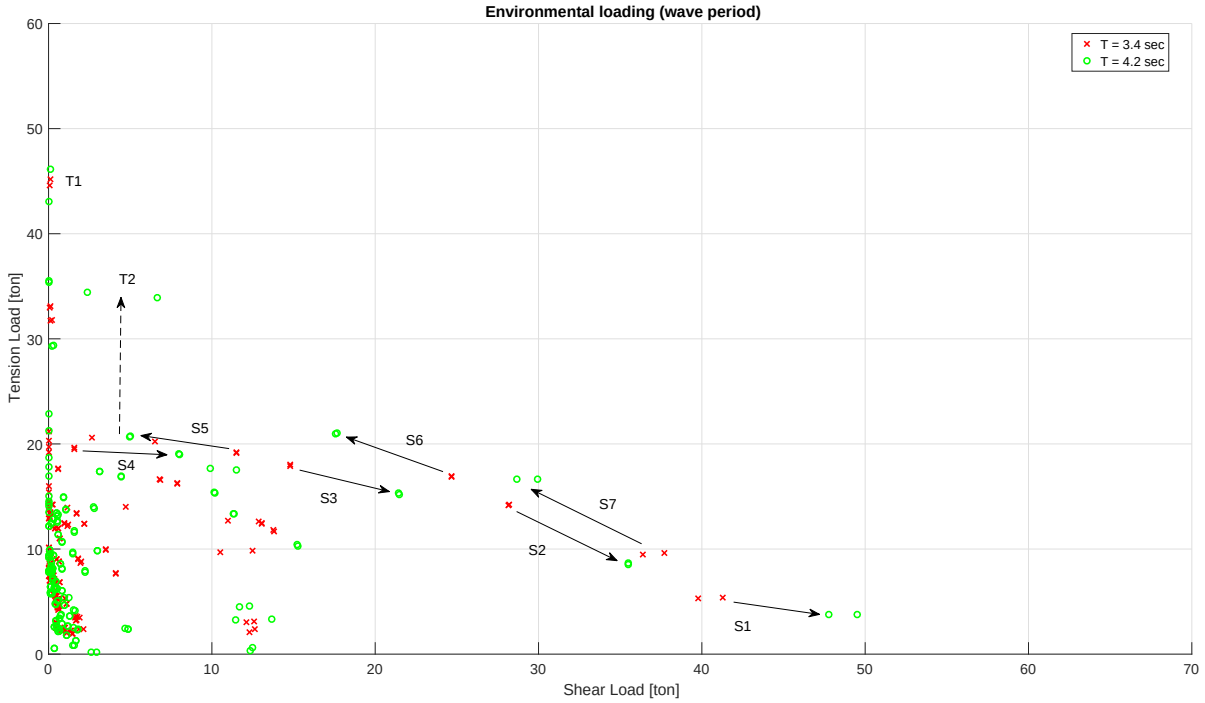

Figure 5.27: Results of the two different wave periods focussing on the load paths of the highest tensional and shear loaded couplings

Tensional Loading

The maximum tensional loading is overall again found at the location labelled as T1 in figure 5.28. For the 3.4 second wave the maximum loading is 45.2 tons. Applying the different wave type does not seem to influence this loading much as for the 4.2 second wave the maximum coupling loading increased with a ton to 46.2 tons. This corresponds to a percentage difference of 2.2 %. However, it must be noted that a similar pattern as in the first part of this study occurs at location T2 in which the tensional loading seems to increase significantly as the load on leeward legs increases. It is expected that under more severe loading the tension in these couplings located at T2 will eventually exceed the tensional loading at T1.

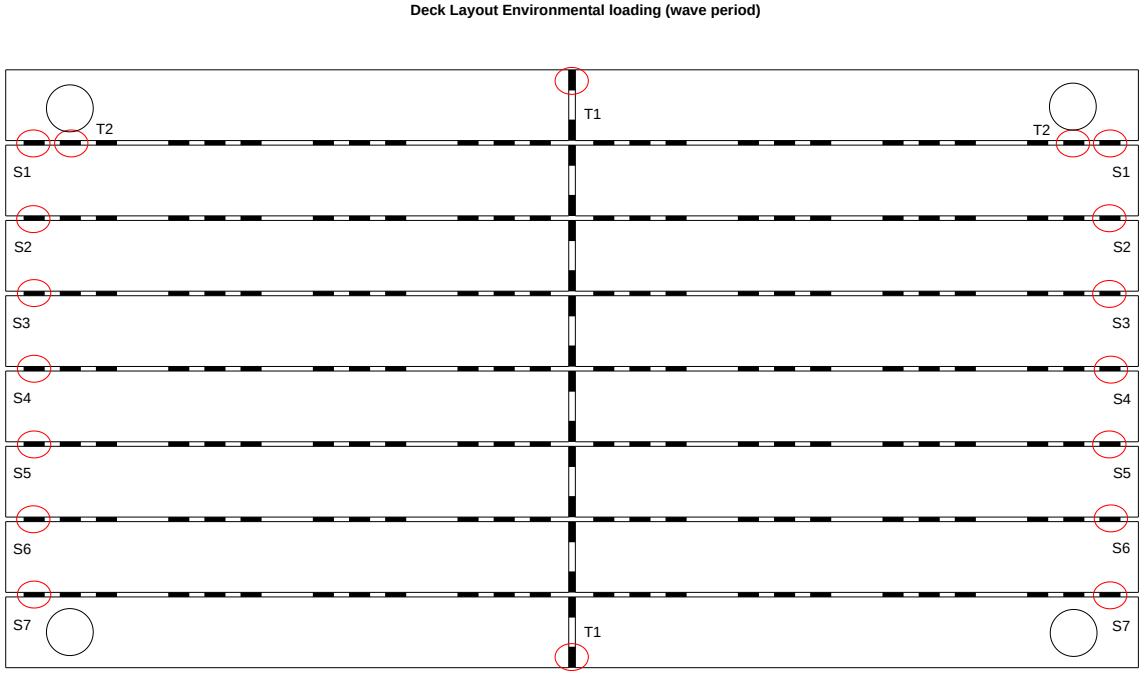

Figure 5.28: Locations of couplings which are loaded highly in shear or tensional loading

Shear Loading
In the shear loading a pattern is distinguishable for all outer couplings in the transverse direction labelled S1 to S7 (figure 5.28). For the initial wave load in which all leg are similarly loaded it is seen again that the couplings near the corners of the structure (S1 and S7) are most highly loaded with higher loading at the leeward side of the structure reaching a maximum of 41.3 tons in this case.
For the second wave, having a length of 27 metres, the time step is chosen at which the leeward legs experience high loading with respect to the front legs. In the results it shows that these outer couplings have all shifted with respect to their shear loading.
Going from S1 to S7 one goes over the structure from the more highly loaded rear legs towards the lesser loaded front legs. This is also visible in the coupling loading as the couplings located close to the rear have increased significantly where the couplings close to the front decrease.

A summary of the maximum results is shown in table 5.6 below. It can be concluded that a different wave period has a significant influence on the maximum loading on the couplings. Mostly with respect to shear loading.

Table 5.6: Summary of maximum loadings for different wave lengths

Case	max. Shear [tons]	difference [%]	max. Tension [tons]	difference [%]
T = 3.8 sec	41.3	-	45.2	-
T = 4.2 sec	49.5	19.9 %	46.2	2.2 %

5.4.3. Discussion
Considering the questions set up at the start of this study the following can be concluded:

- *What is the influence of the angle of attack of environmental conditions on the loading of the structure?*

  From loading the structure under environmental conditions from design specifications it is concluded that the angle of attack does not have a large influence on the tensional loading of the couplings. Only loading at an agle of 90° results in a gradual increase of 11.9 % to a maximum shear loading of 50.0 tons. This is presumably due to the bending moment introduced into the structure by the legs.
  Considering the shear loading the changes are more significant ranging from 42.6 to 59.0 maximum shear loading over the different angles. This corresponds to an increase of 47.9 %. A possible explanation for the high shear loading in the 90° is found in the combination of shear loading due to gravity and due to the tilting movement of the jack-up. At the leeward side of the structure this movement introduces a shear in the couplings that enforces the shear loading present from gravitational loading.
  Regarding non-linear behaviour it must be noted that in this case with horizontal transverse loading, the P-Δ effect was considerable. The additional overturning moment due to the displacement of the centre of gravity of the jack-up was in the order of magnitude of 20 % and 10 % (x-, and y-direction) of the inital overturning moment created by the external loading. Considering the results, it must be taken into account that the overall displacements due to this effect will be larger, presumably resulting in higher coupling loading.

- *What is the optimal environmental angle of attack for a JUP2420?*

  From the results, the tendency is that the structure can withstand the loading due to environmental conditions best at an angle of attack of 0°. In both tension and shear loading the couplings endure the least maximum loading. Environmental loading at an angle of 90° is least favourable for the structure.

- *How is the load distributed over the set of couplings in the configuration?*

  For the vast majority of the couplings within the structure the influence of the environmental loading is not significant remaining loaded within the region of 20 and 30 tons shear and tensional loading respectively. However, the outliers with respect to shear loading experience large increases. In tensional direction these changes are less significant. For all directions, the couplings located at the edges of the structure (T1 in figure 5.23) mostly experience changes in shear loading but not in tension. It must be

noted that under an angle of attack of 90° the tensional loading at other locations in the structure (T2) also experience high concentrations of tension.

- *How does the wavelength influence the loading of the structure?*

  From investigation of two scenarios considering different wavelengths it is concluded that there is significant influence on the shear loading in the structure. As a result of these different wavelengths the wind- and leeward legs either experience similar or different wave loading. In tensional loading the differences are negligible as the difference in maximum shear loading is only 2.2 %. In shear loading these differences are more significant reaching up to 19.9 % increase in maximum loading. Also the difference between the highly loaded couplings at the corners of the structure (shown in figure 5.23 by S1 and S7) is significant. The situation of large wave load differences between the wind- and leeward legs results in a difference of approximately 20 tons.

5.5. Punch-through

For the case on the punch-through an investigation is performed on different stages during a punch-through. The base of what is examined is a JUP 2420 structure without payload or environmental loading.
Within this study the following questions are investigated:

- *How can the developed model be used in the simulation of a punch-through?*
- *How does a punch-through influence the loading of the structure?*
- *To what extent is the current model valid for analysing a punch-through?*

First elaboration is given on the phenomenon known as punch-through.

5.5.1. What is a Punch-through

A punch-through is defined as "an uncontrolled vertical leg movement due to soil failure in strong overlying weak soil"[28].
Over 38 % of all jack-up accidents are related to geotechnical failure[27] of which the vast majority is in the form of a punch-through.
A jack-up stands on four (or three) legs. At the seabed these legs penetrate the soil up to a certain depth at which the upward reaction force of the soil is in equilibrium with the downward force of the structure. Figure 5.30 shows the relation between the bearing capacity of the soil and the penetration depth of the structure. This graph is a unique representation of the soil characteristics at a certain location.

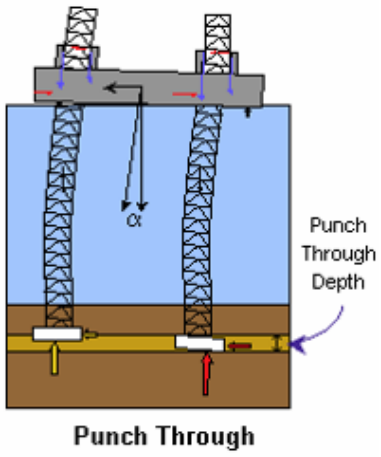

Figure 5.29: Schematic 2D representation of a punch-through[26]

Considering figure 5.29 and figure 5.30, a situation arises in which a deeper soil layer has less bearing capacity than the layer above it. If the downward force on one of the legs exceeds the peak bearing resistance of the top layer, the leg will 'punch through' this layer into the next (weaker) soil layer resulting in a significant additional penetration depth.
The consequences of a punch-through can result in tipping over of the platform or structural failure [9].
The study performed here is not focussed on the soil related specifics but on the effects of a punch-through on the deck structure.

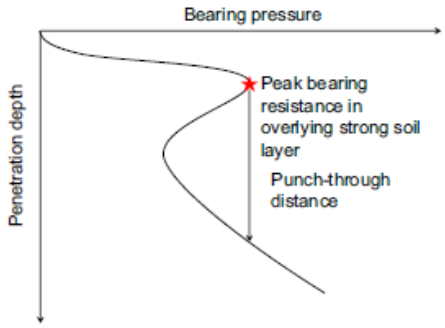

Figure 5.30: Relation between penetration depth and bearing pressure[9]

For the modular jack-ups that consist of the DMBs held together by couplings, it is of great interest to get insight on the effects of a punch-trough on the internal structure.
In section 5.5.2 different stages of a punch-through are examined using the model at hand. As this study may reach the limits of the model a discussion is opened on the results at hand and the validity of modelling such a phenomenon using this model.

5.5.2. Modelling a Punch-through

In the study the downward force on one of the legs is increased due to a horizontal load acting on the structure. It is stated that with the presence of this load a certain punch-through depth will occur.
The starting point of this study is a situation in which a horizontal load of approximately half of the stabilising moment of the structure is applied. This load is directed over the diagonal of the structure increasing the downward force on the leeward leg. This causes a punch-trough leading to an additional penetration of approximately 1.5 metres. Stating that the structure will tilt around its centre axis in the diagonal representation in the event of a punch-through the constraints at the windward and leeward leg are defined in the form of a linear spring representing the resistant forces that are exerted by the soil.
So considering the overall simulation, the structure is loaded by an external horizontal loading and experiences gravitational loading. No form of environmental loading or payload is taken into account. Furthermore, the structure is constrained at the seabed using a combination of simple supports and linear springs.

Spring and Load
As mentioned, the base of this punch-through is set on a displacement of the leeward leg over approximately 1.5 meters. This section elaborates on the values chosen for the loads and linear springs used to mimic soil reaction forces.

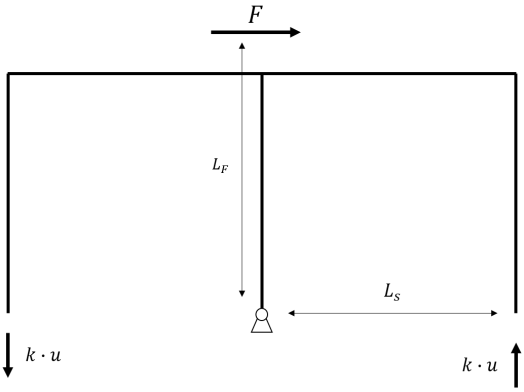

Figure 5.31: Relation between external load and added springs.

Based on a 2D diagonal cross-section of the structure a static relation is set up between the forces acting on the legs and the external force F while assuming a rigid construction.
The load is based on the stabilizing moment around the leeward (right) leg due to the weight (W) of the structure. This moment is described as the weight of the structure working as a downward load in the centre of gravity in the middle of the structure ($W \cdot L_s$). Taking the overturning moment to be approximately half of the stabilizing moment results in an external load as defined in equation 5.2. This load implemented is approximately 980 kN.

$$\begin{aligned} F \cdot L_F &= \frac{W \cdot L_s}{2} \\ F &= \frac{W \cdot L_s}{2 \cdot L_F} \end{aligned} \tag{5.2}$$

For the structure visualized in figure 5.31 the relation between the spring forces at the wind- and leeward legs and the external load is set up (equation 5.3). From the statement that the leg drops down 1.5 metres due to the loading defined in equation 5.2, this results in a spring coefficient k of $\frac{W}{6}$ N/m. This corresponds to a value of approximately 654 N/m.

$$\begin{aligned} F \cdot L_F - 2 \cdot k \cdot u \cdot L_s &= 0 \\ k = \frac{F \cdot L_F}{2 \cdot u \cdot L_s} &= \frac{W}{6} \end{aligned} \tag{5.3}$$

These relations are based on a static representation of the (rigid) system not taking into account possible deformations. The effect of these assumption are shown in the first results as the punch-through exceeds the 1.5 metres and reaches equilibrium at approximately 1.6 metres.

It is appropriate to model a punch-through by three phases. The following sections elaborate on these different phases. The difference between the phases with respect to modelling lie primarily in the methods used to constrain the structure. At the first phase no punch-through has occurred yet while the structure endures the external loading but all legs remain in place. In the second phase the punch-through is initiated as one of the legs punches through the soil. In the third phase the degree of tilting of the structure resuls in an upward displacement of the windward leg.

Phase 1
The first phase is the pre punch-through phase in which the load is executed on the structure but no punch-through has occurred yet. In the modelling of this phase the original set up of the model is used at which the configuration stands on all four legs being simply supported. Figure 5.32 shows a 2D cross-sectional schematic of the modelled situation. The leg on the left is seen as the windward leg and the one on the right as the leeward leg where the punch-through occurs.

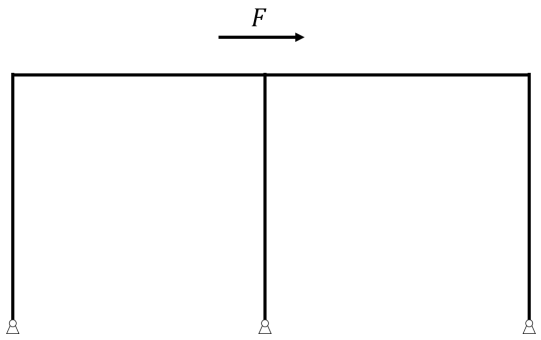

Figure 5.32: 2D cross sectional schematic of phase 1 of the punch-through

Phase 2
In the second phase of the process the soil beneath the leeward leg has failed resulting in the punch-through. At this primary stage of the punch-through the constraint on the leeward leg is changed as it will start sagging into the soil. The simple support on this leg is replaced by a linear spring in the vertical direction. The stiffness of this spring is soil dependant. However, in this simulations the coefficient is based on attaining a final displacement of 1.5 meters due to the presence of the external force as stated above.
In this phase the structure starts to tilt towards the leeward leg. The other legs might tilt due to the movement but still remain in place using simple supports.

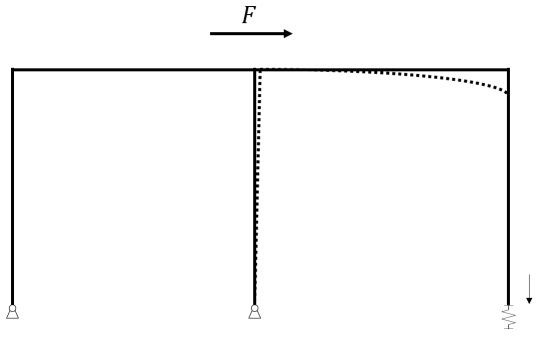

Figure 5.33: 2D cross sectional schematic of phase 2 of the punch-through

Phase 3
As the structure progresses to tilt in the direction of the leeward leg at a certain point the windward leg starts moving upward as it is pulled out of the soil. As the leg moves upward it experiences resistance from the soil surrounding it.
This scenario is modelled by the removal of the simple support at the windward leg replacing it with the same soil spring as installed on the leeward leg. Figure 5.34 shows a 2D representation of this phase.

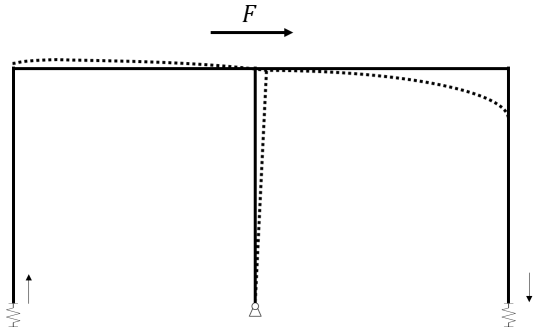

Figure 5.34: 2D cross sectional schematic of phase 3 of the punch-through

Displacements
From the analysis of these three situations the results with respect to the downward displacement of the leeward leg are shown in table 5.7

Table 5.7: Leeward leg vertical displacement

Phase	Leg displacement [m]
1	0
2	0.32
3	1.62

5.5.3. Load Results
For the three different phases the analysis is performed. The results with respect to the coupling loading are combined in a single graph (figure 5.35. The results of the first to the third phase are shown in different colours from blue to red to green respectively. In the following sections the results are discussed with respect to:

- Shear loading (S1, S2, S3)
- Tensional loading (T1)
- Leg couplings (LC1, LC2, LC3)

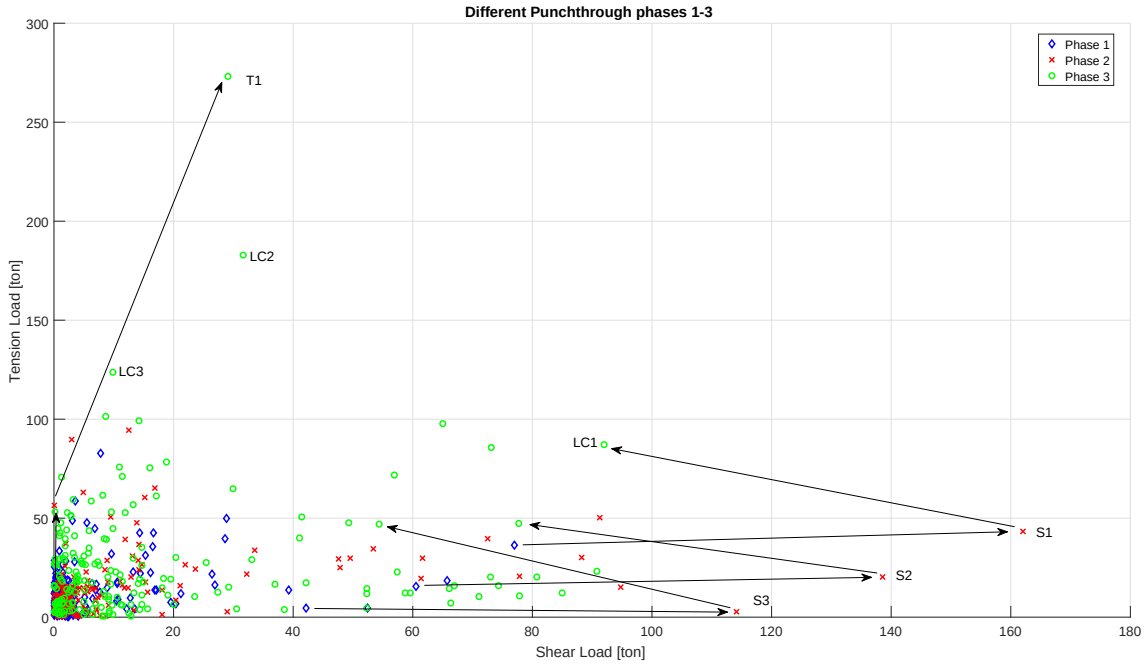

Figure 5.35: Coupling loading for the three different punch-through phases

In figure 5.35 the couplings loaded highest with respect to shear are labelled S1, S2 and S3. Similarly the highest loaded coupling in tension is labelled T1. The arrows show the load path of these couplings from phase 1 to 3. Figure 5.36 shows the locations of these coupling with the circular cross in the right top corner indicating the leg experiencing a punch-through. The couplings close to the leg in the top left corner are labelled as LC1 to LC3.
Note: It is chosen not to use coloured representation of the couplings as the results consist of three different analysis.

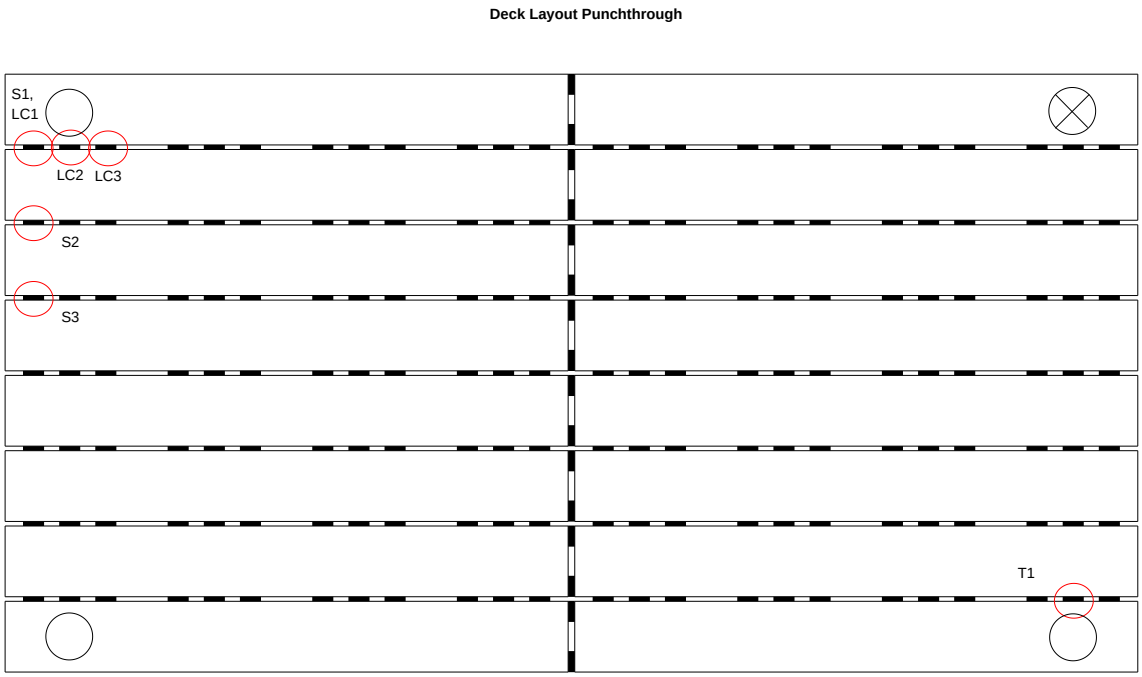

Figure 5.36: Highest loaded coupling locations in modelled punch-through

Shear Loading (S1, S2, S3)
In the shear loading a pattern is found for the three couplings labelled S1 to S3. In each of the phases the highest sheared coupling is found close to the leg at location S1.
Recalling the gravity case scenario of section 5.2, where no external loading was applied on the structure apart from gravity, the highest shear loading was approximately 40 tons. Through the modelling of the punch-through this maximum value increases from 77.0 to 162.0 and decreases back to 92.0 tons in phases 1 to 3 respectively. The highest forms of shear are found in phase 2.

Note that in the first two phases, the concentration of high shearing occurs at these three couplings (S1, S2 and S3). In the third phase the highest loaded coupling is still found near the left top leg, but another string of highly shear loaded couplings is found along the centreline of the structure as depicted in figure 5.37.

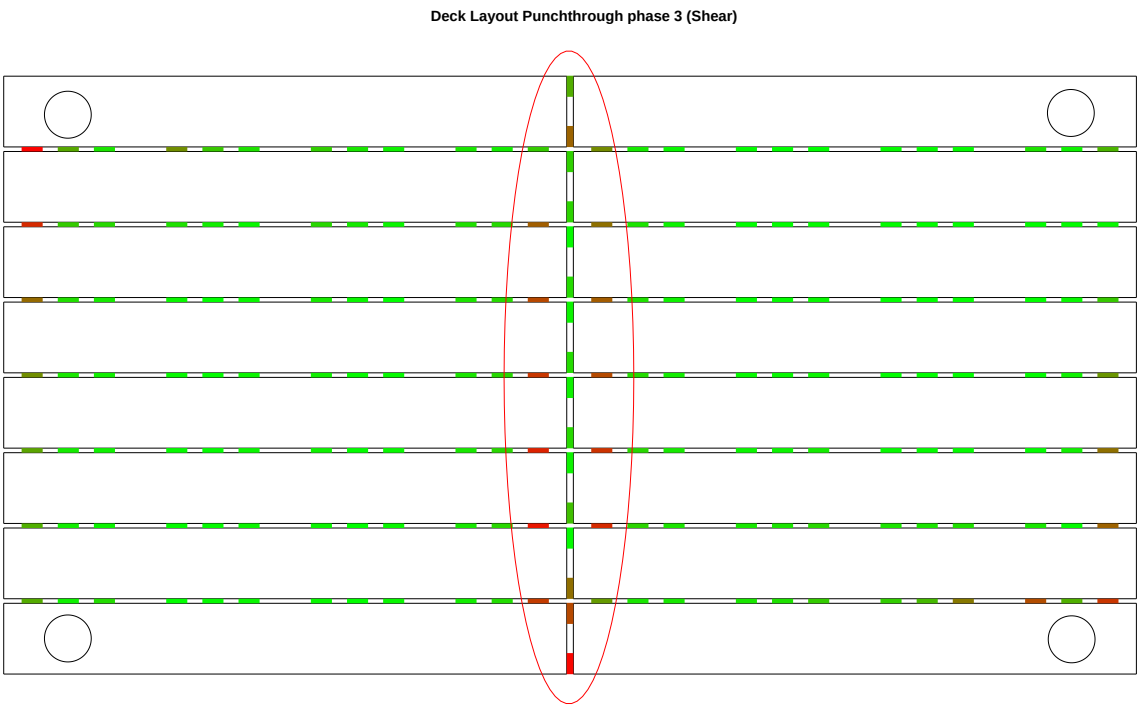

Figure 5.37: Coloured representation of couplings loaded highest in shear in phase 3 of the punch-through

This might be explained as most of the veritcal reaction force from the soil will occur at the legs forming the diagonal supports of the structure.
In addition it is found that the shearing in the couplings around this centreline (figure 5.35) is larger at the couplings leaning towards the left bottom leg. This in comparison to those at the right top of the centreline more in the direction of the leg that endured the punch-through.
When considering the diagonal with the supported legs of the structure again in figure 5.38 it can be noted that on the left half of the figure the shearing force coming from the gravitational loading is enforced by the downward forcing on the left leg caused by the linear spring.
This in contrast to the right side where the upward forcing on the leg from the linear spring counteracts the shearing contribution of the gravitational loading.

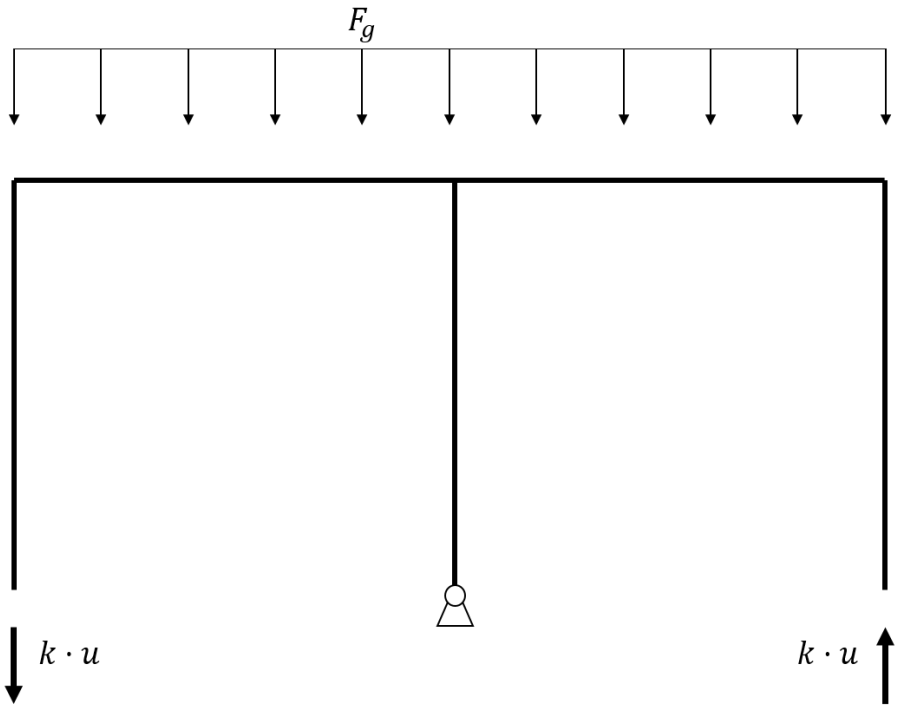

Figure 5.38: Vertical loading contributing to the shear load in the structure

Tensional Loading (T1)
For the tensional loading of the jack-up in the 3rd phase of the punch-through a single coupling located at T1 endures the highest load in tension. From the gravity case scenario where the jack-up is loaded under gravitational force it is recalled that the highest load was found at the centreline (figure 5.6) having a value of approximately 47.2 tons. As can be seen the highest loaded coupling has shifted towards the bottom right leg. Focussing on the load path of this coupling shows that the increase between the first phases of the punch-through is relatively small comparing to the increase of tension to phase 3. Even though the tension of this coupling is more then doubled between phase 1 and 2 from only 22 tons of tension to 56.4, it drastically increases to a value of 273 tons in the final phase.

5.5.4. Leg Phenomenon (LC1, LC2, LC3)

In the final results form phase three another phenomenon is found on the couplings close to the top left leg where the highest shear load is found.
In this 3rd configuration the three couplings at the left top between the DMB that houses the leg and the one below are all highly but also differently loaded (figure 5.36).
In figure 5.35 these are labelled LC1, LC2 and LC3, with LC1 being the outer coupling of the three. As these three couplings are so widely spread within the high loading region of the graph additional research is carried out on the cause of the high loadings at this location.
With respect to shear (x-axis), figure 5.35 shows that LC1 to LC3 are loaded 92.0, 31.6 and 9.8 tons respectively. It appears that the shearing load changes direction over these 3 couplings from LC2 to LC3. A visualization of this is shown in the schematic in figure 5.39. So looking at the values again over LC1, LC2 and LC3 one might say that the shearing is approximately 92.0, 31.6 and -9.8 tons respectively.

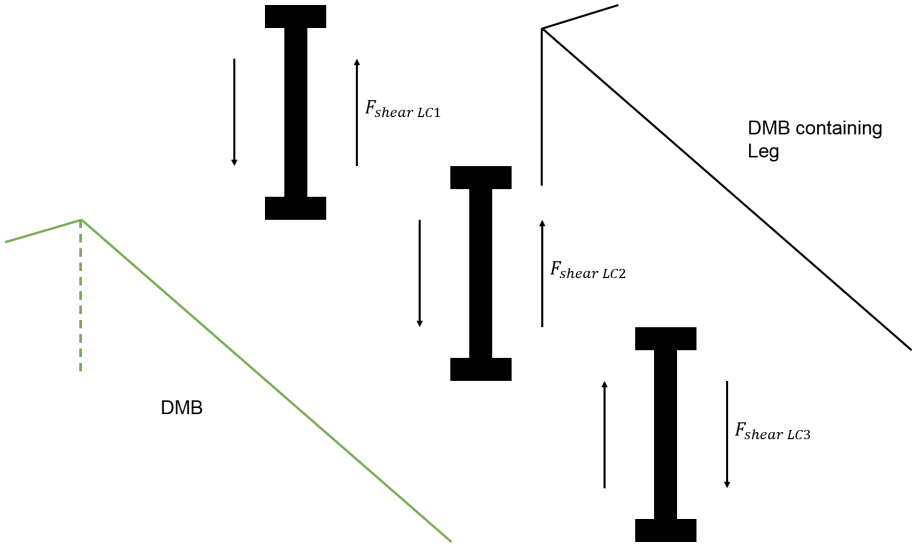

Figure 5.39: Coloured representation of couplings loaded highest in shear in phase 3 of the punch-through

A possible reason for this phenomenon is the influence of the leg on the outer DMB.
As the structure starts to move towards the leg that has endured a punch-through the legs over the diagonal tilt in this direction. As the leg is guided through the corner DMB it will force the outer DMB to make a rotational movement. However, as the DMB is connected to the rest of the deck structure it is withheld to do so. This scenario can cause quite some bending movement in the outer DMB. A simplified visualisation of this scenario is shown in figure 5.40 in which the bending of the outer DMB containing the leg is shown by the horizontal black line.
As the DMB next to it, visualised by the green line, does not house a (stiff) tilted leg structure it is also not forced into the same bending motion. Due to its own structural stiffness it will relatively retain its original form with respect to the outer DMB. The couplings between these DMBs at the leg endure these forms of loading as stated above due to these different occurring displacements. One could say that at the outer two couplings (LC1 and 2) the corner DMB is *pulling* the couplings upward with respect to the 2nd DMB where at the third coupling it is *pushing* the coupling down. Towards the the right the deformations of both DMBs eventually 'align' again.

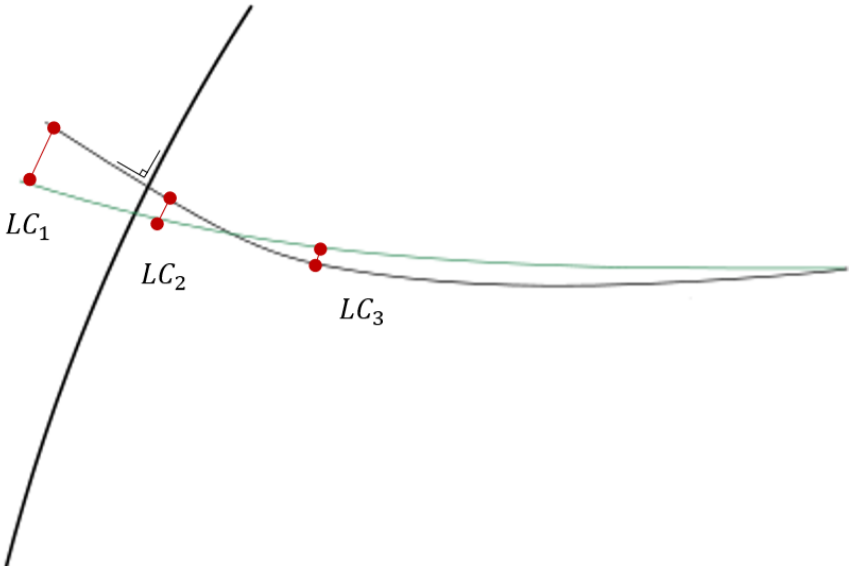

Figure 5.40: Simplified representation of bending movement in DMBs close to the top right corner

5.5.5. Discussion

Based on the methods chosen to model the phenomena of a punch-through and the results, a discussion can be held regarding the questions set up at the start of the section.
As the nature of this study differs from the other cases on environmentals and payload it is chosen not to elaborate on the questions separately but form an overall discussion touching upon all questions defined.

Elaboration on the modelling of a punch-through is performed in section 5.5.2. This type of modelling provides the ability to simulate a specified punch-through scenario. The analysis gives indications on the magnitudes and locations of high loadings that can be expected in the occurrence of such event.
The analysis of the different phases provides additional insight in the changes of these high loadings during the process.

The results differ greatly between the different phases. This makes it clear that the choices made in (especially) the way of constraining the structure has significant effects on the outcome of the analysis.
This sets up a discussion on the results from phase 1 to 3. Considering the maximum shear, the largest loading occurs in phase 2 with the windward leg still constrained to the seabed using a simple support. During a punch-through the change of a windward leg being firmly footed into the soil to starting to move upward is a gradual process. From this it might be found that the extreme results found in phase 2 may never occur as the windward leg might already have gradually started to detach from its original position.
Considering the legs on the diagonal of the punch-through, these are simply supported which implies that throughout the process they do not experience any translational displacement. As a punch-through occurs the weigh carrying capacity of one leg is dropped. As a result the three remaining legs of the structure will exert a higher pressure on the soil as the structure's weight is now divided over three legs instead of four. As a result it is expected that the two legs forming the diagonal will also be driven deeper into the soil. However, when considering this type of analysis from a coupling point of view this also makes that one might view the resulting high loading as a conservative approach.

The results show primarily that the way of constraining has large influences on the outcome. In this area improvements can be made on the modelling method. When for a certain scenario more knowledge is at hand on the soil properties below a jack-up these can be used to constrain the system with a higher accuracy. Specified soil characteristics can help in setting up the values for the linear (and maybe also rotational) springs used to simulate soil interactions.

On the assumptions made and the validity of the outcome the following can be noted: The phenomenon of a punch-through can take place in a slow or fast manner. As the model is of a quasi-static nature possible dynamic effects during a punch-through are not taken into account.
Secondly, the way of constraining the structure highly influences the outcome. Lacking knowledge on site specific soil characteristics implies assumptions made on the simple support and linear spring constrains used within the structure. However, as mentioned this can be improved in future analyses when more site specific characteristics are at hand.

The outcome of the model provides insight on the loading pattern as a result of a specified scenario. Further research can be carried out on different scenarios using this type of modelling to get more insight into the influence of the phenomenon in general.

Concluding this type of modelling of a punch-through can be useful to DAMEN as it indicates the magnitudes and locations of high loadings that can occur.

5.6. Conceptual Assessment on the Operability of the JUP2420

From the results of the case studies a feasibility study is performed on the JUP2420 design based on the capacity of the couplings.

In graph 5.41 the results of the studies have been combined in an overall plot. The included data are the results on:

- The structure under gravitational loading
- The structure with a payload at the edge of the longitudinal end
- The structure with a payload at near the leg
- The structure loaded under environmental conditions from different angles

In appendix C.2 the results of these different cases are visualised separately in combination with the capacity curves.
Combining the results into an overall assessment makes it possible to answer the following question:

- *Is the conceptual design of the JUP2420 sufficient to withstand operational weather conditions and loading experienced from the use of a mobile crane?*

Figure 5.41: Combination of the results of studies performed on gravity, payload and environmental conditions (confidential)

From the studies it is determined that the couplings located near the legs and those located at the edges of the structure in the longitudinal direction are determinative on the maximum loading (figure 5.42). The couplings in these locations have been plotted using a red colour in the results graph.

As mentioned in chapter 3 DAMEN is developing couplings for these modular jack-up configurations and have asked for evaluation based on the three included curves visualised in figure 5.41.
Coupling #1 corresponds to the coupling currently used for other modular (floating) products.

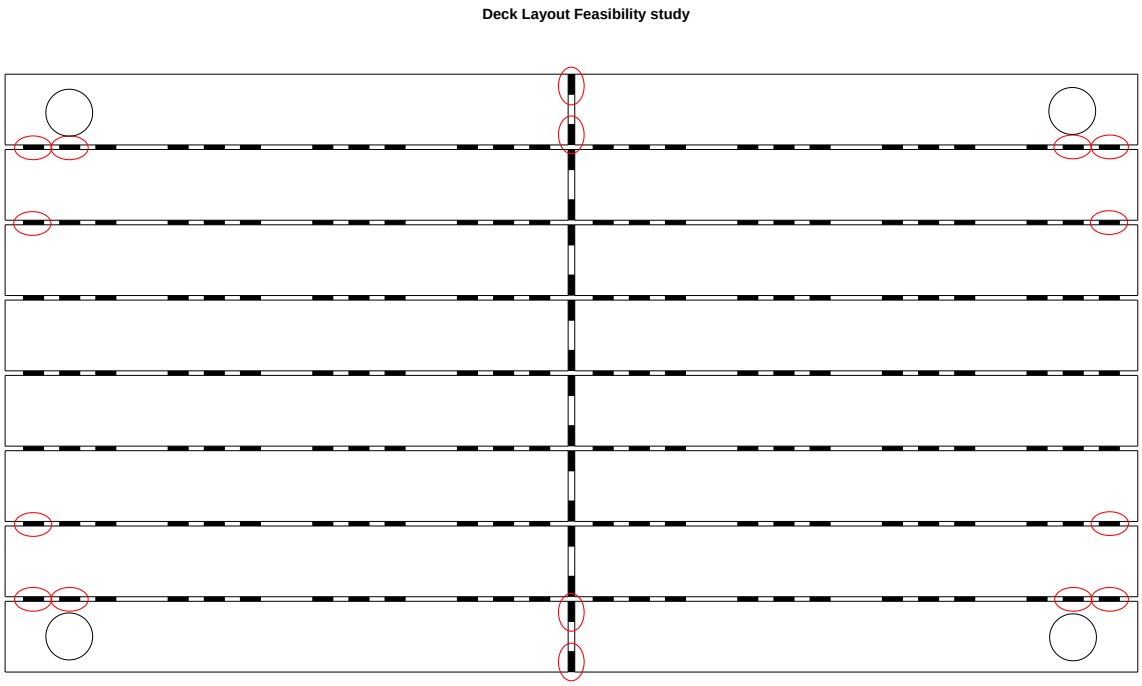

Figure 5.42: layout of couplings highly loaded in the structure

Considering the overall results it can be seen that for the majority of the couplings within the structure coupling #1 would suffice.
However, the outliers located at the edges of the structure often exceed the capacity of this coupling vastly.

The highest forms of outliers are encountered in the case studies on payload. The placement of the payload near the edge of the structure results in the highest tensional loading at approximately 73.0 tons.
The maximum shear load overall is reached in the case study on the placement of the payload near the legs resulting in 69.5 tons.

Considering the maximum loading reached through payload operations coupling types 1 and 2 will not suffice. This conclusion is strengthened by the fact that in operation, a jack-up will endure a combination of loading of *both* payload and environmental conditions.

For the design of the JUP2420 it is advised to focus on the development of the strongest couplings (coupling #3) as this is the only type of the three sufficient to take on the loading of the outliers.

From the studies it follows that there are specific critical areas in the deck but the majority of couplings is loaded within the region of 20 tons shear and 40 tons tensional loading. In the further design of the JUP2420 it is sensible to focus on enforcing the structure and connections at these critical locations.
In addition to this it is found that a large part of the couplings seem never to be highly loaded. It can be considered unnecessary to implement 12 couplings on the sides of each DMB throughout the complete structure. However, in this case further research is necessary on the redistribution of loading in the structure after removal of couplings from the original configuration.

The results on punch-through are not taken into account in the feasibility study shown in figure 5.41 as it is considered not a standard loading endured by the jack-up in operating conditions.
However, the results of the punch-through study indicate that in the occurrence of such event, the loading in the couplings can increase vastly in both shear and tensional loading. These loadings can exceed the coupling capacity resulting in failure. It is reasonable to consider that due to this the deck structure can disintegrate during a punch-through. This is an added aspect in comparison to jack-up designs which are not modular. In designing these types of structure this must be taken into account.

5.6.1. Discussion

For the question set up at the beginning of this section the following is concluded:

- *Is the conceptual design of the JUP2420 sufficient to withstand operational weather conditions and loading experienced from the use of a mobile crane?*

  The overall results of the different studies performed on payload location and environmental loading show that the base design using the current couplings is not sufficient. Even when the design is fitted with the maximum amount of couplings, the outliers in both shear and tensional loading exceed the capacity of the couplings.
  For the development of couplings it is advised to focus on coupling # 3 as this is the only type able to withstand the loading reached by the outliers of the system.
  As the study on payload locations results in the highest loading it is also advised to consider boundaries on the face of the deck structure limiting certain locations where a payload such as the mobile crane is not allowed to be located.
  Furthermore it must be noted that the results of all cases are separately focused on a single load. In operation a jack-up experiences a combination of loading due to gravity, payload and environmental conditions at the same time.
  In further assessment of this conceptual design it is advised to do overall load case simulations on these external loadings combined.
  Regarding the models limitations discussed in section 3.9, comparing the results from the cases to the capacity curves show that especially for the #1 and #2 coupling the resulting loads will probably exceed material yielding properties making them more inaccurate.

5.7. Leg Implementation

The case studies performed show among other things that the legs have significant influence on the loading of couplings surrounding it. For this reason additional research is performed on the leg implementation method chosen in the methodology.
For this additional research the following research question is formulated:

- *What is the influence of the stiffness of the connection between leg and hull on the loadings endured by the couplings?*

In the current implementation method, the leg is connected to the hull using 2 nodes at the top and bottom of the DMB. As discussed in section 3.5.3 the nodes at the top are rigidly connected in all 6 degrees of freedom, whereas the bottom connection only considers the horizontal translational degrees of freedom (x- and y- direction).

It is examined whether reducing the stiffness of this connection reduces the maximum loading in the couplings.
For the external loading, the environmental conditions from section 5.4 are used with an angle of attack of 0 and 90 degrees (figure 5.21).

First the rotational constraints (for ϕ, θ, ψ) applied at the top node are removed, allowing the leg and structure to rotate with respect to each other.
In addition also the constraints in the horizontal translational directions are modified. The rigid connection between the nodes of both DMB and leg, is replaced by a virtual spring introducing a (variable) stiffness in the x- and y- directions.

To investigate the influence of the stiffness of the connection, the simulation is run several times while gradually reducing the stiffness of the spring from rigid to flexible.
Lowering the stiffness between the leg and hull makes it possible for both to attain different displacements. From the specifications of the JUP2420 it is found that the gap between the leg and the guide is approximately 20 millimetres. This 20 mm is taken as the limit for the maximum difference between the horizontal displacements.

The results of the maximum loadings from the simulations are shown in table 5.8 and 5.9.

The first line shows the result from the base case with rigid connections in all 6 DOFs. From the second line downward, the rotational constraints are removed and the specified translational spring stiffness is used. The second line shows that the removal of rotational constraints only, does not affect the loading significantly (for both the 0 and 90 degree cases).

Table 5.8: Maximum coupling loading using translational spring at leg-hull interface for 0 degree case

angle of attack: 0°					
stiffness k [N/mm]	Δ disp [mm]	Shear [ton]	%	Tension [ton]	%
rigid	0	42.5	-	44.5	-
$1 \cdot 10^8$	0	42.6	0.24	44.5	0.00
$1 \cdot 10^7$	0.2	42.6	0.24	44.6	0.23
$1 \cdot 10^6$	2.3	42.8	0.71	44.8	0.67
$1 \cdot 10^5$	*34.8*	44.9	5.65	45.6	2.47
$1 \cdot 10^4$	*82.8*	41.2	-3.06	46.3	4.05
$1 \cdot 10^3$	*26.6*	40.2	-5.41	46.3	4.05

The simulations regarding an angle of attack of 0 degrees do not show an improvement in the results of the maximum coupling loading. The loading even increases slightly in comparison to the base case as the spring stiffness is reduced. In terms of displacement, the use of stiffness below an order of magnitude of 10^6 N/mm exceeds the limitation of 20 mm difference. From further investigation of the result it also appears that these analyses reach outside of the models limits as it produces non-credible results showing negative overall displacements.

Table 5.9: Maximum coupling loading using translational spring at leg-hull interface for 90 degree case

angle of attack: 90°					
stiffness k [N/mm]	Δ disp [mm]	Shear [ton]	%	Tension [ton]	%
rigid	0	59.0	-	50.0	-
$1 \cdot 10^8$	0	58.9	-0.17	49.9	-0.20
$1 \cdot 10^7$	0.1	58.9	-0.17	49.7	-0.60
$1 \cdot 10^6$	0.7	58.1	-1.53	48.1	-3.80
$1 \cdot 10^5$	5.6	52.8	-10.51	47.5	-5.00
$1 \cdot 10^4$	17.9	43.1	-26.95	46.6	-6.80
$1 \cdot 10^3$	*55.9*	40.1	-32.03	46.3	-7.40

For an angle of attack of 90 degrees, reducing the connection stiffness does show improvements on the maximum coupling loading. The shear loading can be reduced by approximately 25 % when using spring stiffness in the order of magnitude of 10^4 while remaining within the limit of 20 mm displacement difference.

These results raise the question on why the modifications provide such different results for these angles of attack.
Comparison of both cases show a significant difference in terms of overall horizontal displacement of the jack-up. Using a rigid connection and the specified environmental loading results in displacements of approximately 580 and 265 mm in the x- and y-direction respectively.
Additional research in NX Nastran shows the stiffness of the guide in the DMB design is significantly different for these two directions. The ratio of stiffness in x-, and y-direction for the guide is approximately 1/3.
This largely explains the difference in displacement of the compared cases. Figure 5.43 shows a top view cross-section of the DMB with leg guide. The lack of stiffeners on the right side of the guide (x-direction) is the probable reason for this directional difference.

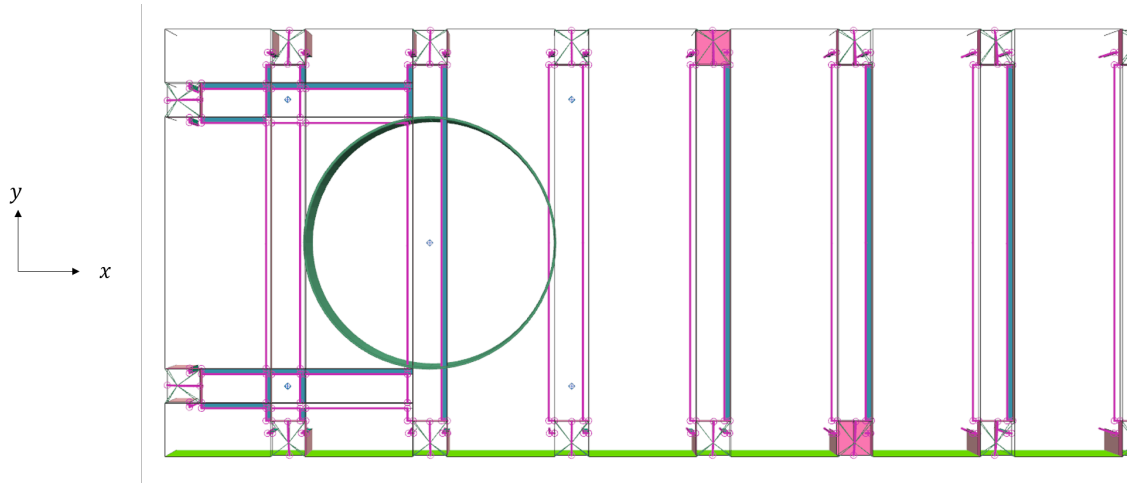

Figure 5.43: NX Nastran Top view cross-section of part of DMB with leg guide

The difference in the loading results in tables 5.8 and 5.9 can largely be explained by this structural aspect. It appears that the connection in the x-direction is already relatively flexible, which makes that further decrease of the stiffness between leg and hull does not have a significant influence.
As in the y-direction the structural stiffness is significantly higher, the influence of the introduced springs can decrease the maximum loading with approximately 25 and 7 % for respectively shear and tensional loading.

As the jack-up is loaded, it attains a horizontal displacement. As a result the centre of gravity of structure becomes eccentric, introducing an additional overturning moment. In case this overturning moment becomes significant the limits of the linear analysis are reached and the results become inaccurate.
For the 0 degree case the structure experiences an overall displacement resulting in an additional moment in the order of magnitude of 20 % of the initial overturning moment due to the environmental loading (with a rigid connection). Reducing the spring stiffness allows for larger horizontal displacements further increasing this moment, reducing the accuracy of the initial linear analysis.
In the 90 degree case these moments are less significant. As mentioned the leg housing appears to be stiffer in this direction, resulting in an additional moment of approximately 10 % of the initial environmental overturning moment (with a rigid connection). Reduction of spring stiffness to an order of magnitude of 10^4 increases this moment to 20 % of the environmental overturning moment.
These additional moments are considered significant, which makes that the results found in this section should be handled with care.
Modifications of the model, accounting for these effects might improve the accuracy of the results.

5.7.1. Discussion

For the question set up at the beginning of this section the following is concluded:

- *What is the influence of the stiffness of the connection between leg and hull on the loadings endured by the couplings?*

The structural stiffness of the leg DMB housing differs in the horizontal x- and y- direction. The stiffness ratio between both directions is approximately 1/3. Due to this, the influences of making the connection between the DMB and leg more flexible are different for both directions.
When loading the structure at a 0° angle of attack (x-direction), reducing the stiffness of the leg-hull connection does not have a positive influence on the maximum coupling loading. In any case the influence is negative, increasing the maximum loading.
In the y-direction the structural stiffness of the leg housing in the DMB is significantly higher. As a result, introducing a more flexible connection (using springs) can significantly reduce the maximum loading. Considering the weather window from the JUP2420 design specifications use of a connection with a stiffness in the order of magnitude of 10^4 has a positive effect and remains within the 20 mm displacement difference limit. With respect to tension the loading is reduced with approximately 7 % and for the shear loading this reaches up to around 25 %. It must be noted that no P-Δ effect is taken into account. As these appear to be significant (10 to 20 % of the initial environmental overturning moment) the accuracy of these load values should be handled with caution.

6

Conclusions and Recommendations

6.1. Introduction

In this chapter the general conclusions and recommendation of this thesis are discussed. In the first section elaboration is given on the overall findings and conclusions of the developed methodology and the case studies performed. Afterwards in the second section recommendations are given on further research on the subject together with advise on the development of these structures.

6.2. Conclusions

The main objective of this thesis was to find and develop a methodology suitable for structural analysis of modular jack-ups following the main research question:

How can superelements be used in the development of a methodology to analyse couplings in a modular deck structure in the early design phase?

In modular construction, superelements can be used to describe the components that are repetitive in the structure. By doing so, considering the requirements, an environment is created in which these elements are used as building blocks. This makes it possible to generate different deck layout configurations. Defining these components as superelements decreases the set of equations in the analysis drastically, also decreasing the calculation time. The outcome of such analysis has an accuracy comparable to conventional Finite Element Analysis.
This is achieved and put into practise in a parametric model which has the ability to generate deck configurations and load cases.
The analysis provides reliable results on the loading endured by each coupling in the configuration. As long as the user is aware of the its limitations. The results are validated using a proven software package based on Finite Element Analysis.
Comparing to conventional methods, the time needed to attain results on a conceptual design using this methodology is reduced to less than a minute. In comparison, conventional FEM analysis can take days.

With respect to case studies in the second part of the thesis, the research questions related are answered within the corresponding section. The overall findings and conclusions are discussed here.
From the studies performed it is clear that there is a large difference in the loading of couplings located near the outer edges of the structure comparing to those in the centre. The outer couplings located at the corners of the structure near the legs experience significantly higher shear loading. Similarly, the couplings located on the outer edges of the structure halfway between the legs experience significantly higher tensional loading.
Throughout all case studies these patterns are found, concluding that the couplings in these locations are critical for the design.

Regarding the load cases on transverse horizontal external loading (e.g. environmental conditions), it is concluded that the additional overturning moment from the eccentric displacement of the centre of gravity is

significant. Therefore, the results of these studies should be handled with care and it is expected that the loading values are higher.

From a design and development point of view, it is concluded that for the modular jack-up designs considered by DAMEN the development of higher strength couplings is necessary to ensure safe jack-up designs. It should also be considered to investigate on local reinforcing solutions for the critical locations.

From the study on punch-throughs, it is concluded that this model can provide approximations of the large loading endured by the couplings. As the loading can reach severe values, there is a reasonable risk of coupling failure. As compared to other jack-up designs which are not of a modular nature this adds a safety risk. Next to the possible tipping over of the jack-up, coupling failure can also lead to disintegration of the deck structure. This should be taken into account in designing safe platform operations.

The first case studies show that the leg-hull interaction has significant influence on the results of the (horizontally loaded) structure. Investigation on the stiffness of the connection between leg and hull shows that the current leg DMB design has a significant stiffness difference in the horizontal x-, and y- direction. From this it is concluded that decreasing the stiffness in the relatively rigid y-direction can significantly decrease the maximum coupling loading.

6.3. Scientific Recommendations

After the development of the methodology and performing the case studies on an existing conceptual design recommendations are set up for further research.

The leg-hull interaction shows significant influence on the loading endured by the couplings in the simulation. Further research on the method of implementation of the legs and the structural interaction between the leg, DMB and couplings can provide useful insights in the design of these components. An implementation method can be researched and developed taking into account the effects of leg inclinations and the a gap between leg and hull.

The studies show that there are critical areas within the jack-up configuration where load concentrates. Further research on the placement of the couplings can improve the loading capacity of the structures in general. An optimization study on coupling location can be considered.

The development of the methodology can be continued in the direction of dynamical analysis. The current model provides a solid basis for research in this direction. As a result it becomes possible to do research on e.g. fatigue. Also the simulations of a punch-through can be improved by doing so.

On the phenomenon of a punch-through, much knowledge can be gained on the influence of such event on the structural characteristics of a modular jack-up. Further development of this model and more research on the phenomenon of a punch-through can be of great value to the development of bottom founded offshore units. As mentioned in chapter 5.5, improvements can be investigated on the modelling of soil and the constraints used for the legs forming the diagonal over which the structure tilts. It is suggested to combine the current model with a soil model (describing the stiffness characteristics at the seabed) in a dynamic environment.

6.4. Company Recommendations

From the results of this thesis, recommendations are provided to the company for the development of modular jack-up structures.

The developed methodology and model provide fast results for structural analyses. In terms of accuracy of the results it performs similar to conventional FEM analysis, noted that P-Δ effects are not taken into account. With this knowledge the company is recommended to use the methodology in creating and analysing conceptual modular jack-up designs in an early phase of the design process.

From the case studies on the JUP2420 it is concluded that stronger couplings are needed for the production of modular jack-ups. DAMEN is advised to use the results of the case studies as a benchmark for developing stronger couplings.
In this process it can be considered to use the results of the studies on payload and environmental loading for the required service strength of the couplings. In addition, the ultimate strength should preferably be sufficient to withstand loading in case of accidents like a punch-through.

The case studies also show that the distribution of loading throughout the structure concentrates into several critical locations. As these locations are the same for all cases examined, for the development of these jack-ups one should also consider improving/strengthening the jack-up locally.

A

DAMEN Modular Barge

An excerpt is taken from the official DAMEN modular barge specifications. These are created and provided by the department of DAMEN Trading & Chartering (DT&C).

FOLIO 07087

DAMEN MODULAR BARGE

Type	DAMEN Modular Barge	
Built	New and never used.	
Sizes	These barges are available in different sizes and can be delivered in different versions as per pictures below.	
	Minimum:	Maximum:
Length	6,058 mtrs	12,192 mtrs
Width	2,438 mtrs	2,438 mtrs
Height	1,219 mtrs	2,895 mtrs
Payload with min. 300 mm freeboard	± 8 tons	± 63 tons
Deck load	6,8 tons/m^2	
Class	The DMBs are built to meet the classification rules for “Pontoons”, optional certification under Bureau Veritas or Lloyd’s Register. All DMBs and the Damen Link System can be delivered with 3.2 material certificate.	
Remark	They are 20’or 40’container sized units available in various heights. These units can be coupled together in the water with a specially designed coupling system, called the Damen Link. Because of this system, the entire combination can be transported by ship, truck or train to her final place of destination and assembled locally.	
Position	The Netherlands	

Easy road transporable

FOLIO 07087

DAMEN MODULAR BARGE

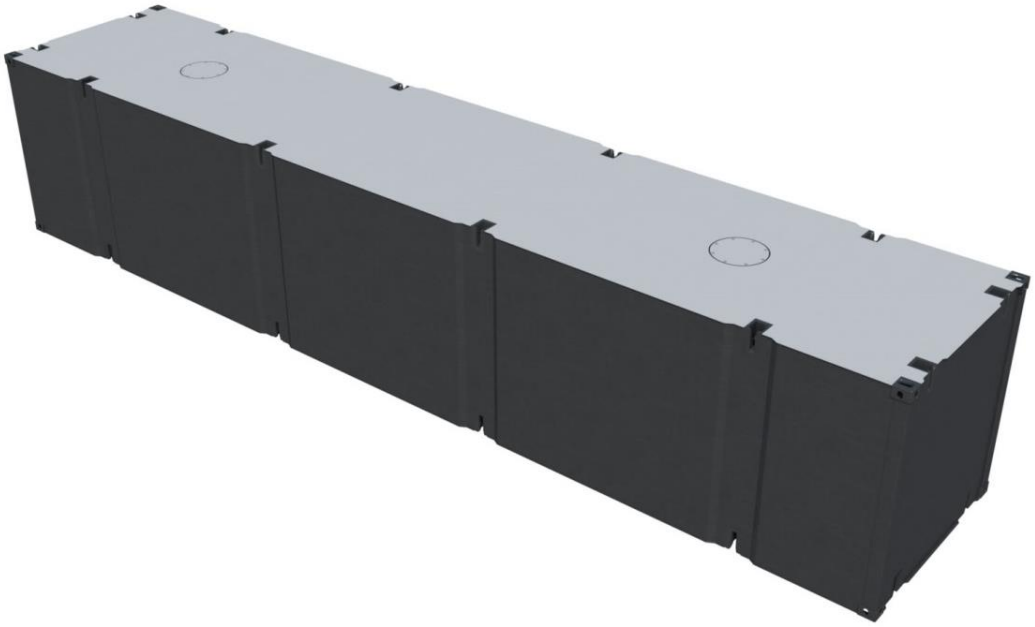

Damen Modular Barge single unit

B

JUP2420

Confidential

C

Case Study

C.1. Payload Location

Confidential

C.2. Feasibility Study

Confidential

Bibliography

[1] Official website of DAMEN Shipyards Group. `http://www.damen.com`. Accessed: 2016-6-10.

[2] Hitachi Sumitomo SCX900-2 Hydraulic Crawler Crane Specifications. Technical report, Hitachi Sumitomo Heavy Industries Construction Crane CO., Ltd.

[3] Guidance Note for the Classification of Self-Elevating Units. Technical report, Bureau Veritas (BV), 2010.

[4] Guideline for Offshore Structural Reliability Analysis: Application to Jacket Platforms. Technical report, Det Norske Veritas AS (DNV), 2012.

[5] Guide for Building and Classing Liftboats. Technical report, American Bureau of Shipping (ABS), 2014.

[6] Design Spiral used in DAMEN. from personal correspondance with H. L. Aga, 2016.

[7] S. Abolfathi A. Dier, B. Carroll. Guidelines for jack-up rigs with particular reference to foundation integrity. 2004.

[8] Bennett, L.L.C. Associates, and Offshore Technology Development Inc. Jack Up Units, A technical primer for the offshore industry professional. 2005.

[9] Britta Bienen, Gang Qiu, and Tim Pucker. Cpt correlation developed from numerical analysis to predict jack-up foundation penetration into sand overlying clay. *Ocean Engineering*, 108:216–226, 2015.

[10] B. Bienen M. S. Hossain C. Gaudin, M. J. Cassidy. Recent contributions of geotechnical centrifuge modelling to the understanding of jack-up spudcan behaviour. *Elsevier, Ocean Engineering*, 38:900–914, 2011.

[11] Robert D Cook et al. *Concepts and applications of finite element analysis, Fourth Edition*. John Wiley & Sons, 2001.

[12] *Modular Barge Specifications*. DAMEN Shipyards, 2016.

[13] V. Daun and F. Olsson. Master Thesis: Impact loads on a self-elevating unit during jacking operation. 2014.

[14] Carlos A Felippa. Introduction to finite element methods. *Course Notes, Department of Aerospace Engineeing Sciences, University of Colorado at Boulder, available at http://www. colorado. edu/engineering/Aerospace/CAS/courses. d/IFEM. d*, 2016.

[15] B. W. Byrne G. Vlahos, M. J. Cassidy. The Behaviour of spudcan footings on clay subjected to combined cyclic loading. *Elsevier, Applied Ocean Research*, 28:209–221, 2006.

[16] P.N. Godbole, R.S. Sonparote, and S.U. Dhote. *Matrix Methods of Structural Analysis*. PHI Learning, 2014. ISBN 9788120349841.

[17] E.J. Greeves, B.H. Jukui, and P.G.F. Sliggers. Evaluating jack-up dynamic response using frequency domain methods and the inertial load set technique. *Marine structures*, 9(1):101–128, 1996.

[18] L. H. Holthuijsen. *Waves in oceanic and coastal waters*. Cambridge University Press, 2010.

[19] J. Capul J. J. Jensen. Extreme response predictions for jack-up units in second order stochastic waves by FORM. *Elsevier, Probabalistic Engineering Mechanics*, 21:330–337, 2006.

[20] M.J. Cassidy J. Mirzadeh, M. Kimiaei. Performance of an example jack-up platform under directional radom ocean waves. *Elsevier, Applied Ocean Research*, 54:87–100, 2016.

[21] W.W. Massie J.M.J. Journee. *Offshore Hydromechanics, First Edition*. Delft university of Technology, 2001.

[22] D. Menglan S. Linsong M. Dongfengm Z. Minghui, Z. Laibin. Sliding risk of jack-up platform re-installation close to existing footprint and its countermeasures. *Petroleum exploration and Development*, 42, 2015.

[23] H. L. Aga O. Shelest. DAMEN Modular Barge, Capacity graph DMB couplings (confidential). Technical report, DAMEN Shipyards, 2015.

[24] R. Hydra O. Shelest. DAMEN JUP2420 Coupling concepts, Strength and buckling analysis (confidential). Technical report, DAMEN Shipyards, 2015.

[25] The Society of Naval Architects and Marine Engineers (SNAME). *Recommended Practice for Site Specific Assessment of Modible Jack-Up Units, First Edition, Revision three.* 2008.

[26] Section Offshore and Dredging engineering. Lecture notes on Offshore Engineering, Desing of Jack-ups, 2013.

[27] JJ Osborne, D Pelley, C Nelson, and R Hunt. Unpredicted jack-up foundation performance. In *Proceedings of the 1st Jack-up Asia Conference, Singapore*, 2006.

[28] ISO Petroleum. natural gas industries–Site-specific assessment of mobile offshore units–Part 1: jack-ups. *International Organization for Standardisation ISO*, pages 19905–1, 2012.

[29] P. D. Marsh R. J. Hunt. Oppertunities to improve the operational and technical management of jack-up deployments. *Elsevier, Marine Structures*, 17:261–273, 2004.

[30] Zhang W. Kang, C and J. Yu. Stochastic extreme motion analysis of jack-up responses during wettowing. *Elsevier, Ocean Engineering*, 2016.